U.PORTO

FEUP FACULDADE DE ENGENHARIA
UNIVERSIDADE DO PORTO

RELIABILITY-BASED ASSESSMENT OF SCOUR PROTECTIONS IN OFFSHORE FIXED FOUNDATIONS

ISRAEL NETO DOS SANTOS RIBEIRO LEÃO

Dissertação submetida para satisfação parcial dos requisitos do grau de

MESTRE EM ENGENHARIA CIVIL — ESPECIALIZAÇÃO EM HIDRÁULICA

Orientador: Professor Doutor Francisco Taveira Pinto

Coorientador: Mestre Tiago João Fazeres-Ferradosa

(Final Version – Versão Final)

JUNHO DE 2016

MESTRADO INTEGRADO EM ENGENHARIA CIVIL 2015/2016

DEPARTAMENTO DE ENGENHARIA CIVIL

Tel. +351-22-508 1901

Fax +351-22-508 1446

✉ miec@fe.up.pt

Editado por

FACULDADE DE ENGENHARIA DA UNIVERSIDADE DO PORTO

Rua Dr. Roberto Frias

4200-465 PORTO

Portugal

Tel. +351-22-508 1400

Fax +351-22-508 1440

✉ feup@fe.up.pt

🌍 http://www.fe.up.pt

Ao meu avô

"Melhor é experimentá-lo que julgá-lo, mas julgue-o quem não pode experimentá-lo"

Luís Vaz de Camões

AGRADECIMENTOS

Em primeiro lugar queria agradecer ao meu orientador Professor Doutor Francisco Taveira Pinto. Foi pela aprendizagem que obtive em unidades curriculares com ele que optei pela especialização de hidráulica, e todo o conhecimento que ele transmite é indispensável para qualquer estudante de engenharia civil.

Em segundo, ao meu coorientador e amigo Tiago Ferradosa. Sem ele, esta dissertação não seria possível. O apoio foi constante ao longo do semestre e com ele aprendi algo de muito valioso: Sem trabalho, nada se consegue. O seu conhecimento na área é algo fascinante e a forma como discute ideias incentiva os outros a quererem ser melhores.

À Eng. Vanessa pela ajuda na revisão de todos os elementos bibliográficos.

Quero também agradecer a todos os elementos das seções de Hidráulica e Materiais que de alguma forma contribuíram para a realização da dissertação. A ajuda foi incondicional e a disponibilização de recursos foi a melhor possível.

À minha família (familiares e amigos). Eles são tudo pelo qual uma pessoa luta e sem eles a vida perdia sentido. Eles são uns grandes pilares de tudo e todo o apoio ao longo desta fase da minha vida foi imprescindível. Eles são o meu hoje e serão o meu futuro.

Obrigado pai, mãe e Carol.

Por último ao meu avô… Ele sabe.

RESUMO

Devido à escassez de recursos não renováveis, mas não só, o investimento em energias renováveis tem vindo a demonstrar-se uma ótima e sustentável solução para o mundo.

A implementação de acordos como o Protocolo de Kyoto ou mais recentemente o acordo de Paris de Abril do presente ano, têm em vista a redução da emissão gases como o dióxido de carbono que representam uma ameaça constante para o planeta Terra e para os seus habitantes e representam um grande apoio à politica de investimento em energia renováveis.

Dentro do capitulo das energias renováveis, a energia eólica tem-se destacado não só pela sua razoável produção, mas também por ser uma energia sustentável e as estruturas offshore em particular, têm vindo a ter um forte desenvolvimento tanto no investimento como na qualidade devido ao sustentável desenvolvimento tecnológico.

Assim sendo, esta dissertação no ramo de hidráulica compreende o estudo do dimensionamento de uma proteção em riprap de uma estrutura offshore. Este tipo comum de solução visa os problemas associados à infraescavação, que é um dos principais problemas em qualquer obra realizado num meio aquático, seja ele estuarino, marítimo ou fluvial.

Este tipo de erosão localizada, cujo termo inglês é scour e o mais utilizado na comunidade cientifica, dá se quando um determinado escoamento encontra no seu caminho um obstáculo, estrutura, originando perturbações no escoamento e no fundo do mar que poderão levar à erosão nas proximidades da estrutura e consequente falha/colapso da estrutura.

O objetivo passa por garantir uma medida de segurança estrutural relativa ao sistema de proteção de estruturas do tipo fixo, com tecnologia riprap, associando à mesma um estudo de fiabilidade.

O presente trabalho permitiu obter estimativas da probabilidade de falha em proteções contra erosões localizadas em monopilares, sujeitos a correntes e ondas

A presente dissertação foi realizada na Faculdade de Engenharia da Universidade do Porto com especial enfase para um trabalho laboratorial no Laboratório de Hidráulica da SHRHA (secção de hidráulica, recursos hídricos e ambiente) do Departamento de Engenharia Civil.

PALAVRAS-CHAVE: Probabilidade de falha, fiabilidade, proteções contra erosão localizada, estruturas offshore, monopilares

ABSTRACT

Due to the scarcity of non-renewable resources, investment in renewable energy has been shown to have a great and sustainable solution to the world.

The implementation of agreements such as the Kyoto Protocol or more recently the Paris agreement made in the present year, are aimed to reduce the emission of gases like dioxide carbon that is a constant threat to the planet Earth and its inhabitants and are of great support to the investment policy in renewable energy.

Within the section of renewable energy, wind energy has been studied not only for its reasonable production, but also for being a blue energy and offshore structures in particular, have come to have a durable development equally in investment and quality due to sustainable technological development.

Therefore, this dissertation in the hydraulic branch comprises the study of the design of a riprap protection of an offshore structure. This common type of solution aims the problems associated with scour, which is a major problem in any work carried out in an aquatic environment, estuarine, ocean or river.

Scour occurs when a certain flow finds is in its way an obstacle, structure, leading to disturbances in the flow and on the seabed that may lead to erosion near the structure and consequent failure / collapse of the structure.

The objective of this dissertation is to develop a reliable system with riprap techonoly, which is the most used in offshore fixed fundations.

This present work permitted to obtain approximations of the probability of failure in protection against scour induced by currents and waves.

This work was carried out at Faculdade de Engenharia da Universidade do Porto with special emphasis for the laboratory work performed in the Hydraulics Laboratory of Civil Engineering Department.

KEYWORDS: Probability of Failure, Reliability based assessment, Scour Protections, Offshore Fixed Foundations, Monopile Foundations

INDEX

INDEX OF FIGURES

INDEX OF TABLES

NOMENCLATURE

A – Amplitude of the wave orbital motion [m]

D_{85} – Sieve aperture with 85 % of passing material [m]

$D_{67.5}$ – Sieve aperture with 67.5 % of passing material [m]

D_{50} – Mean diameter of the protection blocks or of the sediments in the sand bed [m]

D_{15} – Sieve aperture with 15 % of passing material [m]

D^* – Dimensionless grain size [-]

D_{n50} – Nominal mean diameter of the protection blocks or of the sediments in the sand bed [m]

D_{cr} – Critical grain size[m]

D_p – Pile diameter [m]

d – Water depth [m]

d_s – Sediment grain diameter [m]

Eu – Euler number [-]

e – Euler/Neper constant [-]

Fr – Froude number [-]

f_c – Friction factor for currents [-]

f_w – Friction factor for waves [-]

G – Limit State or performance function [-]

g – Gravity acceleration [$m.s^{-2}$]

H – Wave Height [m]

H_s – Significant wave height [m]

$H_{1/10}$ – Average of the ten per cent highest waves [m]

KC – Keulegan-Carpenter number [-]

k_s – Bottom roughness [m]

k – Constant Von Karman equal to 0.4 [-]

L – Wave Length [m]

L_{liquid} – Water free surfce [m]

L_{flume} – Flume Width [m]

L(t) – Load over time [-]

m – Mass [kg]

N – Number of simulations [-]

$N_{minimun}$ – Minimum number of simulations [-]

O(i) – Order of magnitude [-]

P – Pressure [Pa]

P_f – Probability of failure [%]

Q – Flow [$m^3.s^{-1}$]

R(t) – Resistance over time [-]

Re – Reynolds number [-]

S – Strouhal number [-]

SF – Safety factor [-]

Stab – Stability parameter [-]

S_{3D} – Dimensional damage number [-]

T – Period [s]

T_p – Peak Period [s]

T_w – Wave Period [s]

U_c – Current Velocity [$m.s^{-1}$]

U_{cr} – Critical Velocity [$m.s^{-1}$]

U_m – Amplitude of the horizontal velocity just above the bed [m]

U_{med} – Mean Velocity [$m.s^{-1}$]

Xn – Number of values in the failure region [-]

Z – Floodgate Height [m]

u* – Critical friction velocity [$m.s^{-2}$]

V – Volume [m^3]

W_{50} – Medium weight [N]

z_o – Roughness length [m]

α – Bed shear-stress amplification factor [-]

θ – Shields parameter [-]

θ_{cr} – Critical Shields parameter [-]

μ – Mean of a variable [-]

v – Kinematic viscosity of water [$m^2.\ s^{-1}$]

ρ_s – Sediment density [$kg.m^{-3}$]

ρ_w – Water density [$kg.m^{-3}$]

σ_i – Standard Deviation – where *i* is a random variable [-]

σ_D – Uniformity Coefficient [-]

γ_s – Sediment specific weight [$N.m^{-3}$]

γ_w – Water specific weight [$N.m^{-3}$]

τ_c – Current induced shear-stress [$N.m^{-2}$]

τ_r – Resistant shear-stress [$N.m^{-2}$]

τ_s –Loads shear-stress [$N.m^{-2}$]

τ_w – Waves induced shear-tress [$N.m^{-2}$]

τ_0 – Bed shear-stress [$N.m^{-2}$]

τ_∞ – Undisturbed bed shear-stress [$N.m^{-2}$]

1
INTRODUCTION

1.1 INTRODUCTION

1.1.1 OBJECTIVES AND RESEARCH QUESTION

Civil engineering is one of the oldest fields' existent in engineering. From the first day, civil engineers are responsible for finding solutions to society's problems. Since the birth of society, an engineer is a person who can solve problems and develop solutions. A good example is the construction of aqueducts – firstly built by Romans - with the objective of providing of water across complex terrains.

The water has a vital relation to Man and the use of its resources and conditions brought new ideas and achievements that ultimately led to society's development. At the present days, Man's relation to water and oceans goes far beyond the typical water supply. Perhaps one of the best examples is the blue energy investments made in strong relation with the ocean exploitation. Offshore wind farms installed at challenging locations, in the open sea, are certainly a good example concerning on how civil engineers have been contributing to the development of energy resources, at the societies' disposal.

Fig. 1.1 – Burbo Bank Offshore Wind Farm (HTB Eletrical, 2016)

In the recent years, the development of offshore wind farms' planning and construction has been increasing. Due to the increasing scarcity of financial and material resources, the need to improve the design of these structures and to optimise the costs of their implementation has become more and more evident (Fazeres-Ferradosa, 2016). The supporting structures of offshore wind turbines are estimated to represent about 30% of the total cost of an offshore windfarm (LeBlanc C., 2004). Therefore, the study and optimization of the structure's behaviour can contribute for a better management of resources in offshore construction industry.

One of the major problems, concerning offshore fixed foundations, is the local scour, which can lead to structural instability and eventually to collapse (Sumer & Fredsøe, 2002; Whitehouse, 1998; Hoffmans & Verheij,1997). Several problems as fatigue, excessive vibrations and top displacements are related to scour issues, e.g. Prendergast *et al.* (2013; 2015), as shown in figure 1.2. Therefore, taking into consideration this problem is essential to avoid potential problems in the offshore foundation. For example, scour is much related to the frequency of the monopile foundations, which are typically designed in the soft-stiff range.

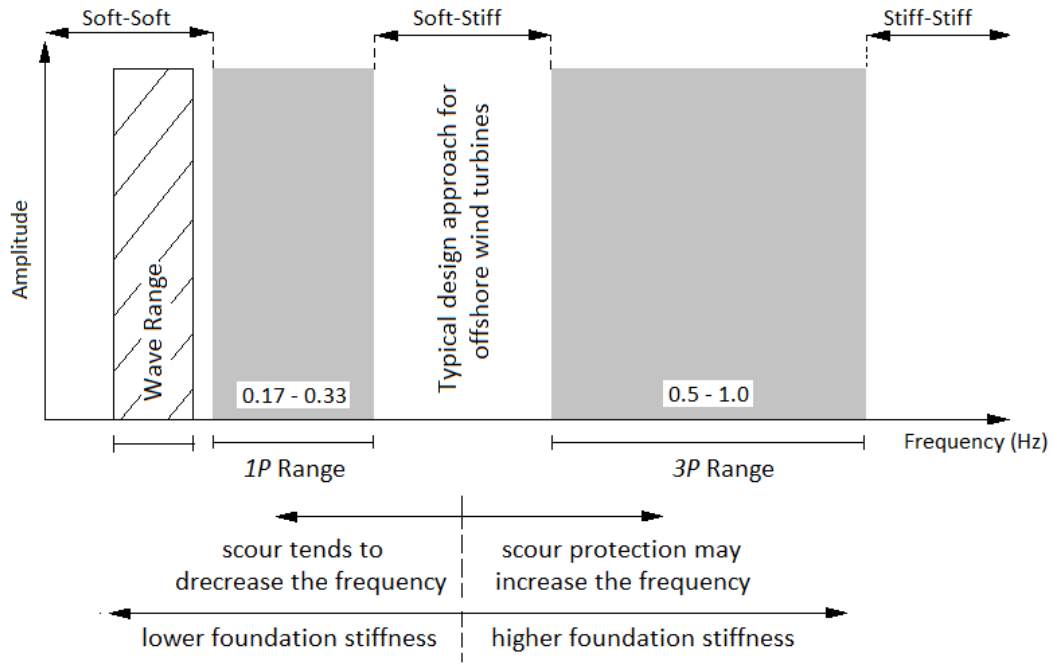

Fig. 1.2 – Frequency ranges for a typical offshore wind turbine and scour influence; Frequency design approaches (adapted from Prendergast *et al.* (2015).

where P is the armour layer thiknesses.

Scour has been the focus of research for several years. However, in offshore foundations, due to the complex hydrodynamic related to waves and currents combined, only recently scour has been continuously researched, e.g. Breusers & Raudkivi (1991), Whitehouse (1998); den Boon *et. al.* (2003, 2004), De Vos (2008), De Vos *et al.*, (2011, 2012), Fazeres-Ferradosa (2012; 2014; 2015), among others.

Nevertheless, according to Whitehouse (2010) there is still a high level of uncertainty as the potential depth of scour in relation to offshore wind turbine foundations and, therefore, uncertainty as the need for scour protection.

Scour protections are a requirement of many offshore projects, particularly for foundations installed in sandy sediment environments (Whitehouse *et.al*, 2014). Such protection systems may be designed taking into consideration two main variables: the armour layer thickness (*P*) and the armour extent (*E*). The armour layer thickness is often described as a function of the number of layers that compose the protection. Hence, this thickness is often studied by means of the research related to the protection blocks' dimensions. Typically, the design of the protections is made according to a certain choice of the mean diameter of these protection blocks (D_{50}) and *P* tends to range from 2 to 3 times the D_{50} value, over a filter layer with smaller thickness (Whitehouse *et.al.*, 2014).

Taking into consideration the present state-of-the-art of scour protections, it can be stated that the stone size (protection blocks) needed for a certain protection is commonly based on the criteria of the threshold motion (Kirkegaard *et al.*, 1998). On one hand, the majority of the existing design criteria are empiric in nature and do not account for the uncertainty of the phenomena, on the other they do not provide a measure or quantification of the reliability of the protection employed.

A possible way to analyse the variability of scour phenomena and the scour protection is to compute the failure probabilities associated to a specific block dimension and the characteristic load values that are acting on the structure.

According to Fazeres-Ferradosa (2015) probabilistic techniques allow the project criteria to be defined taking into consideration the variability of scour phenomenon, instead of only using the analysis performed purely based on the global safety factors, which do not directly account for such uncertainties.

The use of probabilistic techniques focused on the reliability of the protection enable a more accurate and systematic assessment of the protection's failure and its possible construction features. By doing this, it is possible to save considerable amounts of financial resources, due to the protection's optimisation and the prediction of maintenance and refill operations needed.

The present thesis is focused on the following research question:

"Is it possible to reduce the empiric nature of scour protections design by adopting a methodology that is able to assess the reliability of the protection system?"

In order to answer to this, the present thesis main goal is to seek for a methodology, which provides a starting point for a reliability-based assessment of scour protections used in offshore foundations. Such methodology is essential for an informed evaluation of the offshore blue energy investments, which nowadays face new challenges, with higher water depths, installations far away from shore and more severe sea-states.

1.1.2 MOTIVATION AND INTEREST

Nowadays, civil engineers are responsible for the design, production and construction of infrastructures such as buildings, dams, water systems, among others. The importance of civil engineer is recognized and his value to the society's development is crucial.

The proposed theme "*Reliability based-assessment of scour protections in offshore fixed foundations"* is turned to the growth and bet on offshore wind structures. This thesis was proposed taking into

consideration the growing tendency of the offshore wind market and its importance as a way to produce renewable energy, as an asset that not only contributes for mankind development but also to a greener and more sustainable future.

From the authors' view, this is an interesting area because the emergence and bet of the economy's stakeholders and governmental players in such offshore structures is a present reality and this field is presenting itself with a large progression (Athanasia, 2012). Offshore wind energy and its infrastructures are a recent issue, which leads to several non-solved problems. Scour is one of them. Although scour research has mainly been developed for currents alone, e.g. Breusers *et al.* (1977), Chee (1982), Johnson (1992), Chang (1994), Fazeres-Ferradosa (2012), Porter (2012), the research of this phenomena in marine environment is yet far from being completely understood.

The present work was focused on two different contributions:

1. An attempt to research scour under waves and currents combined, in the Hydraulics Laboratory of the Hydraulic, Water Resources and Environmental Division of the Civil Engineering Department at FEUP.
2. The study of a first measure of uncertainty and reliability in design of the riprap type protection used to account for scour around monopile foundations.

The "riprap technology" is a mixed solution of rocks typically employed around monopiles. It is considered as reliable solution and it is widely used in the most common offshore support structures (Matutano *et al.*, 2013), which is indeed the monopile, as shown in figure 1.3.

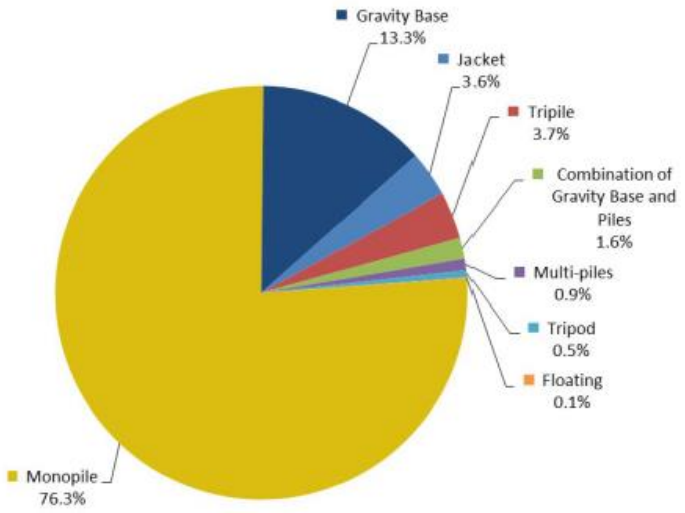

Fig. 1.3 – Monopiles as the most common structure employed as support structure in offshore environment (Navigant Consulting Inc., 2014).

Since these structures are associated to large financial investments, the money savings acquired when designing the protection can be quite significant. This becomes even more evident if it is taken into consideration that offshore wind farms, such as Burbo Bank, Horns Rev I, II and III, Arklow Bank, among others present a number of monopiles that can easily overcome several hundreds of wind turbines, each supported by a single monopile. For example, London Array is one of the largest wind farms existent in offshore environment and has 175 monopiles. Therefore, a small saving in one

protection is easily multiplied by a large number of turbines, leading to significant optimisations in the whole wind park (De Vos, 2008).

In this sense, the studied probabilistic approach is considered as a possible way to optimise the cost/benefit ratios used to assess the viability of these investments. Besides the potential contribution for the financial criteria of these type of investments, the present thesis also aims to provide a positive social impact. At a large-scale impact, this research tries to contribute for better conditions to explore the offshore energy resources, and at a micro-scale impact it can be pointed the tentative made to improve the conditions of the Hydraulics Laboratory to be adapted for scour research in waves and currents combined.

The present thesis was developed within the objectives and work outline of the NEMAR research group (Núcleo de Estudos da Energia do Mar) and corresponds to the author's intention to make a scientific contribution for such an important research field with remarkable links to the nowadays economic evolution.

1.2 Brief Background Notes

1.2.1 Energy supply, consumption and market

With the shortage of non-renewable resources, at a human life scale, such as oil, the world is facing a new era, the renewable energy era. The world started to become aware and to care about climate changes and global warming. The primary objective is to replace the non-renewable resources for the renewable ones, however the humankind dependency is too high. To change this, protocols like the Kyoto Protocol were made but it is not enough and the nations' needs to review their environmental and energetic policies is becoming more and more noticeable.

The Kyoto Protocol signed at 11 December 1997, extends the 1992 UNFCCC (United Nations Framework Convention on Climate Change) and has the objective to reduce greenhouse gases emissions, because of the global warming threat posed to the planet Earth as we know it. The investments made in renewable energy have been increasing in order to reduce the emissions of CO_2 (Fazeres-Ferradosa, 2016). At the present date new policies, e.g. the framework of Paris Agreement from UNFCCC with signature prevision is to the 22nd April 2016, are being developed and correspond to the growing tendency of seeking for alternative energy sources. In this matter, the offshore wind market poses itself as a prime leader in terms of the renewable energy exploitation.

In order to have a brief idea of the energy market evolution, figures 1.4 and 1.5 can be analysed, according to information provided by the International Energy Association (IEA). The figures respectively provide the evolution of world's total energy primary supply versus consumption. Taking information from figure 1.4 and 1.5, it can be understood that both have positive evolution by three main reasons (IEA, 2015):

- Industrialization;
- Globalization;
- Increasing Safety.

With industrialization, the emerging markets such as China and India are increasing their energy demand, which is added to other developed countries' needs, such as USA, European Union, Canada and others. The population growth as found a parallel in the consumption increase, which is also an effect caused by the globalisation factor. Globalisation implies higher demands of energy, which needs

to be satisfied by the market's sources, leading to the tendency for developing new ways to produce energy within a sustainable perspective. Such sustainability is of course connected to the exploitation of renewable energy, in this matter, the sea poses an enormous potential energy for society and economy.

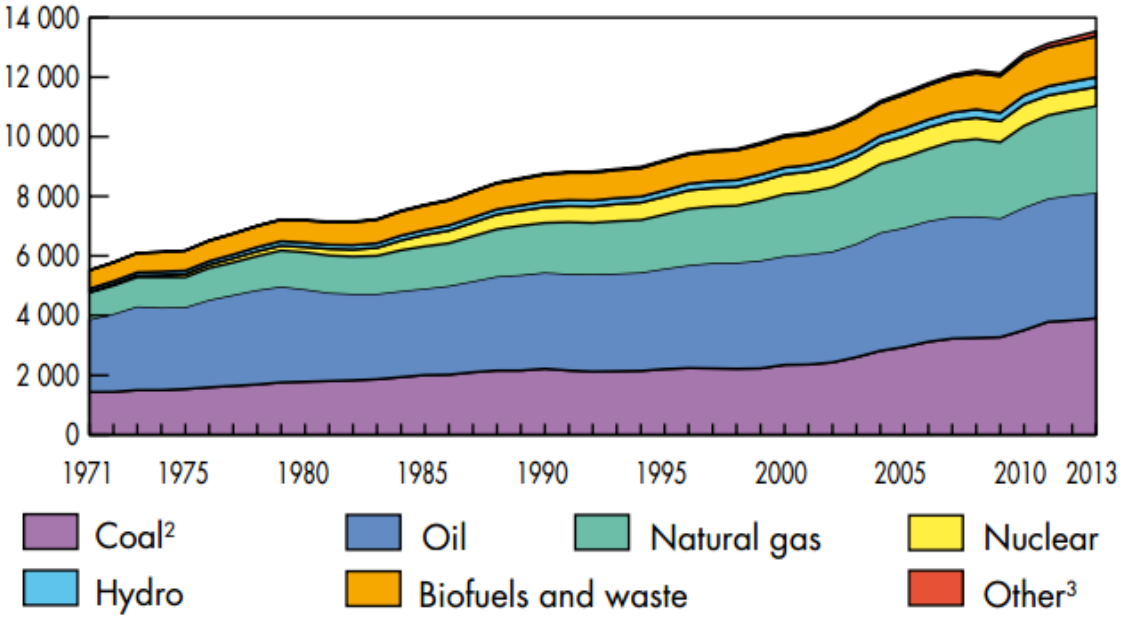

Fig. 1.4 – World Production (IEA, 2015)

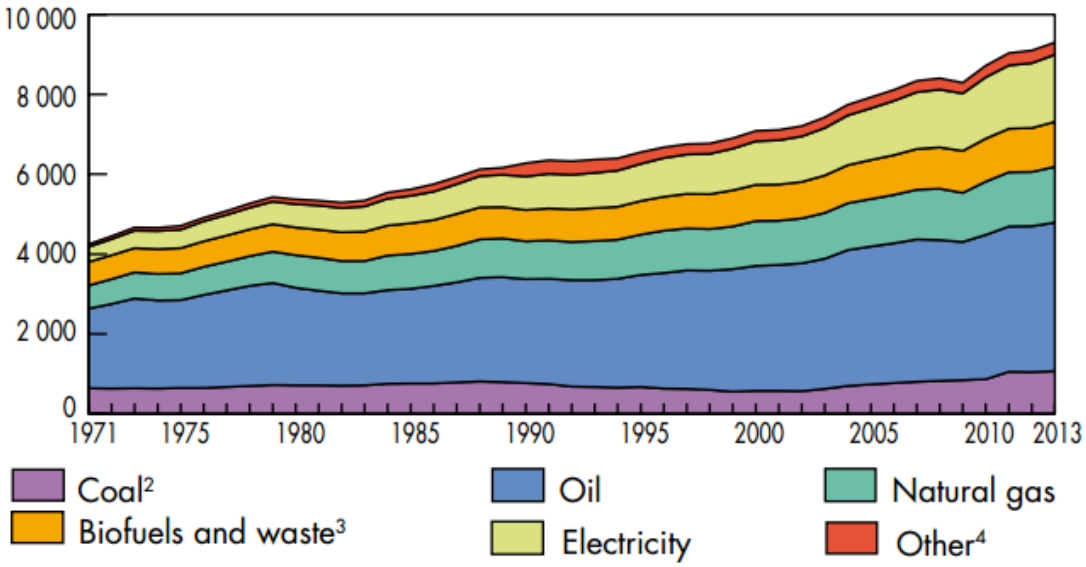

Fig. 1.5 – World Consumption (IEA, 2015)

The increasing safety of the energy production activities also provided a major contribution for the production increase. On the other hand, society is now more aware of possible disasters and threats that must be avoided at all cost. Therefore, their tolerance for catastrophic events, linked to energy investments, for example to nuclear power plants – Chernobyl in 1986 or Fukushima in 2011, is much lower. This also opens a window for the renewable energy market to grow, particularly in countries

where this type of energy production is being shutdown, as it is the German case which is closing all nuclear power reactors till 2022 (British Broadcast Corporation, 2016).

New changes are demanded and the renewable energy market represents a major possibility in this field, due to the energetic potential related to oceans, by means of waves, tidal, currents and wind resources interaction, offshore locations present themselves as one the most favourable sites for energy production.

1.2.2 Renewable Energy - Wind Power Sector

On the renewable field, the most common ways to produce energy are from the wind, hydro and solar sources. This kind of energy has potential because it provides energy services with zero or almost zero direct emissions of greenhouse gases.

The renewable energy is growing and renewable power generation has reached almost 22% of the global mix in 2013 and production as reached more than twice of nuclear power, allowing concluding that wind energy has a significant role on world power sector (IEA, 2015).

According to data from the Global Wind Energy Council (GWEC, 2015), Asia is the world´s largest regional market, with a capacity of almost 33.9 GW with countries such as China and India taking the lead in this region.

Despite the low expectations, caused by the global economic crisis, the year of 2015 was an excellent one for the wind energy sector, beating 2014 record of 51.7 GW and crossing the 60 GW barrier. This development was accomplished as said, by efforts from China and India, with China installing 30.753 GW. This installation represents almost 50% of the global wind power energy installation in 2015 (share of 48.5%) and a cumulative capacity in December of 2015 of 145.362 GW (33.6% of share), doubling the 75 GW installed in 2012. Although China is the leader in wind power energy, as it will be explained further on, in terms of the offshore wind market this is not the case. Nevertheless, a change from onshore to offshore investments is being noticed in the latest years, for example, with the offshore windfarms of Donghai Bridge and Xiangshui Rudong (4COffshore, 2016).

In Europe, the country with more installed capacity is Germany with nearly 45 GW followed by Spain (23 GW) and UK (13.6 GW). A total of 142 GW is installed, which 11 GW were for offshore installations and 131 GW for onshore and comparing the evolution from 2014 to 2015 is known that the investment in offshore is increasing instead of onshore that decreased (-7.8% when compared to 2014).

Another important market is the United States of America. In 2015, USA was the second country with higher investment in wind energy, with 8.598 GW and at the end of 2015 had 17.2% share of the total cumulative capacity in the world. The USA added four thousand new turbines for a total market of 8.598 GW in 2015, a 77% increase over 2014, and a total installed capacity reached 74.471 GW (GWEC, 2015).

As it can be confirmed from the previous numbers, the wind energy market is growing at considerable rates. The general offshore investment in wind energy has played a major role in this sector development, posing new challenges and a more competitive economic environment, which is also extended to the infrastructures used, as it is the case of monopiles.

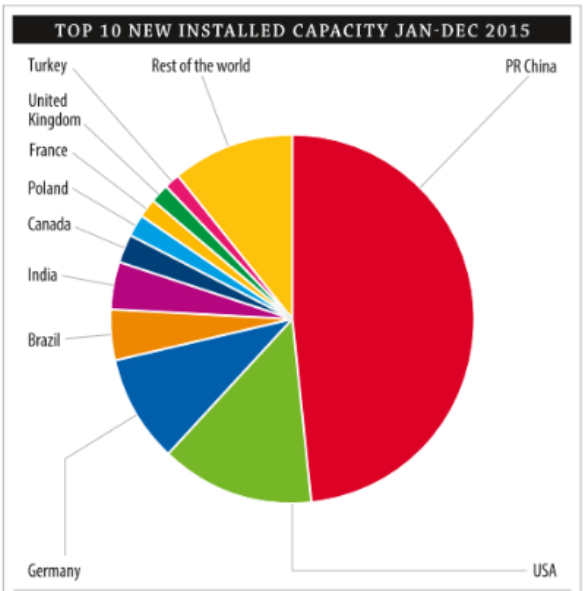

Country	MW	% Share
PR China	30,753	48.5
USA	8,598	13.5
Germany	6,013	9.5
Brazil	2,754	4.3
India	2,623	4.1
Canada	1,506	2.4
Poland	1,266	2.0
France	1,073	1.7
United Kingdom	975	1.5
Turkey	956	1.5
Rest of the world	6,950	11.0
Total TOP 10	**56,517**	**89**
World Total	**63,467**	**100**

Source: GWEC

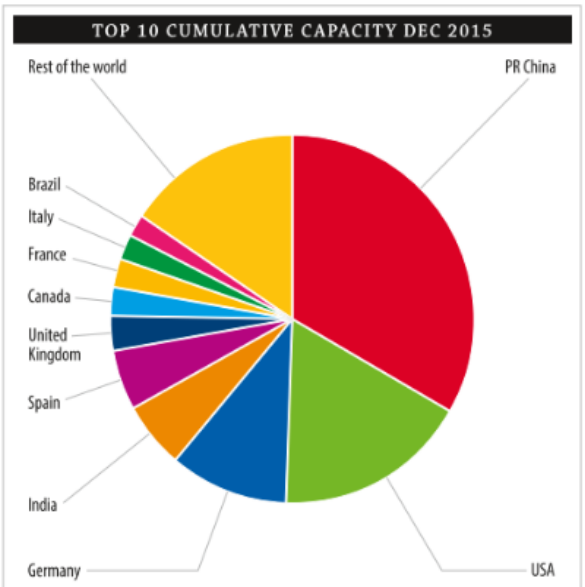

Country	MW	% Share
PR China	145,362	33.6
USA	74,471	17.2
Germany	44,947	10.4
India	25,088	5.8
Spain	23,025	5.3
United Kingdom	13,603	3.1
Canada	11,205	2.6
France	10,358	2.4
Italy	8,958	2.1
Brazil	8,715	2.0
Rest of the world	67,151	15.5
Total TOP 10	**365,731**	**84.5**
World Total	**432,883**	**100**

Source: GWEC

Fig. 1.6 – New installed Capacity (left) and Cumulative Capacity (right) (GWEC, 2015)

1.2.3 OFFSHORE WIND ENERGY – EUROPE SCENARIO

Although the overall investment in onshore wind energy is larger than offshore, offshore wind farms are a new challenge and a new field to invest, full of opportunities. As stated before, the investment in offshore wind resources is clearly increasing.

According to GWEC (2013) report, Europe had 92% of all offshore wind installations made. Such fact is accomplished, because despite the problems related to marine environment, new studies are being performed in this field, with the objective to make cheaper and safer installations. Comparing to the onshore installations, the offshore ones provide considerable advantages. Some of them (Athanasia, 2012; GWEC, 2016) are:

- Availability of large continuous areas, suitable for major projects;
- Elimination of the issues of visual pollution and noise;
- Higher wind speeds, which generally increase with distance from the shore;
- Less turbulence and friction, which allows the turbines to harvest the energy more effectively and reduces the fatigue loads on the turbine.

On the other hand, important disadvantages need to be taken into account from an investment point of view (GWEC, 2016):

- The more expensive marine foundations, in construction, installation and maintenance;
- The more expensive connections to the electrical network and in some cases a necessary increase in the capacity of the weak coastal grids;
- The more expensive installation procedures and restricted access during construction due to weather conditions;
- Limited access for operations and maintenance.

Despite the costs, due to higher potential for power generation, several investments are being made for offshore locations, because the initial funding is more easily recovered, i.e. within less time than it would be for an onshore one. (GWEC, 2016) Nevertheless, several improvements can still be made in order to improve the financial outcome in this sector, which is the case of the offshore foundations optimisation, namely the ones concerning to the riprap protections.

Once again, despite the predictions for 2015 were not the better, the growth was positive. There was an increase of 108.3% over 2014 of new offshore energy connected to the grid. Germany was the main responsible for this development by connecting 10 farms with 546 turbines (a total of 2.282 GW connected to the grid) but on the other hand, Sweden has disable one farm with five turbines connected. In EWEA (2016) the motive is not mentioned, but it is supposed that reasons were security or non-rentable production.

Table 1.1 - Winds farms, turbines and capacity installed through Europe – 2015 (EWEA, 2016)

Country	Germany	Netherlands	Sweden	UK	Total
No. of farms	10	2	-1	4	**15**
No. of turbines connected	546	60	-5	153	**754**
MW connected to the grid	2,282.4	180	-10	566.1	**3,018.5**

Now, Germany and the UK are faced as the two giants of offshore wind, due to their large project pipelines and positive Government outlooks (Fazeres-Ferradosa, 2016). A solid and mature state was reached by Europe and the future is promising because over the past 22 years, the development of offshore renewable energy has increased considerably (Matutano, 2013).

Figure 1.7 and tables 1.1 and 1.2 show the evolution of the cumulative and annual offshore wind installations in MW and the distribution of winds farms, turbines and capacity installed and fully connected to the grid at the end of 2015 throughout Europe.

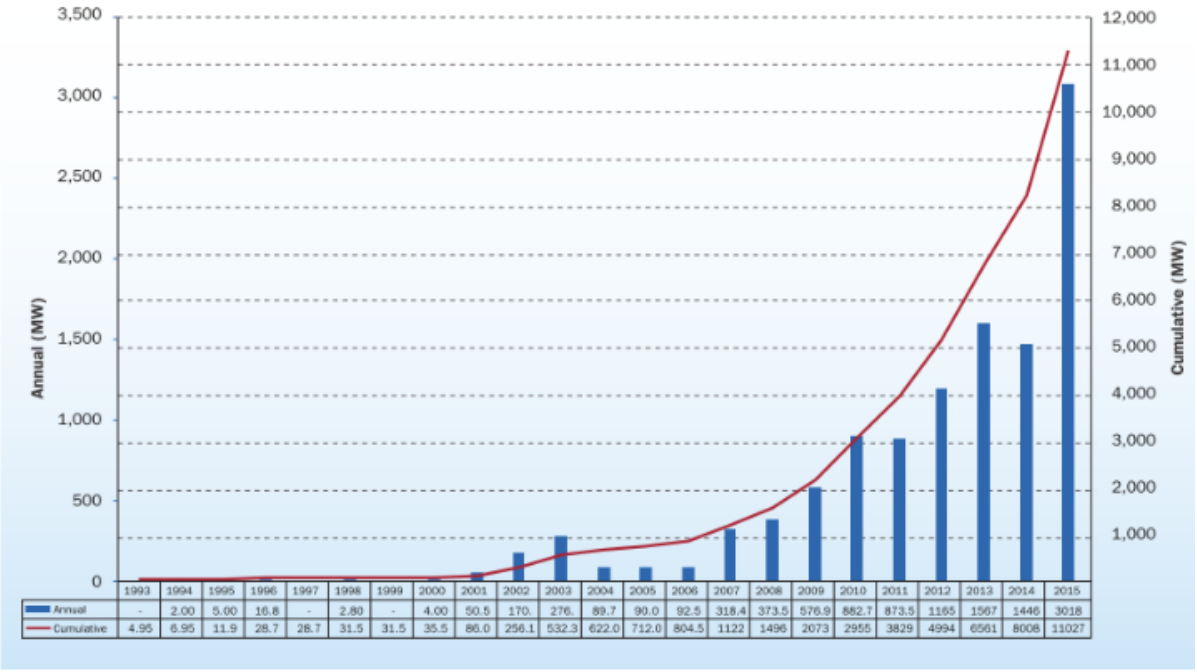

Fig. 1.7 – Cumulative and annual offshore wind installations (MW) (EWEA, 2016)

Table 1.2 - Winds farms, turbines and capacity installed through Europe – Cumulative (EWEA, 2016)

Country	BE	DE	DK	ES	FI	IE	NL	NO	PT	SE	UK	Total
No. of farms	5	18	13	1	2	1	6	1	1	5	27	**80**
No. of turbines	182	792	513	1	9	7	184	1	1	86	1,454	**3,230**
Capacity installed (MW)	712	3,295	1,271	5	26	25	427	2	2	202	5,061	**11,027**

Analysing tables 1.1, 1.2 and the figure 1.8, the idea of a growing market is achieved and we can realize that investments from Germany, UK and Netherlands increased the 2014 value of 1.446 GW to more than the double 3.018 GW.

UK has 1454 turbines with a capacity installed of 5.061GW, representing 45.9% of total installations. Next to them are Germany, that as said, in 2015 made a huge investment changing their capacity with more 2.282 GW, which was more than the total at the end of 2014, 1.013 GW.

Another conclusion it is that most of investments in 2015 were made in the North Sea. The North Sea represents 86.1% (nearly 2.6 GW) against the 9.2% of Baltic Sea and 4.7% of Irish Sea. From the total cumulative value of 11.027 GW of offshore wind capacity, the Atlantic Ocean represents 0.1% followed by Baltic Sea (12.9%), Irish Sea (17.6%) and North Sea (69.4 %).

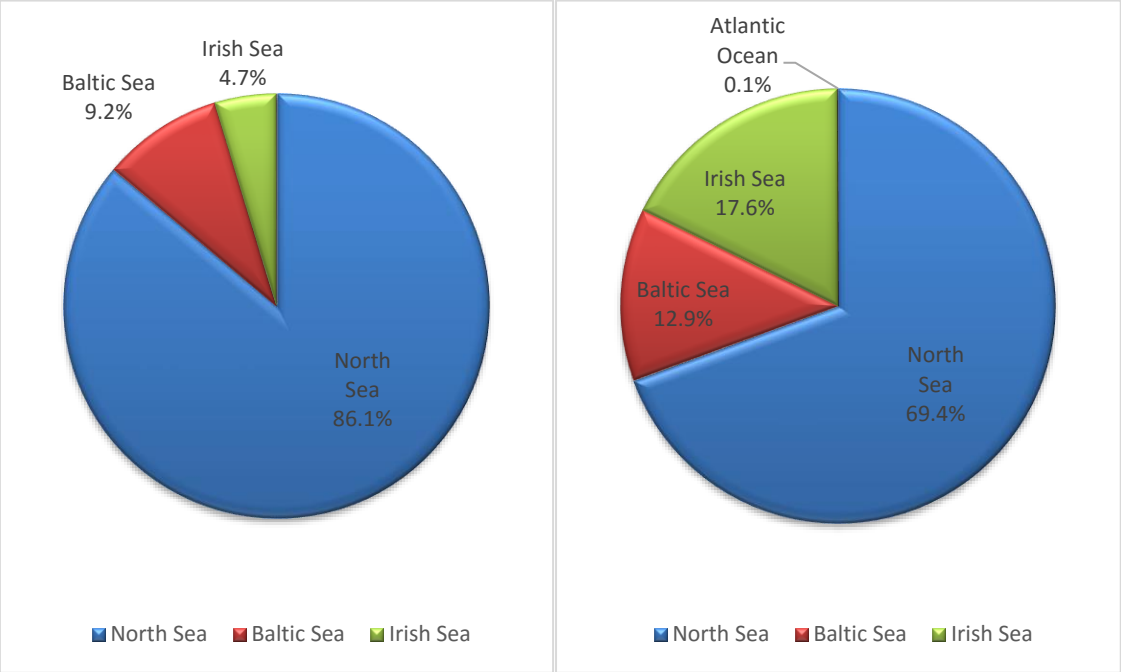

Fig. 1.8 –Share of 2015 net annual installations of (Left) and Cumulative Share by (Right) Sea basin, adapted (EWEA, 2016)

1.2.4 TRENDS

The construction of a wind farm is a complex and thrilling challenge for civil engineers and with the growing market and opportunities, there are trends that for some reasons need to be taken into account with different scenarios.

A few of them (Rodrigues *et al.*, 2015) are:

- Installed capacity;
- Area and number of turbines;
- Distance to shore;
- Water depth;
- Costs.

On installed capacity, the growth rate from 2010 to 2015 and the average capacity of new wind turbines increased. This increase was of 41.1% from 3.0 MW to 4.2 MW as it is shown in figure 1.9 (Rodrigues *et al.*, 2015). Following this lead, it is expected that the project average capacity will increase 27% to 2018 according to Rodrigues *et al*. (2015).

Two of the most important trends in terms of monopiles design and respective protections are the distance to shore and the water depth. Since the first project, the average distance to shore has increased considerably, hence the water depth as also increased. The average distance to shore of projects commissioned in 2013 was around 25 km and in 2015 the value was 42 km. In the same year, the maximum water depth construction was 45 m, in Alpha Ventus Windfarm (jacket foundation) (Rodrigues *et al.*, 2015). Furthermore, monopiles usually used between 0 to 30 m of water depth (DNV, 2011) are now being adapted to new concepts, e.g. XL Monopile that is able to be fully installed and operational up to 45 m (Leite, 2015).

Concerning the costs, the offshore wind sector is experiencing a good financial situation, since the financial markets are favouring the investments in this kind of technology (Navigant Consulting Inc., 2014). Figure 1.10 shows the evolution from 2010 to 2015 of total investment required for new assets. The last year had an enormous investment, almost doubling 2014, representing an evolution of 104%.

It may be concluded that offshore wind market is an important field in the development of the renewable energy sector.

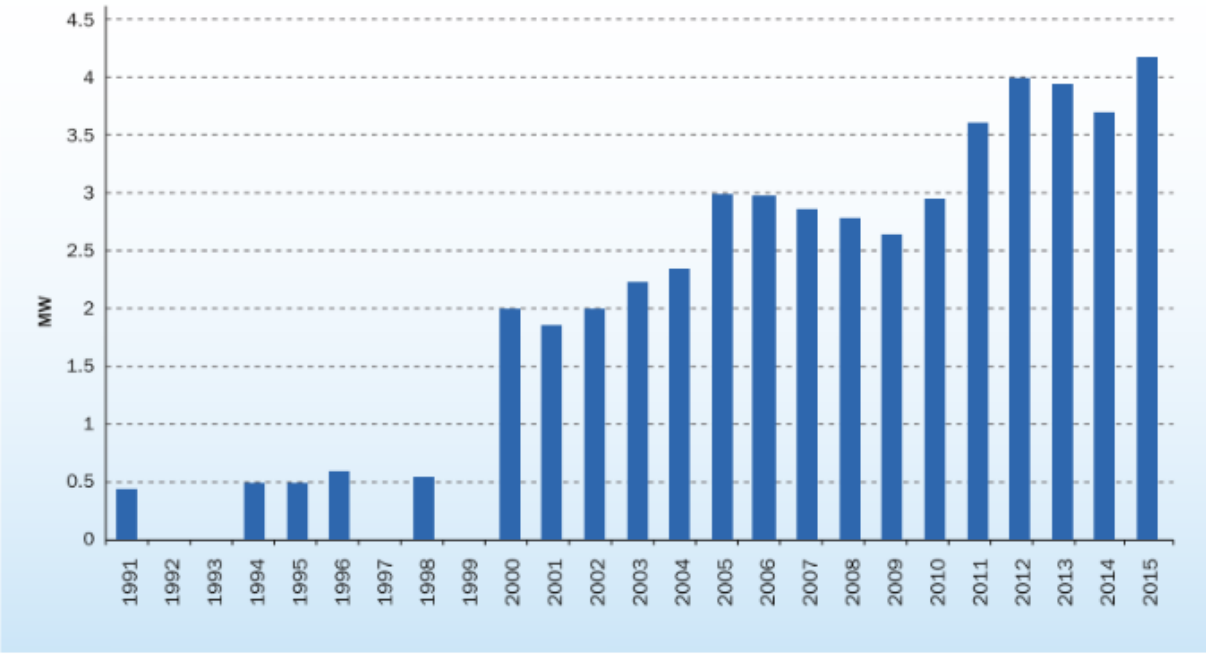

Fig. 1.9 – Average offshore wind turbine rated capacity (EWEA, 2016)

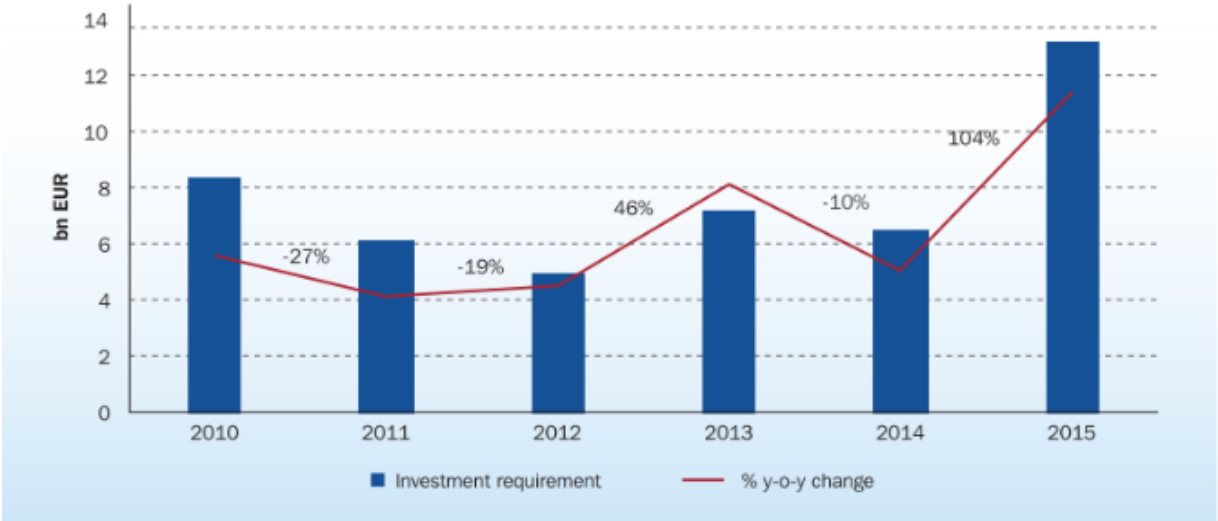

Fig. 1.10 – Total investment requirements for new assets 2010-2015 (EWEA, 2016)

1.3. THESIS ORGANIZATION

This thesis includes six chapters. The first one, Chapter 1, introduces the present theme, and the respective research question to be approached. The motivation and objectives of this investigation are also provided, along with the background context concerning the offshore wind energy sector. Due to the theme of this thesis, the wind energy gets the attention, with North Sea being the zone most used as a background (reference) and with the protections of monopile foundations as the analysed example.

Chapter 2 gives a summarised version of the state-of-the-art concerning scour protections in offshore foundations. In this chapter, basic concepts that are needed to understand the work made and its background. The scour phenomenon plays a major role in this thesis and all the important concepts and literature related to it are cited.

The reliability and probabilistic subjects are presented in Chapter 3. This part of the thesis provides the major concepts for reliability-based design in scour protections and summarizes its major problems and concerns. The analysis of the probabilistic model and mathematical algorithm is also given for further understanding of the results analysis performed in the following chapters.

In Chapter 4, a description of the experimental work and tests procedures is made, related to the scour experiments performed aiming research concerning scour protections subjected to waves and currents combined. The details about the experimental setup, wave tank characteristics and its equipment, scale considerations and experimental results are presented. The conclusions of this experimental work are also summarised, with a particular focus on the improvements needed for future research using similar physical modelling techniques.

Concerning the reliability-based design, the results and their discussion are presented in chapter 5. In this chapter, the methodology explained in chapter 3, regarding the reliability analysis and its applicability is described. The validation of the algorithm is made by using De Vos (2011) example and the protection used in Horns Rev I is analysed as a case study. Based on this case a preliminary assessment to test the algorithm and the results obtained are studied and discussed.

Chapter 6 reviews the main conclusions obtained from this dissertation and provides some inputs and guidelines for future research, concerning the reliability and probabilistic assessment of riprap protections, in offshore foundations. This chapter exposes the most useful outcomes of the research, their implication and introduces a discussion to the non-solved problems in this work.

2
STATE OF THE ART

The state of the art is the latest and most sophisticated stage of an art, science or technology. It refers commonly to the highest level of development of an area, which in this case is the development and achieved goals for the studies of scour protections.

The design of any structure placed in a marine environment is hard to complete because there are too many unpredictable elements. However, several studies have been performed providing considerable contributions to this field. This chapter provides a review on them, explaining the main concepts involved in scour phenomena and protections design. Scour phenomenon is one of hardest and most expensive problems to solve, particularly in sea environment. Therefore, this reading can be complemented with further literature, e.g. Whitehouse (1998), Sumer & Fredsøe (2003), among others.

2.1 SCOUR PHENOMENON

Scour is a process related to the movement of bed materials around a marine structure. There are two different types of scour, local scour and global scour.

The development of scour problems is related to both but because global scour is very site specific and depends on the location of the wind farm (De Vos, 2008), only the local scour is studied and discussed in this thesis.

Local scour is a process whereby bed materials are removed around a marine structure due to the disturbances of the uniform flow, which typically results in a higher degree of turbulence and erosion capacity (Pang *et al.*, 2016). The local sediment transport capacity is increased by the changes in the flow pattern caused by a structure placed within the flow (De Vos, 2008).

Related to this, the stability of a foundation might be at risk and failure can occur. Actually, one of the main causes of bridges' failures are scour problems (Kobayashi and Oda, 1994). With this reality, many studies were made in this field. However, from bridges to wind farms large differences exist in the acting forces that cause scour. At a river, only exists unidirectional flow but in a marine environment, the waves (oscillatory flow) can make a difference in scour problems.

2.1.1 BED SHEAR STRESS CONCEPT

As said before, scour phenomena relate to the movement of material at the bed of a marine environment. This transport of sediment results from a current, a wave or both at same time. This theme was studied by many authors, Nielsen (1992), van Rijn (1993) and Soulsby (1997), are a few of them. Their works were mainly focused on the behaviour of non-cohesive sediment combined with current and wave conditions, which is the case of the present thesis.

It is indispensable to analyse first the sediment transport before introducing the bed shear concept. Soulsby (1997) defines the sediment transport from three processes: entrainment, transportation and deposition, as shown in figure 2.1.

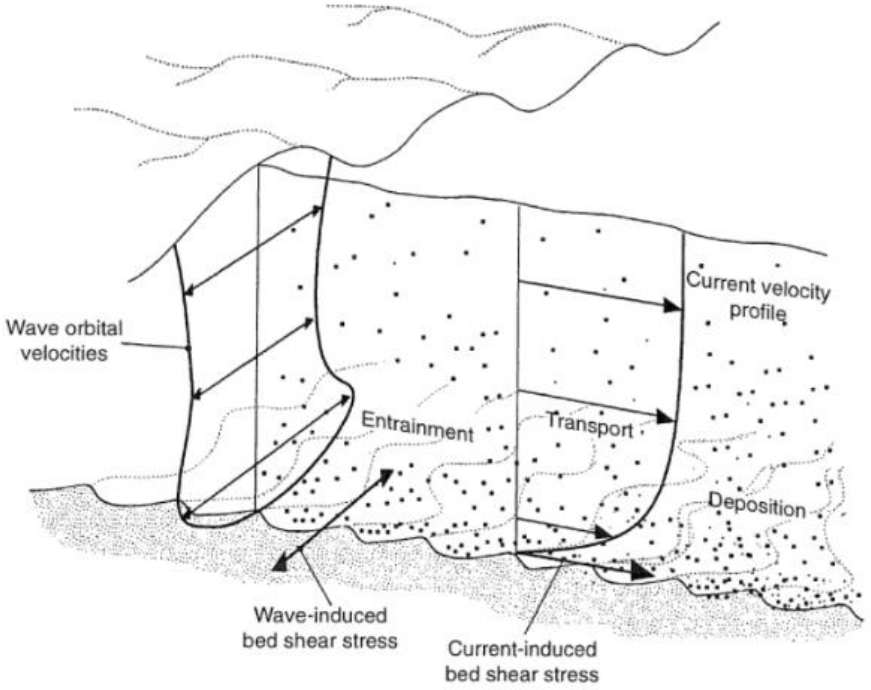

Fig. 2.1 – Sediment transportation, Soulsby (1997)

These three basic processes are related and dependent. Figure 2.1 shows (from left to right) that first occurs entrainment, followed by transport and finally deposition. This analysis is only valid for a little grain/particle because these three phenomena occur at the same time for all particles.

Entrainment is the result of the friction exerted on the seabed by the current and waves and it is related to the bed shear stress. In this process exists the possibility of grains going into suspension due to turbulent diffusion (De Vos, 2008).

After this, transport can be made in two different ways, bedload or suspend. Their difference remits to different flows and consequent size of grains and is represented in table 2.1.

Table 2.1 – Difference between bedload and suspended transport (adapted from De Vos, 2008)

Transport	Flow	Grain Sizes	Importance
Bedload	Slow	Large	Lower
Suspended	Fast	Small	Higher

The deposition is the last process. Occurs when a grain finishes is suspension status, the movement has finished and the particle rests.

From these three processes, the main concern is entrainment due to be relation to the bed-shear stress. This concept has a large importance and its definition is one of the basic concepts that needs to be understood.

The bed shear stress, τ_0 (N.m^{-2}), is the main "force" that causes scour which leads to the collapse of structures in many cases. It can be defined as the frictional force exerted by the flow per unit of bed area and is a function of flow speed as well as the roughness of the seabed (Soulsby, 1997). This dependence is further described later.

It is important to know, that this "frictional force" may result from a combination of the three different possibilities that can occur in a marine environment:

- Currents (steady flow);
- Waves;
- Currents and waves combined.

The analysis of these three cases is important because it is known that despite currents are the main force to cause the bed shear stress, waves are also unpredictable due to different wave heights and other factors.

The bed shear stress can also be defined as a distance per unit of time, which is a velocity. This velocity, known by frictional velocity (m.s^{-1}) or shear velocity (Fazeres-Ferradosa, 2016), is another form to represent the influence of flow speed on sediment transport.

According to Soulsby (1997), the frictional velocity and the bed shear stress can be correlated. This can be understood by equations 2.1 and its development to equation 2.2.

$$\tau_0 = \rho_w u^{*2} \tag{2.1}$$

$$u^* = \left(\frac{\tau_0}{\rho_w}\right)^{\frac{1}{2}} \tag{2.2}$$

It is necessary to understand that in equation 2.2, the u* does not correspond to the real velocity of the flow. However, it can be related to the turbulence in flow and in its fluctuation. (Soulsby, 1997)

Considering this, it is possible to conclude that the bed shear stress and the sediment transport are difficult to predict because there are many components, that are hard to define. Despite this, Shields

(1936) created a curve associated to the Shields parameter that was and still is one of ways to calculate the bed shear stress.

2.1.2 SHIELDS PARAMETER

The Shields Parameter was one of the first methods to predict the initiation of motion in a sediment bed. This dimensionless variable relates the bed shear stress with sediment and turbulent flow characteristics. This relationship is represented at equation 2.3 where ρ_s is density of the sediment grains, ρ_w is the water's density, and d_s is the grains' size and τ_0 is the threshold bed shear stress. The u* as said before, has a huge importance in this equation because is relation goes to the Reynold´s number and to analyse the original curve of Shields. These relationships are in equation 2.4 where ν stands for the kinematic viscosity and D_{50} is the median grain diameter.

$$\theta = \frac{\tau_0}{g(\rho_s - \rho_w)d_s} \tag{2.3}$$

$$Re = \frac{u^*.D_{50}}{\nu} \tag{2.4}$$

Another point from this parameter is that equation 2.3 was made taking only in account a steady uniform flow. However, new adaptations to Shields diagram were done and the analysis can now contemplate the other situations, namely the ones that can occur in a marine environment which were referred before, waves and a combination of currents and waves.

One of these studies was from Hoffmans and Verheij (1997), which is represented in the next figure 2.2.

This curve was a reformulation of the original Shields Curve but taking in account the studies from Soulsby (1997). The main objective was to relate directly the bed shear stress with dimensionless grain sizes, D*. The D* was used for Soulsby equation 2.5. This curve and equation are both reliable to be used with currents and waves.

$$D_* = d_s \left[\frac{g(s-1)}{\nu^2}\right]^{\frac{1}{3}} \tag{2.5}$$

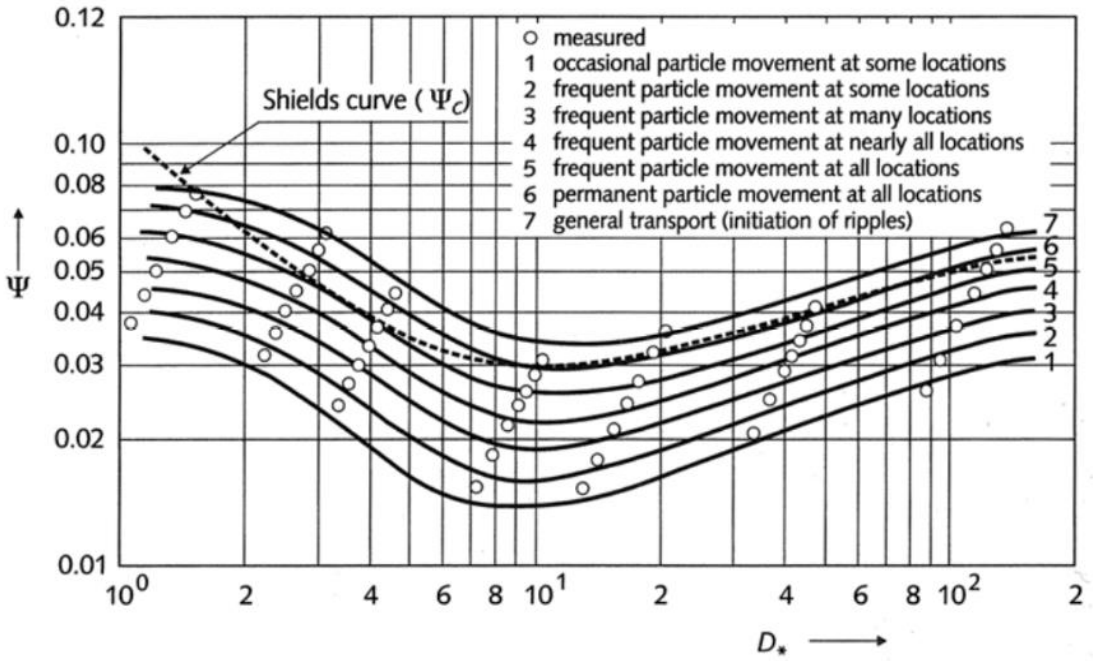

Fig. 2.2 – Shields Curve - adapted by Hoffmans and Verheij (1997)

2.1.3 AMPLIFICATION FACTOR

The amplification factor emerges as an amplification of the bed shear stress, i.e. this factor corresponds to the ratio of the shear stresses with and without the structure placed in the flow. Placing a new structure in the marine environment represents an increase of the stress and turbulence level, which leads to an increasing sediment transport (Sumer, 2002).

Therefore, this factor is a ratio between the bed shear stress after the implementation of a structure and the value of undisturbed bed shear stress. This ratio is represented in equation 2.6.

$$\alpha = \frac{\tau_0}{\tau^{\infty}} \tag{2.6}$$

With this new problem, some studies were made and developed this change in the bed shear stress concept. Whitehouse (1998), combining knowledge from the studies made from Niedoroda & Dalton (1982) among others, compiled in a table the typical values for shear-stress amplification factor alpha around structures.

Table 2.3 – Typical valued for amplification factor, adapted from Whitehouse (1998)

Flow/structure type	α	Source
Steady flow Slender Pile	4	(Hjorth, 1975)
Pipeline	4	(Fredsøe, 1993)
Squat Pile	2 to 5	(Baker, 1979; Eckman and Nowell, 1984)
Bridge caisson (rectangular)	4 to 6	(Hebsgaard et al., 1994)
Wave flow Circular Pile	2 to 3	(Sumer et al., 1992b)
Wave-current flow Bridge caisson (rectangular)	4 to 6	(Hebsgaard et al., 1994)

There are several conclusions and appointments to make. It is understandable that are many things that changes the amplification factor like the velocity of the flow or the complex geometries of structures.

Regarding the first, it may be concluded that with the increase of flow speeds, the bed shear stress also increases leading the amplification factor to a higher value. This occurs because nearby the structure, flow gets more disturbed (Whitehouse, 1998).

For steady current situations, the amplification factor can reach values around 11 or 12 below the horseshoe vortex in the upstream side of the pile (Niedoroda and Dalton, 1982).

Finally, an important aspect to take into account is when the amplification factor equals one. This concept leads to equilibrium scour depth, which is treated below but the main idea is that when the scour hole reaches an equilibrium stage, equation 2.6 is equal one.

2.1.4 Equilibrium Scour Depth

Understanding the amplification factor of the bed shear stress leads to this new and important concept. The equilibrium scour depth can be defined as the equilibrium stage, which is reached after a certain amount of time and allows evaluating the dimension of the hole created by scour.

The relation to the amplification factor is when it equals to one, which can be understand as said before as an equilibrium stage.

The study of Sumer and Fredsøe (2002) is obviously recommended and from it, we can use a graph that describes the evolution of scour depth versus time, the figure 2.3

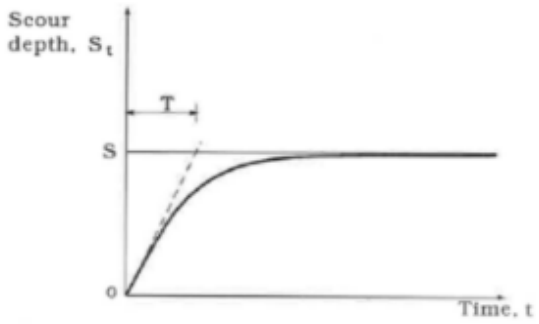

Fig. 2.3 – Time vs Scour Depth (Sumer and Fredsøe ,2002)

In figure 2.3, it is displayed the time (t) versus the scour depth (δt). Despite the logarithmic behaviour of function, which is important, the main concept to understand is that from a certain time, the scour depth almost reaches an equilibrium scour depth, as in logarithmic function. This is called an asymptotic value, which can be used as the highest scour depth that can be reached.

The importance of this concept is major by itself. Studying scour process is extremely hard and reaching a value that corresponds to maximum scour depth is very important to design scour protections.

Through this, time is always an important part of scour depth evolution. The term Time Scale surges when the elapsed time is intending to refer a certain amount of scour, this term is used. This importance is referred in Fazeres-Ferradosa (2012) due to the situation in which the scour hole can be backfilled after a storm or can be slowed down knowing the time scale.

2.1.5 SCOUR PREDICTION

Many formulas were developed to predict scour depth. Most of them are semi-empirical formulas but despite this, they cannot be applied for every case because their concerns to very specific situations.

These formulas can be divided by the type of interacting loads as said before. The literature recommend for the different types is:

1. Steady flow:
   1.1 Carstens (1966);
   1.2 Breusers (1971);
   1.3 Franzetti *et al.* (1982);
   1.4 Kothyari *et al.* (1992).
2. Waves action:
   2.1 Sumer *et al.* (1992);
   2.2 Whitehouse (1998);
   2.3 E-Connect (2002);
   2.4 Den Boon *et al.* (2005);
   2.5 Fazeres-Ferradosa (2012);
   2.6 Matutano *et al.* (2013).

2.1.6 THRESHOLD OF MOTION

After the introduction to the bed-shear concept, evaluate and understand the moment that a particle stars to move is also important. As said before, when a particle is excited by a steady current flow, i.e. when the forces produced by the last one are higher than the stabilizing forces, the movement can occur. (Breusers & Raudkivi, 1991). The moment when the particle stars to move is called the threshold of motion. So the critical value of bed shear stress, this corresponds to the threshold of motion. This concept has a huge importance in the analyses of Shields Parameter.

The Shields Parameter and diagram, associated to the sediment transport, when the non-dimensionless shields shear stress θ is higher than the critical shields parameter $\theta_{cr,}$ the movement of particles starts to happen. This critical shields parameter can be calculated and its dependent to the sediment size.

Regarding the Shields parameter there is still two important reference and studies to be referred together with its conclusions. The first (1.) is from Whitehouse (1998) and the second by Sumer *et al. (*2007) (2.)

1. No scour occurs for values of the undisturbed bed shear stress which are smaller than 25% of the critical value for shear stress;
2. The scour depth becomes independent from shields parameter when large values for Θ are prevailing in comparison to the shields critical value θ_{cr}.

2.1.6.1 UNIFORMITY COEFFICIENT

Sediments are a really important part of the study of scour phenomena. There are several ways to define them but the main characteristic to this kind of studies is its uniformity. Due to this, sediments can be divided in two ways, uniform and non-uniform sediments.

To distinguish these two terms, a new term is presented, the called uniformity coefficient (σ_D). The equation that defines this coefficient is 2.7.

$$\sigma_D = \frac{D_{85}}{D_{15}} \tag{2.7}$$

For practical cases, when the value of σ_D is higher than 1.5, the sediment is considered a uniform sediment but it is to understand that there is no such perfect uniform sediment.

This concept is important and will be use often later in this work

2.1.6.2 CRITICAL VELOCITY IN UNIFORM SEDIMENTS

To calculate and predict sediment transport and scour under different flow conditions this concept can be useful.

Critical velocity can be used instead of the Shields parameter and its use is justified to some limitations of Shields analysis.

One of these limitations is referred in Fazeres-Ferradosa (2016), which state that the Shields Parameter does not take into account the variations in the instantaneous values of the critical shear-stress that may always be varying with the flow. This parameter considers one fixed value for the beginning of motion.

Regarding this, some studies need to be taken into account and will be used to compare the laboratory results of the critical velocity, which will be analysed in Chapter 4 – Experimental Work.

Neil (1967)

$$\frac{U_c^2}{\sqrt{\left(\frac{\gamma_s}{\gamma_w}-1\right)\times g\times D_{50}}} = 2.5\times\left(\frac{d}{D_{50}}\right)^{0.2} \tag{2.8}$$

Garde (1970)

$$\frac{U_c}{\sqrt{\left(\frac{\gamma_s}{\gamma_w}-1\right)\times g\times D_{50}}} = 0.5\times log\left(\frac{d}{D_{50}}\right)+1.63 \tag{2.9}$$

Goncharov (1964)

$$U_c = log\left(8.8\ \frac{d}{D_{50}}\right)\sqrt{\frac{\left(\frac{\gamma_s}{\gamma_w}-1\right)\times 2g\times D_{50}}{3.5}} \tag{2.10}$$

2.1.7 Flow around a Monopile foundation

When a flow finds an obstacle in its way, there are some changes that occur to it and new patterns are assumed by the flow streamlines. Through this, several studies explain these changes, e.g. Breusers & Raudkivi (1991) and Sumer & Fredsøe (2002) divided these changes in four steps considering a vertical pile in sea bed. These changes are described in following sub-chapters and are:

1. Downflow;
2. Horseshoe vortex;
3. Lee-wake Vortex;
4. Streamline contraction.

Figure 2.4 taken from De Vos (2008) provides an outline of these features

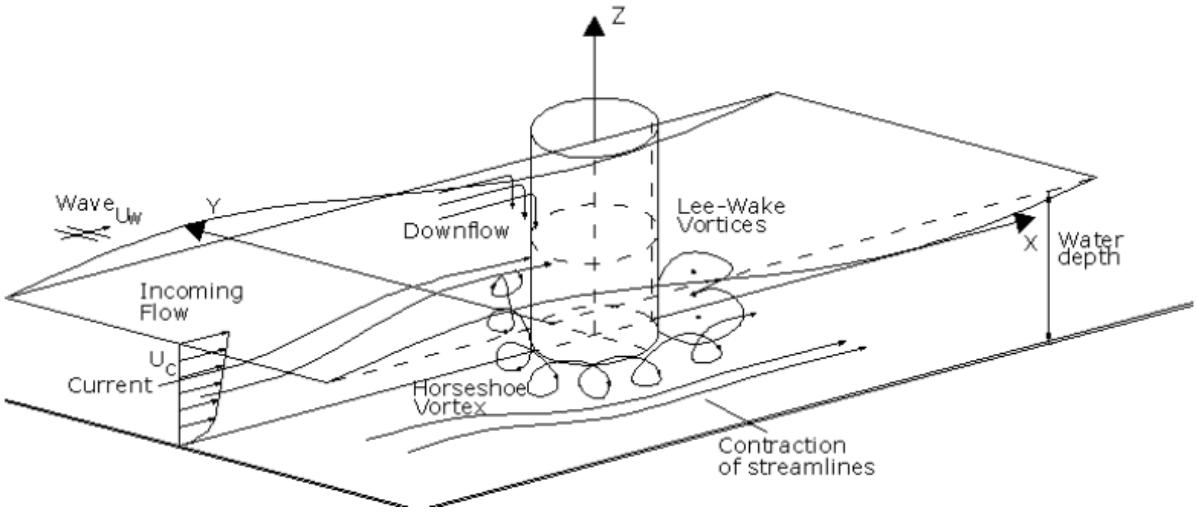

Fig. 2.4 – Definition sketch of the flow-structure interaction for a vertical pile (De Vos, 2008).

2.1.7.1 DOWNFLOW IN FRONT OF THE PILE

The downflow occurs when the flow comes to rest at the front of the pile (De Vos, 2008). With this, the velocity and the stagnation pressure decreases creating a downward pressure gradient (Breusers & Raudkivi, 1991). This gradient leads to a downward movement, which increases the turbulence in the foundation's vicinity. Higher values of turbulence generate higher shear stresses that ultimately contribute to the scour process.

2.1.7.2 HORSESHOE VORTEX

The horseshoe vortex is one of the main phenomena that occurs in sediment transportation and it is according to Whitehouse (1998) the major mechanism that leads to scour around monopiles.

It is formed by the rotation of the incoming flow and its development is due to the separation of the flow at the upstream edge of the scour hole (Breusers and Raudkivi, 1991).

Through this, several vortices are generated developing the scour hole and increasing the bed-shear stress, which leads to the sediment transportation. This amplification is extremely important.

A description of this scenario is represented in figure 2.5, taken from Whitehouse (1998).

Understanding this concept is extremely important and despite this brief introduction to the concept, a few literature is recommended. Whitehouse (1998), Sumer (2002) and De Vos (2008) are the most important because they explain in detail the influence of the boundary thickness, the KC number, and other important parameters. They will be also referred in this dissertation.

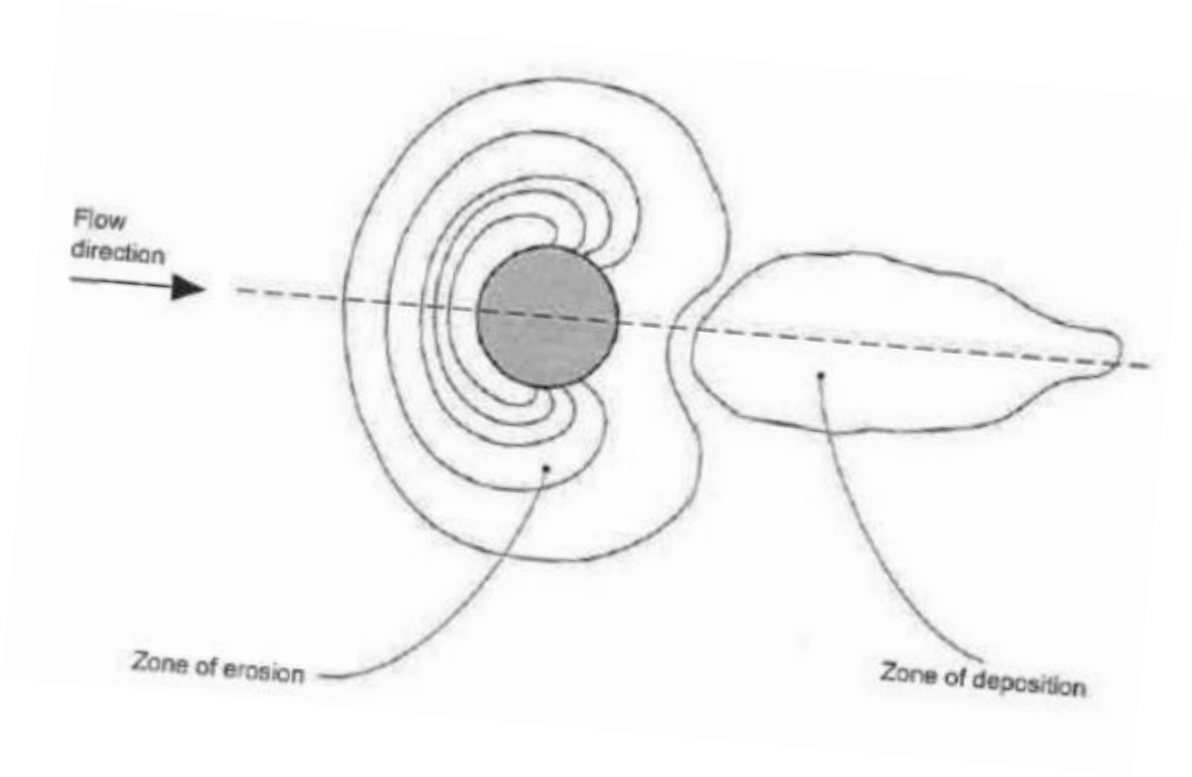

Fig. 2.5 – Characteristic equilibrium scour hole pattern for a vertical cylinder in a steady flow (Whitehouse, 1998)

2.1.7.3 LEE-WAKE VORTEX

Another important concept is the lee-wake vortex. This occurs on the lee side of the pile and is another mechanism that leads to scour phenomenon.

According to Fazeres-Ferradosa (2016), this can be described as the separation of the flow due to the presence of a pile, which leads to a rotation in the boundary layer over the surface of the pile creating vortices. The presence of these vortices creates fluctuations in the flow velocity and it also increases turbulence.

This leads to an increase of the bed shear stress like in horseshoe vortices and the sediments can be moved. These sediments accumulated as seen in figure 2.5, at the deposition zone. Some important studies and conclusions about this theme were made by Sumer & Fredsøe (1997). They are represented in figure 2.6 and 2.7.

a) 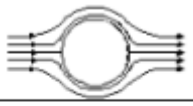	No separation. Creeping flow	$Re_D < 5$
b) 	A fixed pair of symmetric vortices	$5 < Re_D < 40$
c) 	Laminar vortex street	$40 < Re_D < 200$
d) 	Transition to turbulence in the wake	$200 < Re_D < 300$
e) 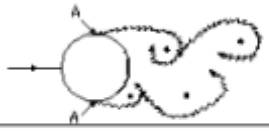	Wake completely turbulent A: Laminar boundary layer separation	$300 < Re_D < 3 \times 10^5$ Subcritical
f) 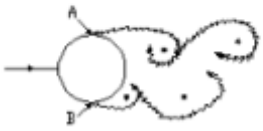	A: Laminar boundary layer separation B: Turbulent boundary layer separation: but boundary layer turbulent	$3 \times 10^5 < Re_D < 3.5 \times 10^5$ Critical (Lower transition)
g) 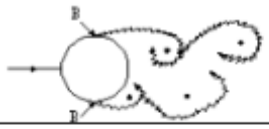	B: Turbulent boundary layer separation: boundary layer partly laminar partly turbulent	$3.5 \times 10^5 < Re_D < 1.5 \times 10^6$ Supercritical
h) 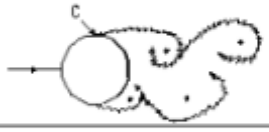	C: boundary layer completely turbulent at one side	$1.5 \times 10^6 < Re_D < 4 \times 10^6$ Upper transition
i) 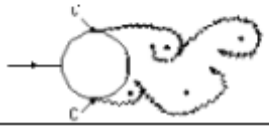	C: boundary layer completely turbulent at two sides	$4 \times 10^6 < Re_D$ Transcritical

Fig. 2.6 – Lee-wake flow regime around a smooth, circular pile in steady current as a function of Re_D (De Vos, 2008)

From this figure, the authors conclude that when the Reynolds number increases, the flow change strongly. Despite this brief information, analysing and understanding the influences of the pile Reynolds number, the pile's surface roughness, the vortex shedding frequency and other concepts is important but it is not the objective of this work to describe all of them. Sumer (2002) is recommended for more details.

Another important is that the lee-wake vortices present a huge importance when analysing oscillatory flows. In this case, the KC number has a major impact as it is represented in figure 2.7.

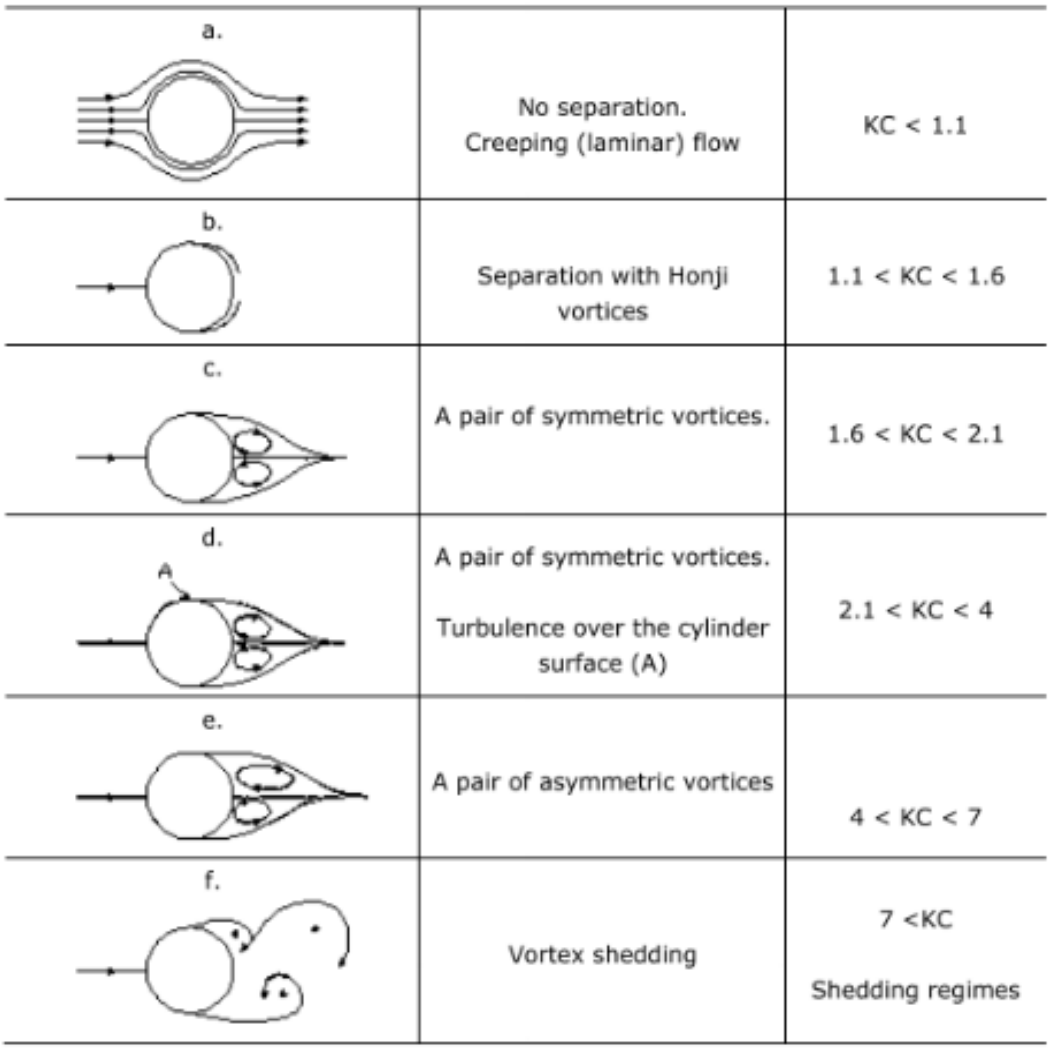

Fig. 2.7 – Lee-wake flow regime around a smooth, circular pile in oscillatory flow as a function of KC number (De Vos, 2008)

2.1.8 STREAMLINE CONTRACTION

There are two important conclusions to make when talking about streamline contraction. Their difference refers to the steady current flow or an oscillatory flow. For a steady-current environment, the amplification factor can be equal to O (10). For an oscillatory flow, this value only reaches O (4) (Sumer, 2002).

This difference is due to the stronger presence of the horseshoe vortex in the steady current situation.

2.1.9 CLEAR-WATER SCOUR AND LIVE-BED SCOUR REGIMES

When no sediment transport occurs outside of pile´s zone or near to the pile´s, this moment or phase is called clear water regime. In this moment, the Shields parameter is compared to both situations (near to pile and away from it) and in the first case (clear-water regime), some motion exists which leads to conclude that shear stress present is higher than critical shields parameter ($\theta_{cr} < \theta$). So is understandable that Shields Parameter has a larger influence in flow´s regime. Despite this, from studies of Sumer & Fredsøe (2002), when θ is too low compared to θ_{cr} there is no sediment transport.

Far from this, there is a second stage which is called the live bed regime. This one defines the moment when sediment transport is initiated over the whole bed. Sediment transport is all over the place, near and far away from piles zone. Another important note is that in theory, live bed regime stars when the values of shear stress are equal to Shields parameter. This can be understandable from Breusers & Raudkivi (1991) literature when they presented a graph where live bed regime and clear water regime are distinguished. The figure 2.8 taken from De Vos (2008), describes and compares scour depth with the bed shear stress present.

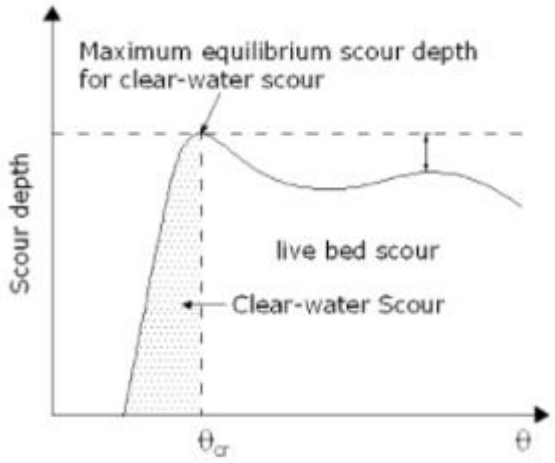

Fig. 2.8 – Scour depth vs Bed shear stress (taken from (De Vos, 2008))

Finally, Breusers & Raudkivi (1991) also conclude that the maximum equilibrium clear-water scour depth is approximately 10% higher than the mean of live-bed equilibrium scour depth

2.2 SCOUR PROTECTION DESIGN

Studying scour protection design is one of the objectives of this thesis. After introducing which are the main basic concepts related to scour and what they do, it is interesting to know how can the scour phenomena be countered the and which are the main methods to analyses the failure of such protection

As said before, studies for scour around bridge piers and its design criteria were addressed by many authors of which should be highlighted Chiew (1995), Hoffmans and Verheij (1997) and May *et al.* (2002). Their criteria only consider steady currents, however it is known, for a protection in a marine environment, a combination of currents and waves must be considered.

For this point, only recently some works have been done, Hansen and Gislason (2005), Grune *et al*. (2006), Whitehouse *et al*. (2006) and De Vos (2011) concerned this part and their studies focus on situations that both (currents and waves) occurs.

The development of a scour protection for an offshore monopile foundation still is an area that has to be developed because only a few group of researchers/engineers has the knowledge and experience to design scour protections (De Vos, 2008).

This part of the state of the art refers to the main failure problems, the needed for scour protection and the parameters that influence scour protections design.

2.2.1 NEED FOR PROTECTION

First, the need for scour protections needs to be evaluated. An analysis of costs/benefits should be always required because the structure's safety must be guaranteed at economically viable rates. In this European crisis, the costs represent always a problem when it is evaluated the reliability and importance of building any structure with Government or Stakeholder's money.

There are two different ways/alternatives for a scour protection around a monopile foundation (May *et al*., 2002):

1. Allow scour and use extra structural measures;
2. Take scour reducing measures.

A full description of these two alternatives is made in De Vos (2008), but for this work only a failure mode is studied and scour protection is a required measure. For deep studies the following works are recommended: Zaaijer and Van der Tempel (2004), Hjorth (1975), Hoffmans and Verheij (1997) and May *et al*. (2002)

2.2.2 FAILURE MODES

Chiew (1995), Sumer & Fredsøe (2002) and Hoffmans and Verheij (1997) studied mechanism of failure in scour protection around a monopile foundations. From their works, it is possible to conclude that four different failure mechanisms exist that can lead a structure to fail. These mechanisms are presented in figure 2.9 and described next:

1. Erosion of the top layer;
2. Loss of subsoil through the scour protection;
3. Edge scour;
4. Scour hole is too steep.

Only the first one will be used and studied in this thesis. The erosion of the top layer can lead to scour around the structure if the scour protection was not properly designed. The dimensions of stones around the monopile foundations have a huge importance in this theme as it will be discussed later. To distinguish between movement or no movement allowed in scour protection is always also important and needs to be taking in account

In the second mechanism, some bed material is lost through the scour protection. Sinking is a problem that can occur near to pile and the stability of the structure can be putted in dangerous. De Vos (2011) describes this mechanism as an iterative process over the time.

At the edge scour, abrupt change in roughness between the riprap and the bed can lead stones to disappear at the edge of the scour protection. This may cause security near to pile to decrease.

Last mechanism occurs when the scour hole is too steep. Flow slide may damage the scour protection from the edge (De Vos, 2011).

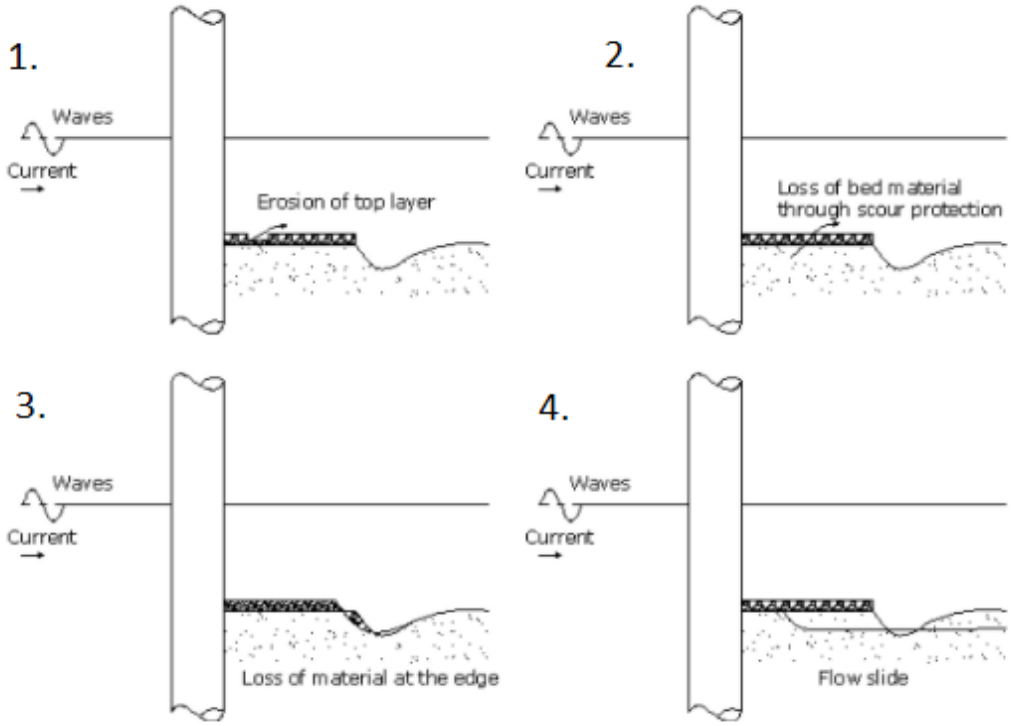

Fig. 2.9 – Mechanisms of failure (adapted from De Vos, 2011)

2.2.3 STRUCTURAL PARAMETERS

In the structural parameters, there are two important parts: the type of foundation (in this case a monopile foundation and the scour protection characteristics.

In the first part, there are two important factors in foundations, shape and size. The most common monopile foundation used are cylindrical shape. This shape is used because it minimizes the influence of the structure on the flow (Sumer *et al.*, 1997). The size refers to pile diameter, which needs to be sufficient to resist to currents and waves.

About scour protection characteristics, De Vos (2008) defines five important parameters, stone density, stone size, stone grading, stone shape and settling velocity.

The density of a stone (equation 2.18) is the mass (m) per unit of volume (V), usual used in $kg.m^{-3}$ and the common value for stone/sand is 2650 $kg.m^{-3}$.

Density stone $$\rho_s = \frac{m}{V} \quad (2.18)$$

Stone size refers to the median diameter of the stones. This characteristic is very important in the design due to its relationship to weight of the stone. Transportation of stones is very difficult to make and depending on its size and weight, transport and placement of stones in works are dependent of it. Normally it is expressed in meters and the reference value is the nominal diameter.

The size of the stones is not only important to determine the resistance against the loading condition, it also influences the bed shear-stress through its impact on the roughness, and thus influences the load on the stones as well (De Vos, 2008).

Stone size $$D_{50} = \left(\frac{W_{50}}{\rho_s}\right)^{\frac{1}{3}} \quad (2.19)$$

Related to stone grading, coefficient of uniformity was already a subject treated before in chapter 2. Its importance is enormous and it depends on D_{85} and D_{15} (eq. 2.7). It is a dimensionless value.

For last, shape refers to the form that stones fit in the protection. A sample wide grading is necessary and stones should be blocky.

2.2.4 ENVIRONMENT PARAMETERS

When talking about marine environmental, there are some parameters that are extremely important for the design of the scour protection. These parameters are current velocity, wave characteristics, sediment properties and the water depth.

The wave characteristics and water depth d determine the horizontal component of the orbital velocity U_w at the bottom, which is needed to calculate the resulting bed shear stress (De Vos, 2008).

3

RELIABILITY BASED DESIGN IN SCOUR PROTECTIONS

3.1 PROBABILISTIC CONCEPTS

3.1.1 PROBABILITY MEASURE OF RELIABILITY

When we want to quantify a certain reliability of a structure, there are some measures that need to be scrutinized. One indispensable variable is the return period. Any structure has a certain life time expected and when is designed it take into account that return period. The return period can be defined as a statistical measurement, normally based on historic data, symbolising the average recurrence interval of an event over an extended period of time (Fazeres-Ferradosa, 2016). Beside this, the return period also takes into account the variation of a certain variable with time but it does not account for the fact that a certain variable has its variability in a certain point in time (Henriques, 1998).

In any structure, the design process always involves two components, the resistances and the loads. Normally these component can be described as a function, which depends on time. From Eurocodes and other regulations, the design criteria normally used is to overrate the loads and to underestimate resistances. This creates a higher security factor and consequently more safety. However, it is know that resistance properties reduced through the time. The figure 3.1 shows this evolution through the time.

Assuming that loads and resistances have Gaussian´s distributions, analysing figure 3.1 it is to understand that despite both distributions intersect each other, the correspondent area should be small. This area represents a probability of failure that occurs when the loads are bigger than resistances. In order to have safety instead of failure, equation 3.1 should be respected. The resistance must be always higher than loads. Another form to evaluate this is from the safety factor (3.2), which are a development of equation 3.1. Safety is guaranteed when this safety factor is higher than 1. However, this value changes from structure to structure.

0

$$R(t) - L(t) > 0 \tag{3.1}$$

$$SF = R(t) / L(t) \tag{3.2}$$

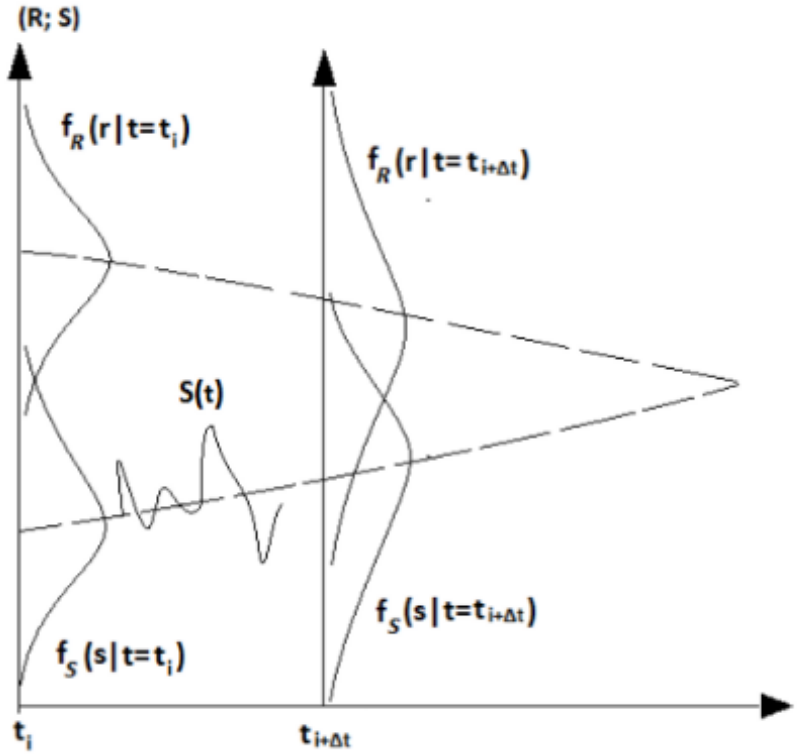

Fig. 3.1 – General reliability problem (Henriques, 1998).

When it concerns time, is known that as said before, it plays a major role. The resistance starts to decrease and loads can easily increase. The fatigue is a characteristic that influence this two variable in a negative way. It can lead a structure collapse.

According to Faber (2009), the major cause of structural failure is the occurrence of extreme events such as extreme series of waves or winds, service loads, and earthquakes. This aspect refers that the loads can reach a high level that for some structures it is not reliable. The risk of failure exists and this factor need to be always studied and scrutinized.

3.1.2 BASIC RELIABILITY PROBLEM

Any reliability problem considers two variables, the resistance (R) and the load (L). For the proposes of reliability problem, they need to be defined as a probability density function which can have various distributions. These distributions are defined in the next subchapter (3.2)

According to Faber (2009), the probabilities of failure in reliability theory must be faced as nominal ones. In other words, probability of failure achieved is not the true probability of failure, instead it is a measure that also includes the lack of knowledge about a structures' performance and the true probability of failure is impossible to achieve since uncertainty is always present.

Through this, it can be defined an important term, probability of failure. This concept can be well defined as the probability that a failure occurs in a specified interval (time).

The function that defines and generalizes the probability of failure is equation 3.3.

$$P_f = P\ (G\ (R;\ S) \leq 0) \tag{3.3}$$

When the function G is equal or lower than the 0 value, a failure of the structure can occur. This function is normally referred as the performance function but some other authors like to described it as limit state function. From one side, it is understandable that this function is no more or less that a performance situation (good and bad performance according to the value comparative with 0 of the function). However, in common lectures and literature relative to civil engineer field, the term limit state function is used more often.

In this thesis the probability of failure is related to a fail by a mechanism (the erosion of the top layer). The resistance forces can be shown by the shields parameters and for the loads, an equation from De Vos (2011) laboratory result will be used. This information is described later.

For a more detailed information about reliability problems and its mathematic background applied to hydraulics problems, including offshore structures, a full review of Reeve (2010) is recommended.

3.2 PROBABILITY DENSITY FUNCTIONS (PDF´S)

A probability density function can be described as the relative likelihood for a random variable to take on a given value. In this chapter, a brief view of some distributions is made to understand them and for later choose in chapter 5. In this chapter, some distributions will be defined to represent the behaviour of the variables related to design. The probability functions will be used to define every possible value correspondent to a situation and calculate its probability which is indispensable for the calculation of the performance function

3.2.1 GAUSSIAN DISTRIBUTION

The Gaussian function is the probability density function of the normal distribution. The normal function can be defined by a mean (μ) and variance (σ^2). This variance is not more than the square of the standard deviation. The equation that defines it is 3.4 and an example graph is showed in figure 3.2.

$$f(\mu\ ,\ \sigma^2) = \frac{1}{\sigma\sqrt{2\pi}} e^{\frac{-(x-\mu)^2}{2\sigma^2}} \tag{3.4}$$

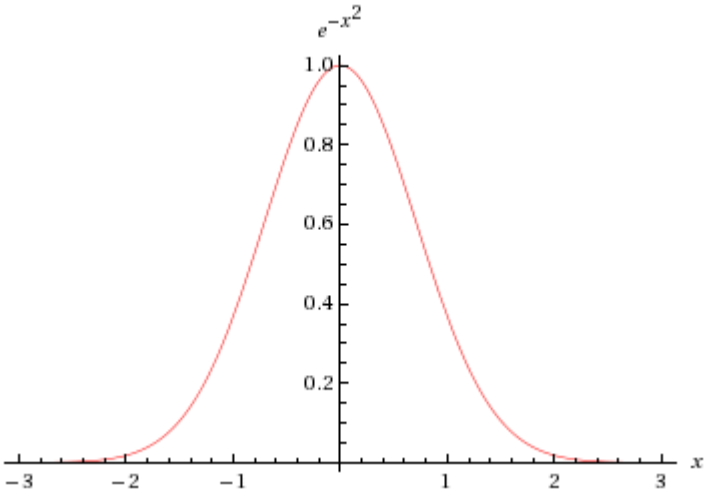

Fig. 3.2 – Gaussian function – made in Math World Website

3.2.2 LOGNORMAL DISTRIBUTION

The lognormal distribution is a continuous probability density function. To define it, the mean (μ) and the standard deviation (σ) are needed. Its relation to the normal distribution is due to the fact that if a random variable is lognormally distributed, the logarithm of the random variable is normally distributed. In this work, in the development of the algorithm, a normalization in variables is made to use in the Matlab program. The equation that defines the lognormal distributions is 3.5 and it is graph is presented in figure 3.3.

$$f(\ln x;\ \mu, \sigma) = \frac{1}{\sigma\sqrt{2\pi}} e^{\left[-\frac{(\ln x-\mu)^2}{2\sigma^2}\right]} \tag{3.5}$$

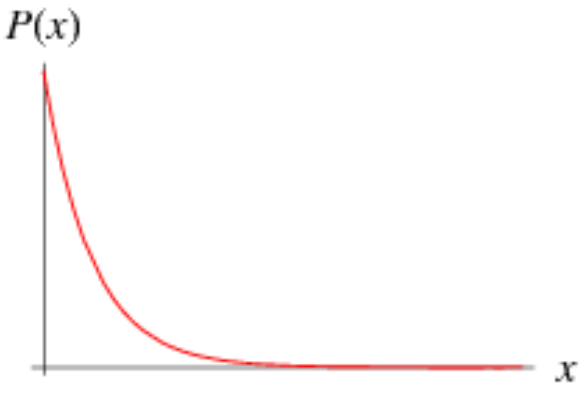

Fig. 3.3 – Lognormal distribution – made in Math World Website

3.2.3 EXPONENTIAL, WEIBULL AND RAYLEIGH DISTRIBUTIONS

These three distributions are similar from their equations type and parameters.

The exponential distribution is one of the most used distributions and is often applied to model the time elapsed between two events. It has one parameter (the scale parameter) to define it, which is related to the mean and the standard deviation. The equation that defines it is 3.6.

$$f(x;\lambda) = \begin{cases} \lambda\, e^{-\lambda x} & x \geq 0, \\ 0 & x < 0 \end{cases} \tag{3.6}$$

The Weibull distribution, in 1951was described by the Swedish mathematician Waloddi Weibull. The Weibull distribution has one more parameter (k) than the exponential distribution, which is a shape parameter. When this parameter is equal to one, the Weibull distribution is similar to the exponential distribution. The equation that describes it is 3.7

$$f(x;\lambda;k) = \begin{cases} \frac{k}{\lambda}\left(\frac{x}{k}\right)^{k-1} e^{-\left(\frac{x}{\lambda}\right)^{k}} & x \geq 0, \\ 0 & x < 0 \end{cases} \tag{3.7}$$

For last, the Rayleigh distribution is a special case of the Weibull distribution. It's commonly used in the calculation of wave parameters due to its relationship with the JONSWAP spectrum. With it, we can obtain the significant wave height and other important parameters. It has a scale parameter, which sometimes can be confused due to the use of same letter to represent the standard deviation (σ).

$$f(x;\sigma) = \frac{x}{\sigma^2}\; e^{\frac{-x^2}{2\sigma^2}} \quad x \geq 0, \tag{3.8}$$

3.3 MONTE CARLO SIMULATION

Commonly used in problems, involving probabilities density functions as referred before in this chapter, the Monte Carlo Simulation method is a technic that provides/generates random variables values following its mean and other statistics characteristics.

Its preference among others in this dissertation is due to the higher simplicity and efficiency of implementation it in a math program like Matlab. This method can solve complex problems with a significant number of basic independent variables, which have their own different distributions functions. This characteristic can be very useful for scale problems because it can work with different values from different realities instead of other methods. Furthermore, the Monte Carlo presents randomness, which plays another important role. The behaviour of values generated from Monte Carlo can be easily described and analysed.

This method is considered a Level 3 method (only for reference when consulting literature) according to Reeve (2010). This level is described as the most used method for reliability techniques.

The Monte Carlo method generates the appropriate pdf values for the limit state function. The values can be treated as being similar to a sample of experimental observations and used to obtain the sample solution (Das & Zhang, 2003).

The Monte Carlo method can be defined by the number of events that belong to the failure region, i.e. number of times that G<0, divided by the sample size. This technique is simple but there are some considerations like the sample size that need to be taken into account. The equation that defines Monte Carlo is 3.9:

$$P_f = \frac{Number\ of\ values\ in\ the\ failure\ region\ (Xn)}{Total\ number\ of\ simulations\ (N)} \tag{3.9}$$

According to Henriques (1998), when talking about the number of samples used, there are some errors adjacent to it. This is because if samples are not exact, the value obtained from it could not be exact. So obviously, increasing the number of samples improves the precision of the answer (Reeve, 2010). The author also refers that the sample size should be at least 10 times the length of return period. Other example is a recommendation from DNV (1992) which recommends for the sampling size a value equal to 100 divided by the probability of failure.

There are several methods that minimize this sampling problems such as variance reduction technique. For these problems, some literature is recommended, e.g. Fazeres-Ferradosa (2015), Henriques (2015) and Reeve (2010).

For the use of Monte Carlo method, there are different procedures that can be put in practice to analyse if the Monte Carlo is an appropriate method. Miranda (2014) refers that the minimum requirements to apply the Monte Carlo simulation method are:

1. Develop systematic methods for the numeric analysis of basic variables;
2. Select an appropriate and reliable technical simulation;
3. Consider the complexity effect of limit status performance through its own dependent variables;
4. Use an appropriate number of samples to obtain a reasonable estimative for the probability of failure.

This simple technique suggested by Miranda (2014) is also referred by himself has not an efficient method and other two methods are proposed but for the purpose of this thesis, only the simple technique is showed to introduce this them. Some literature about other methods is suggested. e.g. Teixeira (2007), Miranda (2014) and Henriques (1998).

3.4 RELIABILITY MODELLING – BRIEF DESCRIPTION OF THE ALGORITHM

The present section aims at briefly describing the algorithm developed in MATLAB software, which was used in order to obtain the probabilities of failure. Due to confidential policies of the present study, the code itself will not be presented. However, it might be checked under author's permission. Nevertheless, the arguments and calculation procedures will be explained and analysed further on.

This algorithm is based on Shields (1936) and De Vos (2008; 2011) methodology. Both theories were respectively used to obtain the resistance and the acting loads on the scour protection. In order to correctly assess the reliability of a certain scour protection, it is important to quantify the environmental

and the structural variables encompassed in the design process, as well as their behaviour within the protection's life cycle. The parameters listed in table 3.1 should be known.

Table 3.1 – Environmental and Structural parameters needed as inputs

Environmental Parameters		Structural Parameters	
Used to: define the acting loads, i.e. the shear stresses		Used to: define the resistance of the protection	
Water depth	d	Protection blocks, i.e. rock density	ρ_s
Significant wave height	H_s	Stone grading – uniformity parameter	$\sigma_D = \frac{D_{85}}{D_{15}}$
Peak wave period	T_p	Initial estimate of the blocks' mean diameter	D_{50}
Current speed	U_c	-	-

Once these parameters are defined it is important to establish how to compute the resistant shear stress (τ_r) and the acting shear stress (τ_s). As seen before the resistant shear stress can be computed according to the Shields (1936) theory, concerning the threshold of motion. This stress must be interpreted as the top layer strength against erosion. Hence meaning that no stones/blocks are dragged away from the armour layer.

In order to obtain this, equation 3.9 can be used (Shields, 1936), where $s = \frac{\rho_s}{\rho_w}$

$$\tau_r = \theta \times \rho_w \times g \times (s-1) \times D_{67.5} \tag{3.9}$$

Where θ is the associated to the Shields parameter, g is the gravitational acceleration and the $D_{67.5}$ is the blocks' dimension for which 67.5% of the stones are not retained in the sieves, i.e. the 67.5% percentile of the stones used in the armour layer.

To quantify the value of $D_{67.5}$ equation 3.10 is advised by De Vos (2008):

$$\log\left(\frac{D_{67.5}}{D_{50}}\right) = \frac{67.5-50}{85-15} \times \log\left(\frac{D_{85}}{D_{50}}\right) = 0.25 \times \log\left(\frac{D_{85}}{D_{15}}\right) \tag{3.10}$$

Typically, equation 3.9 is computed for D_{50}, there specific reasons why the $D_{67.5}$ is applied. Such explanation is further detailed in chapter 5, concerning the analysis of the algorithm results.

Briefly it can be said that the use of such diameter ($D_{67.5}$) as to do with the fact that not all blocks have exactly the same size. Therefore, some stones tend to start their movement sooner than others, a possible

way to account for such fact is to increase the diameter in Shields formula implying that a higher resistance of the protection is being required for design purposes.

Shields parameter as an asymptotic behaviour towards θ = 0.056 (Shields 1936). However, in the present algorithm a consistent value with De Vos (2008; 2011) was used.

The considered value was θ = 0.035. This is also analysed in chapter 5 with more detail. The reason why a lower value than the asymptotic one was applied is, once again, linked to the imperfect uniformity of the protection blocks. Using a lower value for the Shields parameters allows us to take into consideration the fact that smaller stones tend to move faster and sooner than the larger ones.

Considering all these arguments, the following equation 3.11 provides the outcome of the resistant shear stress, as a combination of equations 3.9 and 3.10:

$$\tau_r = \theta \times \rho_w \times g \times (s-1) \times 0.25 \times \log\left(\frac{D_{85}}{D_{15}}\right) \tag{3.11}$$

Regarding the acting shear stress, two components were considered. The shear stress on the top layer is composed by an interaction between the loads from the waves and currents combined. This interaction is a very complex one and linear sum of both terms is not possible (Whitehouse *et al.*, 2011).

The combination of these acting loads, i.e. the acting shear stresses, was assumed as in De Vos (2011). The following figure provides the regression outline made by De Vos (2008) scour tests, which were later on compared with the opti-pile project (E-connect, 2002) and gave origin to equation 3.12 in model scale 1:50, which provides the combined acting shear stress (τ_s):

$$\tau_s = 1.659 + 3.569 \times \tau_c + 0.765 \times \tau_w \tag{3.12}$$

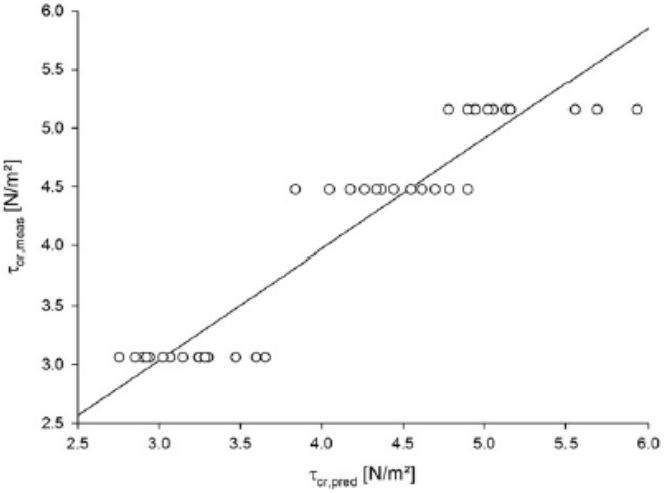

Fig. 3.4 – Scour tests data from De Vos (2008) tests, which established the correlation between the wave and currents induced shear stress

As it can be seen from the previous equation, the algorithm must also include the computation of τ_w and τ_c. This is done according to the following theories and equations stated bellow.

The currents induced shear stress is computed as in equation 3.13:

$$\tau_c = \rho_w \times f_c \times {U_c}^2 \times \frac{1}{2} \tag{3.13}$$

Where f_c is the dimensionless friction coefficient as in Liu (2001):

$$f_c = \frac{2g}{\left(\frac{\sqrt{g}}{k} \times \ln\left(\frac{d}{z_0 \times e}\right)\right)^2} \tag{3.14}$$

Note that k is the Von Karman constant equal to 0.4, z_o is the roughness length corresponding to the elevation above the bed with zero velocity, which can be obtained using Colebrook & White (1937) equation (3.15),

$$z_0 = \frac{k_s}{30}, \qquad with \quad \frac{u_* k_s}{\upsilon} \geq 70 \tag{3.15}$$

where υ is the kinematic viscosity equal to 10^{-6} (T=20 ºC) and e is the Euler's number (≈2.718).

The roughness length depends on the bottom roughness, k_s which depends on the presence of ripples. In this case, since no ripples are assumed to be present, the typical value is ks =2.5d_{50}. If ripples are present, this value is obtained as k_s= (0.5-1) Hr where H_r is the ripple height (Liu, 2001). Note that d_{50} does not concern to the armour layer, it is instead the median sediment grain diameter.

The influence of shear stress caused by the waves is obtained similarly to the currents one, according to equation 3.16:

$$\tau_w = \frac{1}{2}\rho_w f_w U_m^2 \tag{3.16}$$

In the waves case, the shear-stress is an oscillatory one and as an amplitude of τ_w, the f_w corresponds to the friction factor for waves flow. U_m is the amplitude of the horizontal velocity just above the bed, which for monochromatic waves, can be derived from the linear wave theory as:

$$U_m = \frac{\pi H}{T_w} \times \frac{1}{sinh\left(\frac{2\pi d}{L}\right)} \tag{3.17}$$

where H is the wave height (in this case the design wave height $H_{1/10}$=1.27H_s), T_w is the wave period and *d* is the water depth. *L* is the wave length and it can be obtained by means of the dispersion relation.

The wave friction factor can be calculated according to several theories. De Vos (2011) provides a comprehensive summary and analysis of the possible equations that can be used to obtain f_w. In the present case in order to have consistency with De Vos (2008, 2011) work, equation 3.18 was used (Dixen *et al.*,2008):

$$f_w = 0.32\left(\frac{A}{k_s}\right)^{-0.8}, 0.2 < \frac{A}{k_s} < 10 \tag{3.18}$$

where A is the amplitude of the wave orbital motion, obtained as follows:

$$A = \frac{U_m T_w}{2\pi} \tag{3.19}$$

Given all the expressions, for the waves acting loads description is then possible to combine the wave and current bed shear stress, at a prototype scale, by converting equation 3.12 from the previous scale of 1:50 to the prototype values 1:1, as it is explained in De Vos (2011; 2012). Hence obtaining the final equation 3.20 to evaluated the combined acting loads:

$$\tau_s = 83 + 3.569 \times \tau_c + 0.765 \times \tau_w \tag{3.20}$$

At this point of the algorithm all the expressions needed were gathered. However, the reliability assessment implies that the problem is stated as a typical limit state function of resistances minus loads.

This leads to the present interpretation of the shear stresses that was used in order to express the problem as a reliability one. The statically stable status of the scour protection is ensured when the acting loads are not higher than the resistant ones from Shields criterion.

Taking into consideration the equation 3.1, 3.11 and 3.20, the problem can be rewritten for a failure situation (G<0) as in equation 3.21:

$$G = \tau_r - \tau_s = \left(0.035 \times g\rho_w \times (s-1) \times 0.25 \times \log\left(\frac{D_{85}}{D_{50}}\right)\right) - (83 + 3.569 \times \tau_c + 0.765 \times \tau_w) \tag{3.21}$$

In order to assess the reliability of the scour protection, equation 3.21 must be simulated according to the uncertainty of the basic random variables, which is the same as saying that according to the parameters and variances of each variable equation *G* must be calculated several times, and then equation 3.9 must be used to obtain the final value of the probability of failure.

The figure 3.5 presents a final overall scheme of the algorithm, this matrix can be used as a procedure to perform the reliability assessment of the protection. In this scheme, steps 1 and 2 are according to De Vos (2008) procedures and step 3 corresponds to the Monte-Carlo simulations and the reliability or inversely the failure (P_f) assessment. Note that an upgrade to this process is the possibility of pre-defining a certain value of P_f and then design for a required D_{50} in terms of the top layer failure mode. This could be done by reverting the process, and having an initial estimate of the blocks' dimension. An insight on how to perform initial estimates of the mean stone size are given in Whitehouse (1998). Nevertheless, at this point, this work only aims at a probability of failure evaluation and not to the design itself.

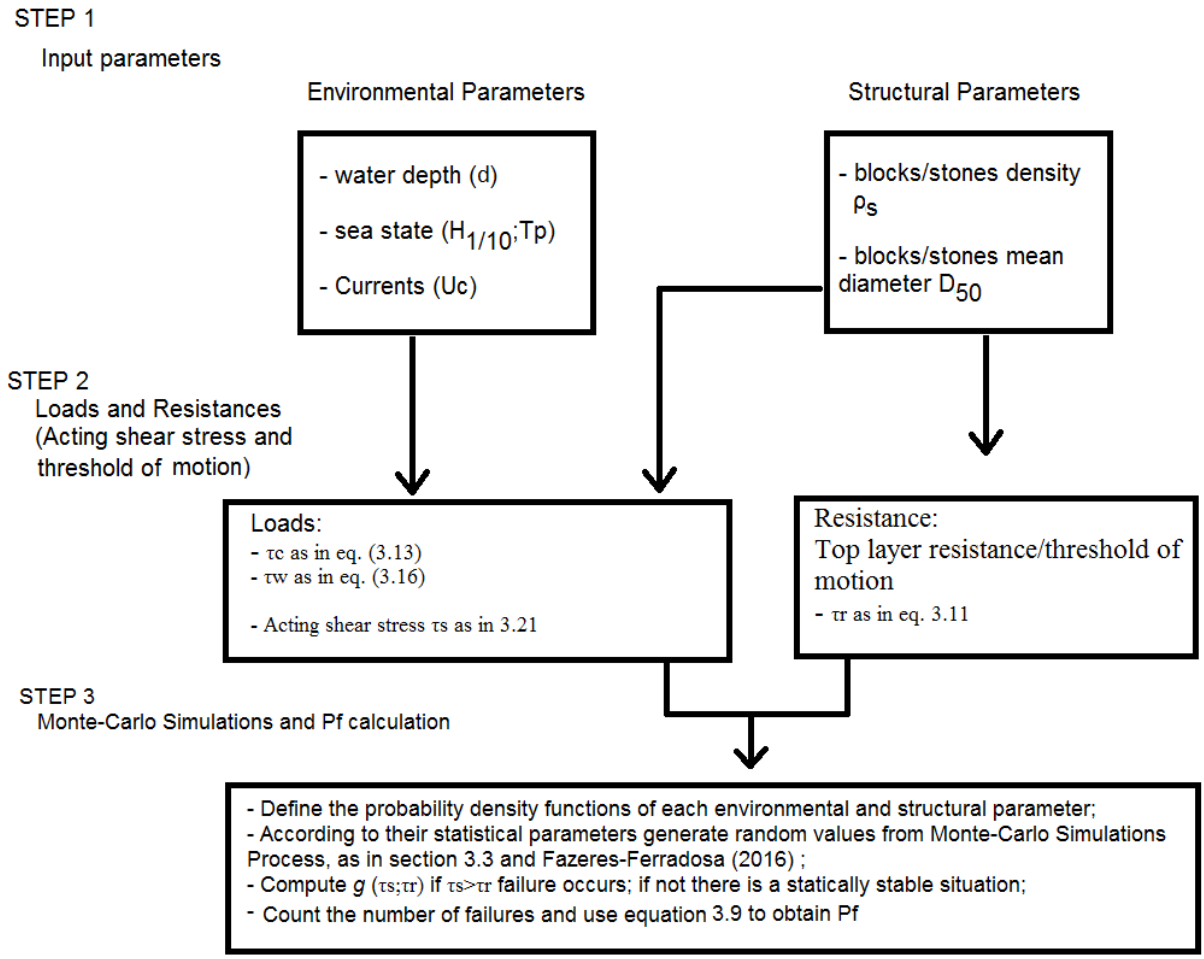

Fig. 3.5 – Final overall scheme of the algorithm

4
EXPERIMENTAL WORK

4.1 INTRODUCTION AND OBJECTIVES

The experimental work is an important subject and plays a major role in this thesis. As said before, this thesis evolves two different works: an experimental work and a reliability study.

This chapter is divided in various phases. The first part introduces scale and modelling considerations which need to be taken to understand some problems due to laboratory facilities and other components. The Froude number is approached and some conclusions are important for the laboratory setup.

In the laboratory setup, a full description of the two experiments is done. The first was made in a flume and the tests intended to the critical velocities in a sea bed. A representation is fulfil described and some formulas recommended in the State of the Art regarding this theme are calculated. In the second part, the tests are carried out in the wave tank which are the most important to this dissertation. This kind of tests try to evaluate the scour around a monopile foundation and measuring it which is one of the main objectives purposed.

This chapter provides the details of the physical modelling performed and analyses the r8esults obtained.

4.2 SCALE CONSIDERATIONS

To represent the real situation – prototype – a model at a different scale depending on circumstances and resources plays a major role in design of structuresThe objective of a physical model is to approximate it to the real situation and when its simulated, the similarity between the prototype and model can be described by non-dimensional parameters (Fazeres-Ferradosa, 2016).

Taking this knowledge, is understandable that not always every scale parameter can be accomplished due to dependencies between them. Concerning hydraulics, some non-dimensional parameters and its formula are:

Froude Number $$F_r = \frac{U}{\sqrt{g\ d}} \tag{4.1}$$

Reynolds number $$R_e = \frac{U\ D}{\nu} \tag{4.2}$$

Strouhal number $$S = \frac{L}{U\ T} \tag{4.3}$$

Euler number $$Eu = \frac{P}{\rho\ U^2} \tag{4.4}$$

According to De Vos (2008), the two important simulate criteria for waves and currents in a laboratory facility are the Froude and Reynolds numbers which need to be preserved. Despite this, it is known that is impossible to maintain both when a model is made at scale due to the geometric parameter, the length.

Concerning this, it is recognized that for scaling hydraulic models, the choose follows on the Froude model law, where prototype and model have both the same Froude number (Hughes, 1993). Despite this, the Reynolds number represents a status that can't be ignored due to its relationship to viscosity. Viscosity problems are important in an experimental work but Hughes (1993) recommends ignore viscosity effects when the Reynolds number is equal or greater than 1.104.

The basic concept of scale parameter, N, is defined in equation 4.5. This is no more than the connexion between the prototype value of any variable($X_{Prototype}$) that need to be considered and the model value (X_{Model}).The division remits to the scale parameter as it is showed next.

$$N = \frac{X_{Prototype}}{X_{Model}} \tag{4.5}$$

Considering now the present case, we have five different variables that need to be defined: water depth, current velocity, wave height, period and pile diameter. Regarding this, since the Froude number was chosen to represent similarity, we know that the length scales it is our real scale (this means that if we have a pile with 1 meter and we want to represent it in the model at a scale of 1:10, the model should have 0.1 meters). Due to this and developing and working in Froude law, we can get the other scale parameters for the other variables. These relations are presented next:

Length Scale	N_L	(4.6)
Velocity Scale (Currents	$N_U = \sqrt{\frac{N_\gamma N_L}{N_\rho}}$	(4.7)
Period Scale (Wave Peak Period)	$N_p = \sqrt{\frac{N_L\, N_\rho}{N_\gamma}}$	(4.8)

All variables can be now correctly defined to be used in the physical modelling.

After this brief introduction to the main scale parameters, it's now to understand the laboratory/physical modelling. This modelling represents one of three different techniques that coastal engineer use to understand the complex of flow regimes that often exist around coastal structure (De Vos, 2008).

Despite the advances in numerical modelling (other technique), a small scale laboratory physical model is the most reliable method to design and test most of coastal structures. Compared to field measurements (last technique), a small scale laboratory also presents better reasons to be implemented. The costs are lower which make it a better choice (Hughes, 2003).

In this thesis, a physical model was used to attempt and test a random case. The conditions are referred later in this chapter but it's important before making that future choices, considerer and refer this considerations and effects.

The model can have several problems due to incorrect reproduction of prototype. A list of this main problems in a scour protection around a vertical pile in a two-dimensional wave flume and some possible solutions are listed in De Vos (2008) based on Whitehouse (1998), Hughes (1993;2003), Kortenhaus *et al*. (2005) which are presented in the next table. This table shows in the left part the major problems mentioned from these authors and in right, some conclusions and improvements. It's also important to note that in the experimental work of this dissertation, it was used a large wave tank, not a wave flume but for similar considerations the studies from these authors can be usefully.

Table 4.1 – Problems in a wave flume and possible improvements

Problems	Improvements and Conclusions
The generation of unintentional non-linear effects caused by the generation of waves and currents	Generating higher order waves can be an improvement
The generation of unidirectional waves	It is known that wave can have multiple directions, like current. Some tests with different waves directions can be done to test if it can improve
The reflection and re-reflection of waves in a wave flume	This type of problem can occur at a small scale facility. It is a hard and complex problem because it cannot be quantified. In this thesis the paddles from wave generator can also absorb waves.
The influence of the side walls on the waves	No influences regard this subject but a more deeply study to analyse its influence needs to be performed.

Other facts can also be referred but for wave tank there is no great importance on them, being the last mentioned the most important. It is to conclude that models effects can represent an important role in the correct design but the scale effects play the major role.

4.3 PRE-LABORATORY SETUP

As said before, this works has two different approaches that need to be mentioned: tests in the flume and tests in the wave tank.

Before going to the test, some preliminary assumptions need to be referred such the scour protection materials. Section 4.3.1 presents an introduction to the materials that will be used in this work. This is extremely important to measure and define.

4.3.1 SCOUR TEST MATERIALS

A. Seabed material

Any scour study/problem in marine environment has characteristics to be taken in account. First, we have the sea bed. The seabed's presents different sediments gradations. For this study, it was used a sand offered from the LHEC which needed to be sieved to know all characteristics. To do this, consulting the Material Section of Civil Engineer Department was useful, and a full analysis with sieves. It's important to notice that all this work was made with the help of a civil engineer that works in the referred section which provided all resources and explained all the norms that were need to be used and satisfied. In Portugal the analysis of sediments uses the NP 1379 norm and it was satisfied. With a sample scrutinized of 310.5 grams, the sieved was completed and the grading curve was constructed and the values that was used are presented next in figure 4.1 and table 4.2.

Table 4.2 – Full description of Seabed Sand

Sieve Aperture (mm)	Restrained mass (g)	Retained (%)	Accumulated Restrained (%)	Passed Accumulated (%)
4	0	0	0	100
2	0	0	0	100
1	0	0	0	100
0.5	0.5	0.16	0.16	99.84
0.25	161.3	51.95	52.11	47.89
0.125	145.3	46.80	98.9	1.10
0.063	3	0.97	99.87	0.13
P	0.4	0.13	100	0

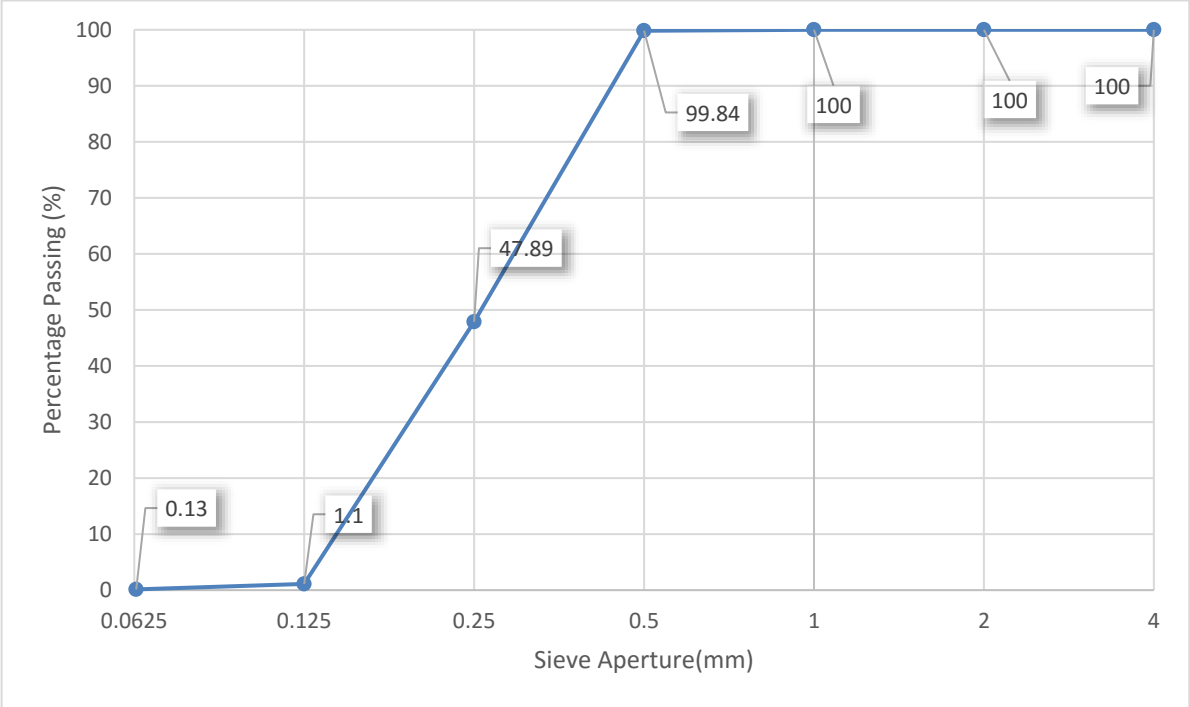

Fig. 4.1 – Grading Curve for Seabed Sand

B. Filter Layer – Sand (0-4mm)

Any scour protection has at least two layers has said before. The filter layer and the cover layer. This filter layer has importance due to its function in the protection which is to prevent the underlying soil layers from being washed out through the pore structure of the protective layers. This primary function is referred in Schürenkamp *et al. (*2012) and they also refer that the filter layer can substantially contribute to dissipate pressure. With this characteristic, when comparing to geotextile filters, granular filters are often preferred (CEM, 2008).

Another important concept and definition to the filter layer are its hydraulic and geometric characteristics. Regarding this, no study was pre announced or done due to not so large amount of resources, but for future works this analysis is recommended. Also consulting other literature is suggested, e.g. Hoffmans (2008) and Schürenkamp *et al. (*2012).

Through this, the choice from the resources available was sand with a size between 0 and 4 mm which were full descripted by the manufacture and the Materials Laboratory of Civil Engineer. With a sample size of 591,3 grams, the grading curve (figure 4.2) was provided and the retained mass and other characteristics are scrutinized in the table 4.3.

Table 4.3 – Full description of the filter layer (Sand 0-4 mm)

Sieve Aperture (mm)	Retained mass (g)	Retained (%)	Accumulated Retained (%)	Passed Accumulated (%)
8	0	0	0	100
6.3	0.6	0.1	0.1	99.9
4	13.1	2.22	2.32	97.68
2	64.3	10.87	13.19	86.81
1	167.9	28.4	41.59	58.41
0.5	189.9	32.12	73.70	26.3
0.25	101.8	17.22	90.92	9.08
0.125	45.8	7.75	98.66	1.34
0.063	6.2	1.05	99.71	0.29
P	1.5	0.25	99.97	0.03

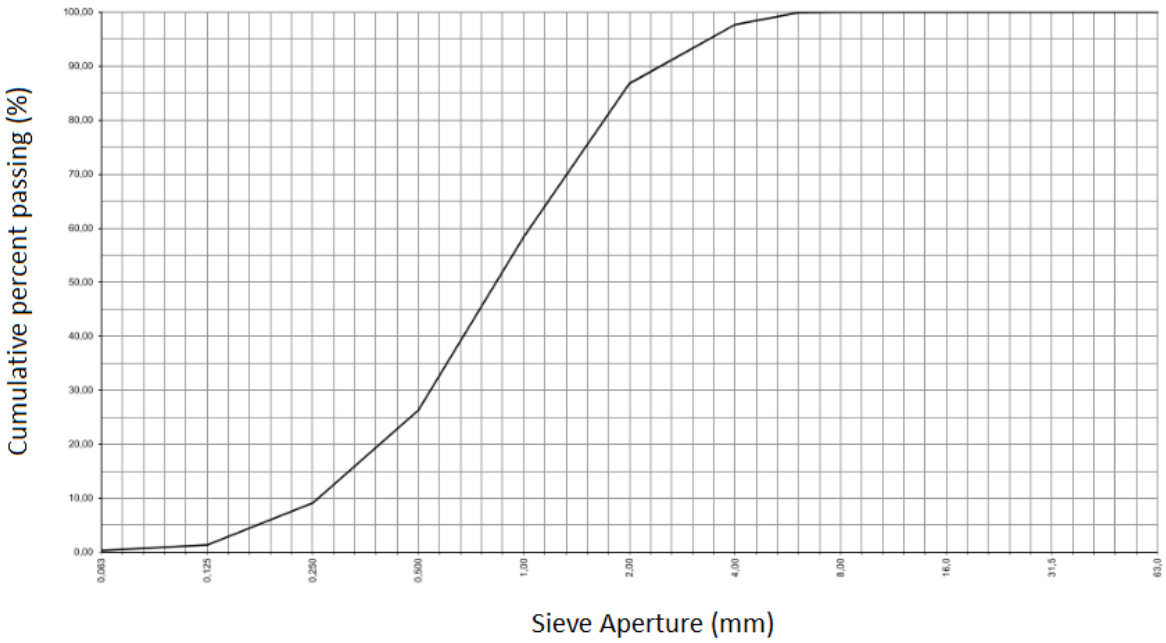

Fig. 4.2 – Grading Curve for the filter layer (Sand 0-4 mm)

C. Cover/Armour Layer – Gravel (4-8mm)

The cover is the most important part of a scour protection because it represents the stabilized/resistant forces that counters the sediment transport. The cover layer diameter is related to the Shields Parameter and is one of the main parameters to evaluate in this work and the erosion of the same can lead our structure to fail. Regarding this, it is also important to notice that with higher dimensions, higher will be the resistance since larger stones are harder to be dragged (De Vos, 2011).

For this experimental work, the objective was to use an armour similar to real situations but the resources available were limited and a gravel with a larger size was used. This was the best option with such resources but for future works, a gravel with a large grading curve – σ_s equal to 2.5 at least – and a lower size will be a better option to test failures and the scour phenomena. Despite this, this study was made with this gravel with a median size between 4 and 8 mm. It was scrutinized by the Materials Laboratory of Civil Engineer with a sample size of 947.1 g. The grading curve is represented in figure 4.3. This curve is constructed taking into account the distributions of mass retained in sieves which are represented in table 4.4.

Table 4.4 – Full description the cover layer (Gravel 4-8 mm)

Sieve Aperture (mm)	Restrained mass(g)	Retained (%)	Accumulated Retained (%)	Accumulated Passed (%)
12	0	0	0	100
10	5.9	0.62	0.62	99.38
8	46.8	4.94	5.56	94.44
6.3	177.8	18.77	24.33	75.67
4	600.3	63.38	87.71	12.29
2	102.4	10.81	98.52	1.48
1	6.5	0.69	99.21	0.79
0.5	1.9	0.2	99.41	0.59
0.25	1.2	0.13	99.54	0.46
0.125	1	0.11	99.65	0.35
0.063	1	0.11	99.76	0.24
P	1.3	0.14	99.9	0.1

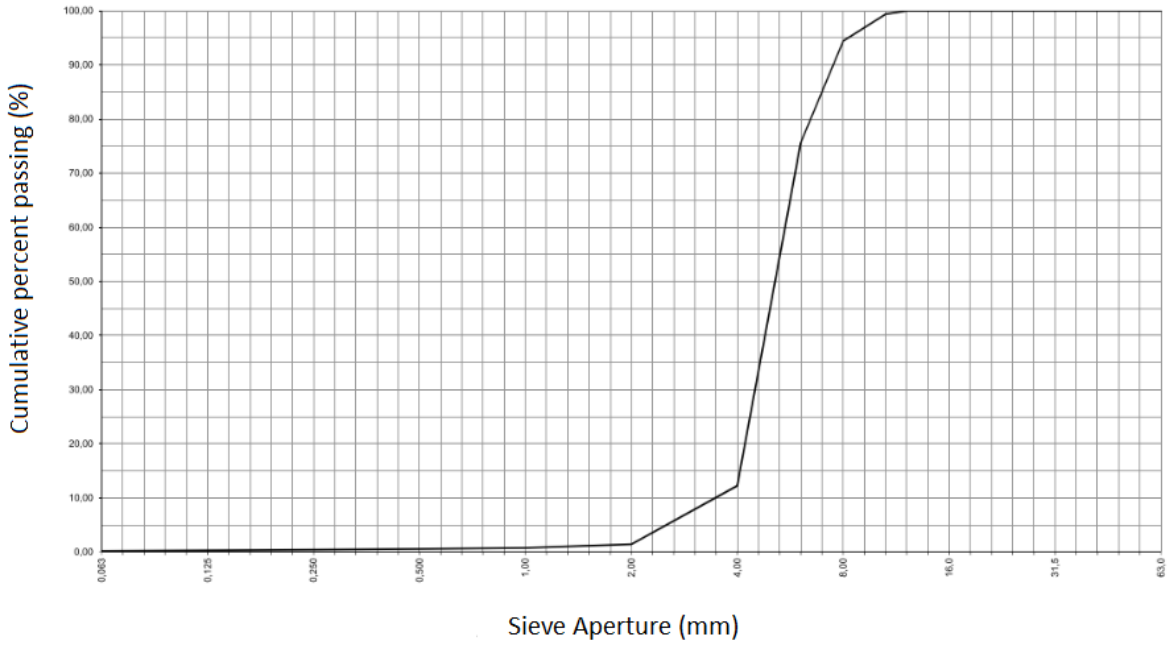

Fig. 4.3 – Grading Curve for the cover layer (Gravel 4-8 mm)

4.3.2 MEASURING EQUIPMENT

For the experimental work, three different measuring equipment were used: a 2D Bed Profile System, an ADV and Wave Probes connected to a computer.

First, the 2D Bed Profile System is an equipment that measures and describes a profile of any surface. It contains a probe that measures the distance between a zero point (starting point) and the bottom of a surface with a horizontal step that can be programed. This equipment can make 2D profiles with a good accuracy, which is extremely important for the purposes of this experimental work, which is a measure of the scour depth. Despite these good characteristics, in this experimental work the equipment was not working well enough to trust 100 per cent in the results of it, which led to the use of other equipment to measure depths. In future works this will be mentioned as an urgent problem to solve. In figure 4.4 the equipment is presented.

Fig. 4.4 – 2D Bed Profile System (HR Wallingford)

With that difficulty, a solution was needed and delegated to the ADV. The ADV (Acoustic Doppler Velocimetry) is an equipment that records instantaneous velocities with a relatively high frequency based on Doppler effect. This equipment was designed by Nortek AS and the model is Vectrino. This velocity measuring device had a maximum output rate of 200Hz and could take measures until 4m/s. with an associated error of ±0.5%.

Despite the fact that the main objective of an ADV is recording velocities, it can also measure distances with a great accuracy and through this it was chosen to make the depth measures in the scour tests. The fact that it only measures variables on a single point lead to a careful transportation through the profile of the equipment. This subject will be treated later when the bed profile measurement is referred and calculated and a full description of movements and other characteristics will be described. The figure 4.5 is a photo that represents the ADV used in this dissertation to measure distances.

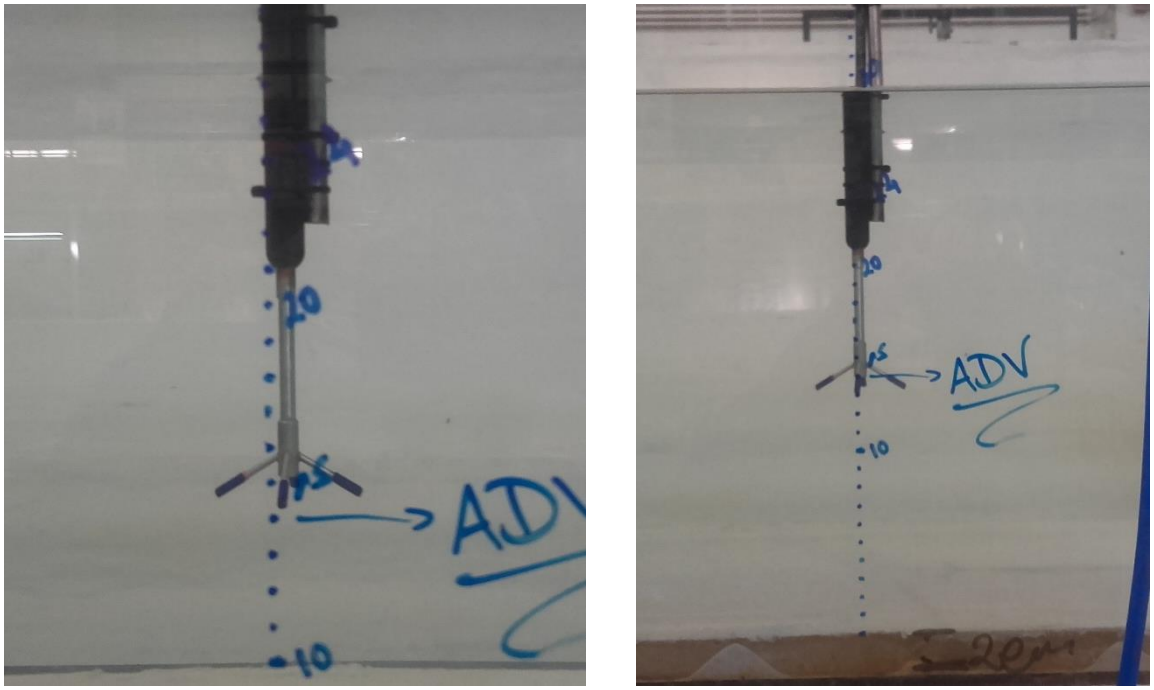

Fig. 4.5 – Acoustic Doppler Velocimetry (ADV) used

The last equipment used were the wave probes which are connected to the acquisition component. The objective of using such equipment is to verify if all conditions pre-stated in laboratory test are correct and if not, introduce a correction factor. The characteristics related to the waves such as wave height or wave period need to be correctly used and scaled in tests and the Probes can verify it. The figure 4.6 shows the probes used which were five of them.

The five probes were used to ensure that the waves characteristics were according to the target values across the flume´s length.

Fig. 4.6 – Wave probes used

4.4 Laboratory setup, Experimental Results and Discussion

After this introduction to the laboratory instruments and some considerations, the experimental work can be now presented. First the preliminary evaluation of the critical velocity will be made in a flume to take some notes and to understand it and obviously it relation to the Shields Parameter. This experience is only to understand the behaviour of sediment transport over currents. After that we can go to the wave tank and perform scour tests which are the main and most important part of this experimental work.

4.4.1 Flume Tests – Preliminary evaluation of the critical velocity

To perform this kind of tests, a flume in the Laboratory of Hydraulics was used. The figures 4.7, and 4.8 represent it which has 17 m of length, 40 cm of width and 50 cm of height. The channel is horizontal and its slope can be changed (0 degrees in this work). Has glass walls covering it and its supporting structure is made of stainless steel.

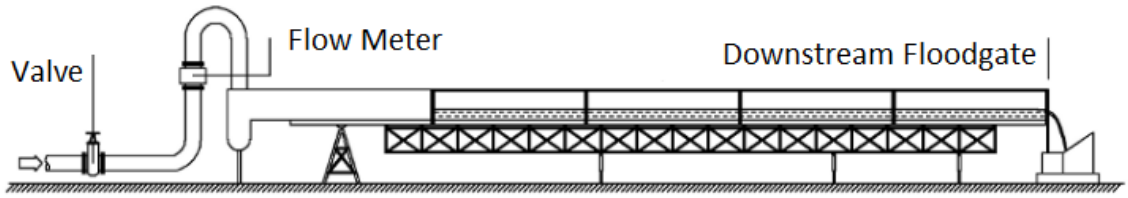

Fig. 4.7 – Flume scheme (adapted from SHRHA)

Fig. 4.8 – Flume to perform velocity tests

To perform this tests other important arrangement was needed in the downstream side of the flume. A retention box to contain sediments was constructed to prevent some problems that could occur in the hydraulic circuit (the pumps could be obstructed and be permanently damaged).

A false bed with a length of 5 m was built to place the sand due to the length of the flume. This false bed provides a similar roughness in the flume´s bottom to correctly simulate the real conditions.

Another important note for the evaluation of these tests is the relation between the critical velocity and the present velocity.

This scenario and the moment when it occurs is too difficult to evaluate due to the difference between some particles started to move before the predicted time and others later.

Through this, the preliminary evaluation of critical velocities was made using formulas already referred in chapter 2 which are from Goncharov (1964), as cited in Fazeres-Ferradosa (2011), Neil (1967) and Garde (1970). The results of these preliminary tests are presented in table 4.5 and that presents the critical velocity for the seabed material, filter layer and armour layer.

Table 4.5 – Critical Velocities

Method	Sediment	U_{cr} (m/s)	U_{cr} (cm/s)
Neil	Cover Layer	0.6854	68.54
	Filter	0.3292	32.92
	Seabed	0.2070	20.70
Goncharov	Cover Layer	0.58155	58.16
	Filter	0.3037	30.37
	Seabed	0.1954	19.54
Garde	Cover Layer	0.7279	72.79
	Filter	0.3383	33.83
	Seabed	0.2062	20.62

From table 4.5 we can conclude that the implementation of the formulas is correctly done and that values are quite similar from different methods. This is considerable important because a bad analysis could lead to an incorrect interpretation of future results. It is understandable that the armour/cover layer has a critical velocity higher than the filter used and the seabed sediments like it should be. Most of these formulas depends on the median diameter and as described before the cover layer is responsible for the protection and therefore needs to be higher, as it is.

Regarding this, we can now perform tests in the flume. The flume contains a valve that regulates the flow that can be measured in the flow meter. A successive increase of the flow rate is made to understand when movement occurs, opening the valve with some number of rotations. In this work, the water height, the free water surface, the opening of floodgate and others characteristics were measured and are presented in table 4.7 but before this analysis, some considerations also need to be taken in account.

The sediment transport phenomena were described and clarified in five different phases that are presented in table 4.6. The first, "No Movement", refers to the case in which there is no movement of any particle. After increasing the flow rate, some few individual particles can start to move and this characterization corresponds to the Stage II. Stage III occurs when some particles, not a few, start to move but some of them also start to move, but stop when find a bigger particle that is stabilized. When all the particles start to move (only a few can stop but only for finding accumulations of bigger particles) we name it the fourth stage (Stage IV). For last, live bed regime occurs when the critical velocity or the Shields Parameter is overcome. This phenomenon was already described in Chapter 2.

The experimentation and the stages are described in the tables 4.6 and 4.7.

Table 4.6 – Preliminary Stages

I	No movement
II	Few Individual Particles Start to move
III	Some Particles Start to move (start and stop)
IV	Movement occurs
V	General movement (Live Bed Regime)

Table 4.7 – Preliminary Tests

	Valve		Floodgate	Water					
	Nº Rotations	Q (l/s)	Z (cm)	Y (cm)	L_{liquid} (cm)	L_{flume} (cm)	$y*L_{flume}$ (cm^2)	U_{med} (cm/s)	Obs
1st Test	0	0	31	29	0	40	1160	0	I
	1	0	31	29	0	40	1160	0	I
	2	0	31	29	0	40	1160	0	I
	3	1.4	31	29	0	40	1160	1.21	I
	4	5.1	28	26.5	0.5	40	1060	4.81	I
	5	10.8	28	29	3	40	1160	9.31	II
	5	10.8	28	26.5	0.5	40	1060	10.19	III
	5	10.8	23	25	4	40	1000	10.8	IV
	5	10.8	22.5	24	3.5	40	960	11.25	IV
	6	16.7	20	24	6	40	960	17.39	IV
	6.5	19.7	18	24	8	40	960	20.52	V
2nd Test	0	0	29	24	-3	40	960	0	I
	1	0	29	24	-3	40	960	0	I
	2	0	29	24	-3	40	960	0	I
	2.5	0.85	29	24	-3	40	960	0.89	I
	3	1.59	28	26.5	0.5	40	1060	1.5	I
	3	1.59	31.5	28.5	-1	40	1140	1.39	I
	3.5	3.47	31.5	30.5	1	40	1220	2.84	I
	3.5	3.47	29	29	2	40	1160	2.99	I

	3.5	3.47	26	24	0	40	960	3.61	I
	4	5.94	26	25	1	40	1000	5.94	I
	4.5	8.6	24	23	1	40	920	9.35	II
	5	11.05	26	27	3	40	1080	10.23	III
	5	11.05	23	25	4	40	1000	11.05	III
	5.5	14.37	21.5	24	4.5	40	960	14.97	IV
	6	17.47	21.5	23.5	4	40	940	18.59	V

Two series of tests were performed to analyse the critical velocity. Their difference is mainly due to the number of rotations used to allow the flow in the flume. In the first case, the step was larger because a simple analysis was the objective but through the results, the second analysis was performed to detail more the different stages that can occur and different flow conditions.

An important note should be made according to the flow. The increase of flow rate if it is not slowly made, can lead our test series to fail because it can create problems in the flume like effects of reflection. To avoid this, the work was slowly made.

So, the test included two series and also two variables that can change the pattern of the flow: the flow itself and the floodgate aperture. Changing both makes our study more complete and more understandable for the many different phases. Analysing now the velocity, we can recognize that it is extremely hard to evaluate a moment that the stages turn from I to II or another change. The distinguish of these different stages is made from human eyes and as it consequence can lead to different analysis. This is a huge problem but as said before, this analysis was only to perform preliminary conclusions

The most important of them is the transition between the IV and the V stage which lead to the live bed regime. Through the tests, a value between 17 and 18 cm/s is expected as the modification of stages.

4.4.2 WAVE TANK TESTS

A. Description of the wave tank

The experimental work of this dissertation focus in the wave tank from LHCE which is a tank with 12 m of width, 28 m of length and maximum water depth of 1.2m. This tank has two large windows, that allow the visual observation of the test outcome. At the rear end a beach with of 6 m length and 12 m wide. This equipment is composed by:

- Generator machine which is composed by two module units with 8 paddles each. These elements are moved by electric motors and incorporates an absorption of reflexion system. It allows to reproduce regular and irregular sea states.

- The unit of control of the generation machine which can acquire and analyse data. This data has its own software (HR Wallingford) and it's easy to evaluate and to transport/transform in other data type that can be readable software's.

The wave tank is presented in the figure 4.9.

Fig. 4.9 – Wave Tank from LHCE

B. Scale hypothesis

The scale used in this experimental work was 1:100. The reason to use it refers to the available resources which are limited. A brief reference to other scales should always be made such as the 1:50 or the 1:25. With a minor scale, the measures and error are less than for 1:100 and we can achieve values with more certain trust.

The table to reference and use latter in this experimental work with the characteristics of some variables are presented next. The model effects were mentioned in 4.2 and all the values are calculated using the prototype-model correct scale referred in that subchapter (Equations 4.5; 4.6; 4.7; 4.8).

Table 4.8 – Scaling Variables

	d (m)	Uc (m/s)	Irregular Waves Hs (m)	T(s)	D_p (m)
Prototype	24	1.8	5	11	5
Model	0.24	0.18	0.05	1.1	0.05

C. Characterization of the side channel

To perform the analyses of scour depth in the wave tank, it is obviously that not all the area of the tank is needed, only a few part, therefore a channel was constructed to do the tests. This side channel dimensions are 75 cm of wide, 12 m of length and the maximum level of water is the same as in the wave tank as it should be. It contains a box of sand (also created for the test) with two ramps in the upstream and in the downstream side of the scour protection The height of this box was 21 cm and ramps have a length of 1 m and height like the box of sand (21 cm) which leads to an angle of 12º degree.

Figure 4.10 presents the setup of the side channel.

Fig. 4.10 – View from the upstream

D. Currents and Waves

As explained before, when referring to marine environmental conditions, there are two important components, the currents and the waves and representing them in the laboratory at a correct scale can be difficult to perform. So, the performed tests series can be divided in the two components and treated separately before and later together.

For the generation of currents, the resources accessible in the laboratory facilities where two pumps each one with a maximum flow rate of 8 m^3/h and both submersible. To use this in the laboratory, a box with one hole before and two later was constructed. This box aims to introduces the flow in our channel for scour test (which is described in the next point). One problem arises when this is done because there is a discrepancy between the box sizes and the channel size and water depth that can chief flow itself not to reproduce well in model as it is in prototype.

The generated waves for the pre-assessment of the setup, i.e. for the present scour tests, were generated according to a JONSWAP spectrum, with peak enhancement factor (γ) of 3.3 and a T_p=1.1 s and H_s=0.05 m. Later on the DAQ suite data for waves monitoring proved that the values measured were not 100% reliable, this means that the results analysed further on in section point H and I should be interpreted within a very careful perspective.

In the preliminary test for our scour protection it was understandable that currents were not affecting at all the scour protection. No movement was reported with one pump first and later with the two and despite the fact that the main objective was to represent a similar situation to North Sea cases where the velocity from currents is not so high (sometimes it isn't even 1.5 m/s as it will be showed in chapter 5) this was not unexpected and a bad scenario for the development of experimental work. One of the main objectives was to compare the value obtained in this experimental work with other that database but with this minus characteristic the comparison is enormously rigid to achieve and it does not have scientific value. We conclude that the analyses of currents would not be appropriately due to some hitches that can be associated with scale considerations (modelling effects or scale effects). Some other

options were though but the shortage of time in laboratory leaded to leave the idea of analyse currents and waves.

So the idea become now to analyse only waves. The wave generator can generate a large cycle of waves. The characterization of the wave (length, period and other parameters) is done in the program of Sea State Generation System. There are two different programs in the system, one to generate the wave and the other to collect data. In the collection of data, every characteristic is described to compare to the want characteristics. Otherwise, simulations and series of tests are not valid if the proposed settings are not accomplished. More information about the wave characteristics is presented in the next point where a full description of setup is made including all the inputs and scale changes.

E. Monopile

The monopile plays a major role in the design of scour protections because as said before, it influences many factors connected to scour referred in the state of the art– amplification factor, horseshoe vortex's, among others)

The monopile shape also influence but in this dissertation and laboratory work only a cylindrical pile was considered. It material can influence but due to the resources available only the pile used could fulfil all parameters wanted for it. (No damage, surface treated, etc.)

Next, a photo taken from the author shows the pile used in the laboratory.

Fig. 4.11 – Physical model pile (D_p = 5cm)

F. Sediments

The sediments used in this experimental work were already referred in section 4.3 but at this point, the objective is to full understand the procedure made to sediments to use it in the experimental work. Table 4.9 presents few important notes from the sediments taken from previous figures should be constructed.

Table 4.9 – Sediments characterization (mm)

	D_{50}	D_{15}	D_{85}	D_{n50}	σ_s
Armor Layer	5.36	4.08	7.14	4.50	1.75
Filter	0.87	0.34	1.94	0.73	5.76
Seabed	0.273	0.163	0.429	0.229	2.63

After these characterization, but before the design of scour protection, an important work needs to be done: paint the scour protection stones. Painting the stones allows to a more detailed analysis after the tests, because with different colours, we can understand the amount and the direction of displacement that occurs to the stones by visual observation, which is important to this work. The colours chosen were red and blue to make it easier distinguish them and their position in scour protection is for the inside position red colour and outside blue colour. It was formed two different rings.

The painting work is showed next in figure 4.12.

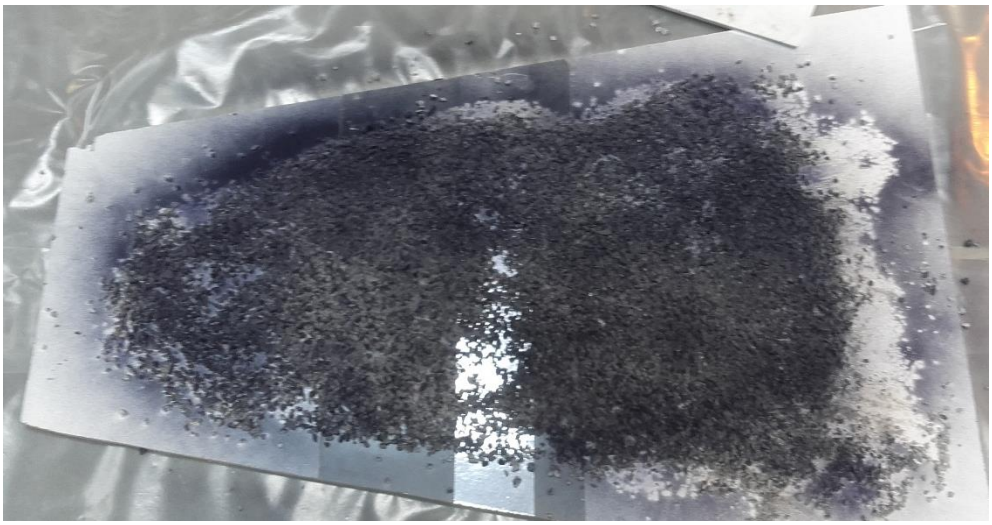

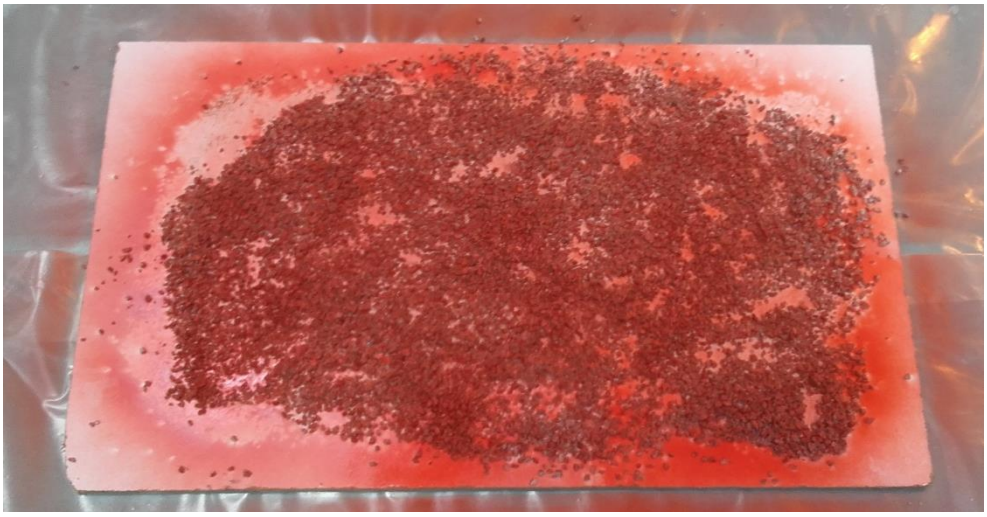

Fig. 4.12 – Painted Stone

There is still other important notes to be taken to full install our armor layer, its thickness and its diameter along the monopile. According to De Vos (2011), the thickness should be $2.5D_{n50}$ and the circle around the pile should have 5 times the pile diameter. This verification is also seen in figure 4.13 (right) and to do this, three models from cork were designed to implement the scour protection (Armor layer) and the filter layer. The diameter of such model was 25 cm ($5\ D_p$) as it can be confirmed in figure 4.13 with the ruler (the ruler show the approximately value of 10 cm). Despite the fact that photo is on 2D, the model also has the correspondent thickness (1.125 cm = $2.5\ D_{n50}$).

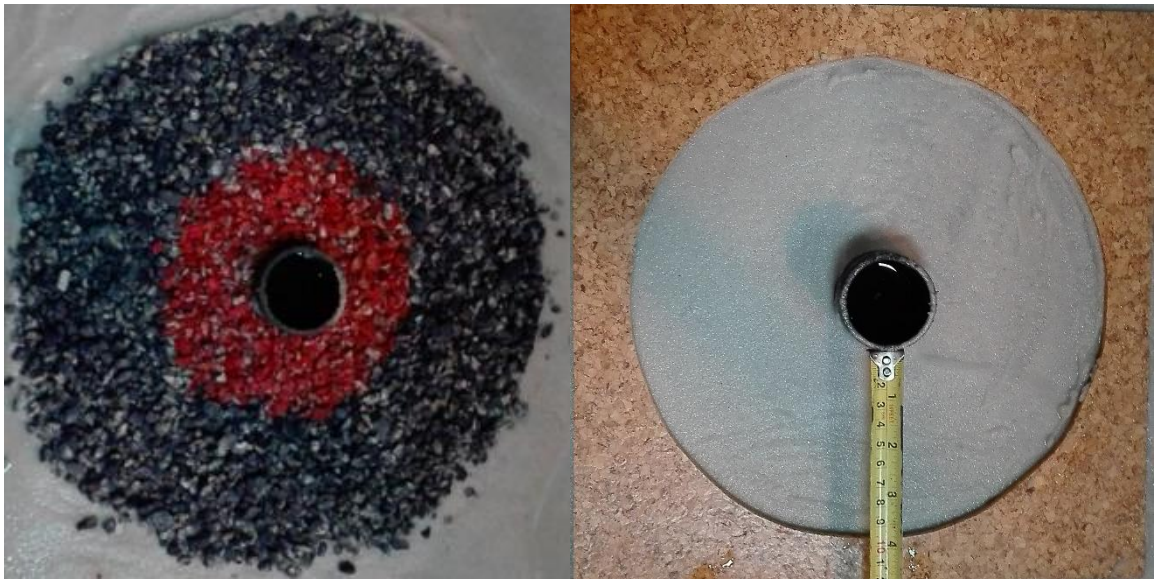

Fig. 4.13 – Coloured Rings (left) and Rings Diameter

G. Setup description

The description of the experiment setup can be divided in two different steps/processes, the pre-test arrangement and the test itself. A full description of steps is made in this point and a full test series is explained.

The steps that need to be considered in the pre-test are:

i. Fill the tank with water by opening the valve;
ii. Put the pile in bottom of the box sand;
iii. Place the sand in the box adding some water to it;
iv. Smooth the sand-bed;
v. Place the filter layer around the monopole;
vi. Add the first and second armour layer;
vii. Full fill the tank to the water level pretended;
viii. Smooth the sand bend.

After that phase, the tests can be performed by a process which is described next.

i. Calibrate the probes in our side channel by setting three different points (Y=-2; Y=0; Y= 2)
ii. Input in the HR Wave maker program the number of waves and time for the test;
iii. Start the Wave maker;
iv. Start data acquisition in the program DAQ Suite;
v. Stop the wave maker;
vi. Analyse data from DAQ Suite to check if the values input were met;
vii. Place the ADV in our side channel;
viii. Start to measure with ADV the scour depth created by wave action and construct a table with such values;
ix. Repeat all the process from i to vii if we add more cycles of waves is required/desired.

In this process, the measures with ADV need to be described because this equipment only measures the distance and velocity to a single point. With this, a matrix was created to choose the points that are measured. Steps of 2 cm were taken in X (flows direction) and in Y (perpendicular to X) steps of 5cm. The boundaries are X= [-24.5; 24.5] and Y= [-15 ;15]. The movements are described next:

i. Settle the zero values on top of the monopile – this leads to a bad measure of ADV and doesn't count for calculations;
ii. Fix the Y value.;
iii. Advance through X;
iv. Return to 0 values and move to other Y value;
v. Repeat these steps until finish the profile.

From each test series, the above mentioned steps need to be carried out. This is a long work due to the amount of time spent in the pre-test, because the fill of the tank, the drain out, the remove of the sand and do all steps over again. From each test series if the results are not the desired ones, all this work needs to be completed which leads to a constant use of the laboratory facilities that is not always available.

Through this explanation, some works were done in the laboratory to test the scour protection pre designed (assuming similar values to the North Sea). These tests are explained as follows, in points H and I.

H. First trial – Test with Scour Protection

The first test series was named a trial because there was no idea of how sediments would respond to currents, waves and other important. As said before, the currents were a problem because no scour effects were created which leaded to dismiss it. Generating waves and measure the scour depth associated to it was the objective of each test. The water depth was equal to 24 cm and wave height was set to 5 cm with a period of 1.1 seconds. According to other experimental works such as e.g. De Vos (2011) and Fazeres-Ferradosa (2015) the tests were performed in wave trains of 2000 waves, from 0 to 4000 waves.

The figure 4.14 presents the simplified profile matrix:

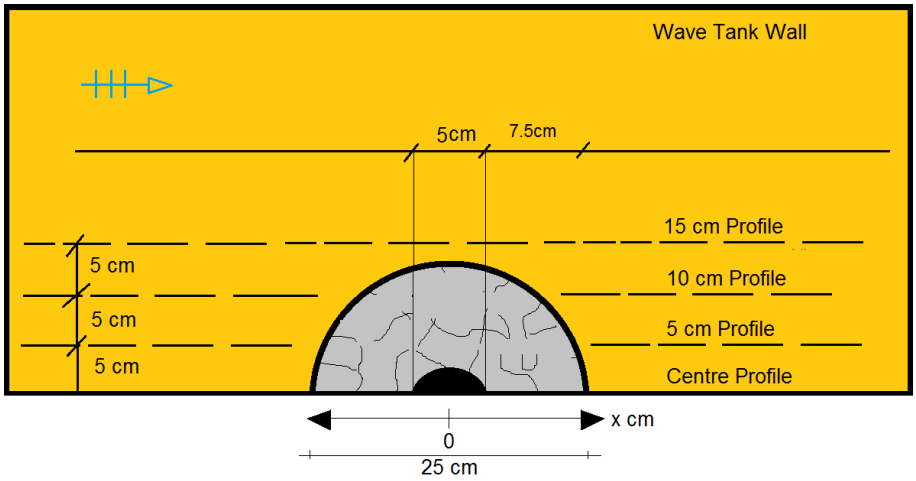

Fig. 4.14 – Simplified Profile Matrix with the centre of the pile as the *xOx* origin.

This first trial was performed with a scour protection with a thickness of 1.125 cm at model scale, i.e. 1.125 m in prototype. The grey cells on the left correspond to the protection zone. Several profiles were taken, although as it will be discussed in chapter 5, the most severe scour depths tend to occur near the central profile, aligned with the currents and waves direction.

Therefore, the discussion hereby presented will mainly concern to this profile only, future work should also consider a deeper analysis of the other ones taken, eventually with a 3D comparison between the profiles for different wave series.

As it can be seen in table 4.10, in the outlined blue cells, a failure occurs at 6.5 and 10.5 cm way from the pile, respectively downstream and upstream of the pile. These locations are quite further away from the pile walls, which might be due to a misplacement of the stones, hence not being a real failure, or due to the high values of turbulence on top of the scour protection in these places.

As an overview it is obvious that some erosion has occurred, but mainly non-sufficient to expose the filter layer, despite the two values that were mentioned before at 6.5 and 10.5 cm away from the pile's centre. A particular mention must be made to the fact that the profiles were not exactly taken at the surface of the pile's walls, because the ADV and the Profiler probes are intrusive equipment which

required a 1 to 2 cm space between the pile and the first measuring point. This affects the results reading and acquisition. Further analysis is needed in order to assess the effect of this problem in the tests made.

Table 4.10 – Differences between the Initial Profile and the Final Profile (4000 waves) – With Scour Protection (cm)

Profile at Centre			
Distance (X)	**Upstream Value**	**Distance (X)**	**Downstream value**
Pile	0	0	0
2.5	-0.4	2.5	-0.7
4.5	-0.4	4.5	-0.6
6.5	-0.4	6.5	**-1.3**
8.5	-0.4	8.5	-0.4
10.5	**-1.3**	10.5	0.4
12.5	-0.8	12.5	-0.1
14.5	-0.6	14.5	-0.4
16.5	-0.6	16.5	0
18.5	0	18.5	-0.2
20.5	0	20.5	-0.5
22.5	0	22.5	-0.2
24.5	0	24.5	-0.4

The following figure 4.15 also provides a photographic record of the final feature with the pile and the protection placed before the test.

Fig. 4.15 – Photographic record of the final profile with Scour Protection

I. Second Trial – Test without Scour Protection

Due to the non-reliable values of the tests with the scour protection, another test series was done, without protection, to analyse the scour severity in terms of maximum scour depth and scour extent. This was done also to qualitatively evaluate the magnitude of the shear stress present in the combination made, between waves and currents.

All the procedures named in G point were followed, similarly to the previous test. The results of scour between the initial and final profiles are presented next in table 4.11.

Table 4.11 – Differences between the Initial Profile and the Final Profile (4000 waves) – Without Scour Protection (cm)

Profile at Centre			
Distance (X)	**Upstream Value**	**Distance (X)**	**Downstream value**
Pile	0	0	0
2.5	0.3	2.5	-0.2
4.5	0.3	4.5	-0.4
6.5	0.4	6.5	-0.2
8.5	-0.2	8.5	-0.5
10.5	-0.2	10.5	-0.5
12.5	-0.2	12.5	-0.5
14.5	-0.2	14.5	-0.5
16.5	-0.2	16.5	-0.5
18.5	-0.2	18.5	-0.5
20.5	-0.2	20.5	-0.5
22.5	-0.2	22.5	-0.5
24.5	-0.2	24.5	-0.5

Surprisingly, no significant scour was noticed near the upstream side of the pile. This could be due to the reading error of the ADV, which were not able to exactly ready the real scour depth at those points.

On the other side, taking into consideration the irregularity of the flow, it is not possible to confirm if the generated combination of currents and flow is correspondent to the one generated in the previous test. Therefore, this leads to the conclusion that the present setup must be improved in order to ensure the tests reproducibility. Also the wide section used for these tests (0.75 m wide and 0.24 m depth) with only one pump working at 8 m^3/h did not provide enough flow velocity for a very significant erosion.

Future works should consider the use of more than one pumps to increase the currents velocity and the acting bed shear stress.

Fig. 4.16 – Photographic record of the final profile without Scour Protection

Despite the non-trustable results another aspect can be mentioned. When the scour depth is not placed, and the pile is subjected to waves and currents combined the maximum scour depth does not occur at the centre profile (Melville & Coleman, 2000). Actually, it tends to move to a 30^{o} line (figure 4.16 shows it) on the upstream side of the pile, which is not registered by the ADV and the profiler. This could also be a reason for the apparent non-significant scour near the pile, for example at position 2.5 cm and 4.5 cm positions.

Although the scour tests did not provide the expected results and the present work was important as a first approach to combine currents with waves and adapt the existing laboratorial facilities at the LHCE. Future studies should be performed in order to improve the concepts and adaptations made in this dissertation.

Also during this work several problems were encountered in the probes to control the waves' height, for a target model value of H_s=0.05 m the probes measured 0.062 m. Such difference should also be considered, and the probes must be further inspected before future research is done.

The probes also stopped measuring during 4 other tests with scour protection. Therefore, it was not possible to use this information for this dissertation.

5
RESULTS AND DISCUSSION

5.1 CASE STUDY

To analyse and discuss results and to make conclusions, a case of study is needed and its characteristics too. In this thesis, the objective was to analyse the conditions and the factors at the North Sea.

There are a significant number of wind farms in the North Sea to choose to analyse and introduce in this chapter but only offshore fixed foundations are taken into account for this thesis.

Regarding this, Horns Rev I was chosen for his characteristics and information's availability.

Horns Rev I is an offshore wind farm located in the eastern of North Sea near to Blåvandshuk, in western coast of Denmark.

It has an area of 20 Km^2 with a distance from each turbine of 560 meters. The project started in June of 1999, but the construction of foundations only started 3 years later in February of 2002. The first power generation was made after 6 months in July of the same year.

Fig. 5.1 – Location of Horns Rev I, II and III

This offshore wind farm is known for being the world largest offshore project in 2002 and its main objective was to reduce the Danish CO_2 emissions.

It has a total of 80 turbines which are Vestas V80 with 2 MW from Vesta Wind Systems manufacturer making a total of 160 MW installed capacity and generating over than 600 000 MW.h per year.

After this construction, two other projects with the same name and both in North Sea were created.

Horns Rev II was inaugurated in 2009 with a total of 91 turbines with a 209.3 MW capacity installed and can generate 956 030 MW.h per year.

Horns Rev III is still in a phase of development and its construction is predicted over the next years. The objective is to have a total project capacity of 400 MW.

5.1.1 SUPERSTRUCTURE

The superstructure is a tower and its information is resumed in table 5.1 represented below.

Table 5.1 – Superstructure – Tower Details (adapted from LORC,2016)

Structure Type	Tubular
Structure Material	Steel
Height	61 m
Weight	160 000 kg

5.1.2 SUBSTRUCTURE AND SCOUR PROTECTION

The construction of Horns Rev I had two main phases, building the substructure followed by the superstructure.

For the first, substructure, many details are needed to be taken into account like soils parameters, wave heights and others. The focus of this thesis concerns this part, the substructure.

From data acquired from LORC website, we can describe geotechnical conditions. Horn Rev is consisted of sand, gravel, pebble gravel and stones with only few pockets of fine materials.

Related to this, the foundation chosen were monopiles (a total of 80, same number as turbines) and they were driven 25 m into the seabed. They have a diameter of 4 m and a thickness of 0.05 m. The total weight of this substructures are between 180 000 and 230 000 kg.

For the scour protection, two layers of gravel with different diameters and thickness´s were used. The first layer has a gravel diameter between 0.03 and 0.2 m and thickness of 0.5 m. The second one, have a large diameter with size between 0.35 and 0.55 m and thickness of 0.8m.

All this information is summarized in table 5.2.

Table 5.2 – Substructure (adapted from LORC,2016)

Structure Type	Steel Monopile
Foundation Type	Monopile
Filter Layer	Gravel: 0.03-0.2 m Thickness 0.5 m
Cover Layer	Gravel: 0.35-0.55 m Thickness: 0.8 m
Support Structure Description	Diameter: 4 m Thickness:0.05 m Length: 18 m Weight: 180 000 – 230 000 kg

5.1.3 DESCRIPTION OF SCOUR PROTECTION VARIABLES

To full fill the information's about Horns Rev I to work in the algorithm, there are still some few variables that need to be defined.

These variables are important to the design of scour protection and related with stress´s at it. Some of them belong and are inputs of the stabilized stress like diameter of stones and others are not stabilizing such as the wave height.

These variables and their description are listed below:

I. Water depth (d)

In Horns Rev I, the water depth is not always the same since the sea bed has a certain slope. With a distance of 17.9 km from the shore, we have three different situations: the shallow, deep and intermediate waters.

According to Nielsen *et al.* (2014) the water depth has a large variation and its values are between 6 and 13 m.

II. Wave height

The North Sea is known for not having so higher wave heights when compared to other seas or oceans.

Wave height is very important because the load stress formula presented in this thesis has a huge dependency on wave height but smaller than on the current´s velocity. Despite this, we know that from the description above the current´s velocity in the North Sea are not so high, making wave height an important part of equation.

To define the wave height, figure 5.2, taken from Nielsen *et al.* (2014), is the best option. It has the values for the significant wave height and with Rayleigh distribution we can define it. This records are between 1 March 2002 and 30 April 2005 at Turbine 44. This turbine is placed in central part of Horns Rev I with an intermediate deep.

Analysing the figure, it can be understandable that there is no high variation of the wave height. As in matter of fact, all over the farm the wave height is almost constant (Nielsen et al., 2014).

The highest value presented is 3.5 m and the most common is 1.5 m.

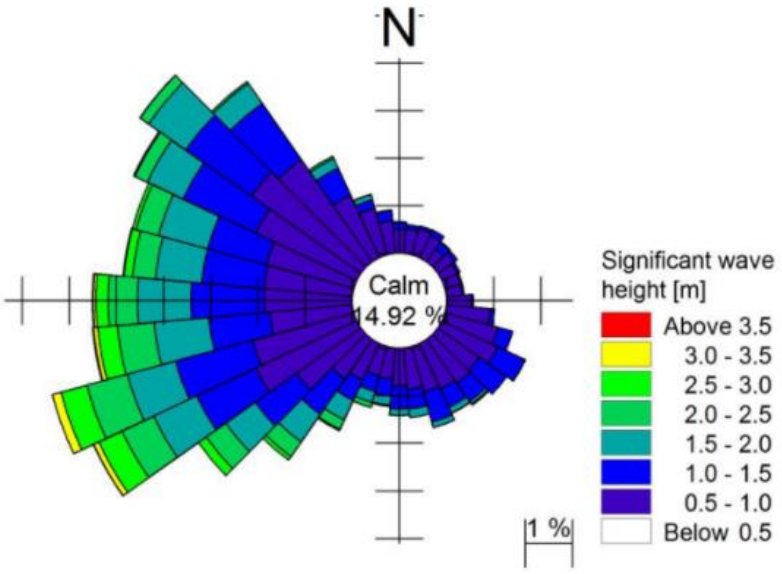

Fig. 5.2 – Wave rose for the significant wave height (taken from Nielsen *et al.*, 2014)

III. Currents Speed and Period

For velocities, Nielsen *et al.* (2014) used linear theory and based on peak period and wave height to define it. To do this, the maximum orbital velocities were measured between the same date of wave height measures at figure 5.3. A distribution was created and it is showed next and with it, the turbine 44 is again referred with its variation of velocities.

From left part of figure 5.3, a distribution of maximum orbital velocities with an interval of 0.2 m/s related to periods is done for five different turbines, each of them with different properties – water depth, location, etc.

Analysing this, it is understandable that there is no value higher than 1.5 $m.s^{-1.}$ The most mutual are lower value in the range between 0 and $1m.s^{-1.}$ Through this, the figure of current speed can be made.

At turbine 44, the values of current velocity are lower. This is good for scour protection because it is known from formula of destabilized stress´s, that velocity has a square behaviour.

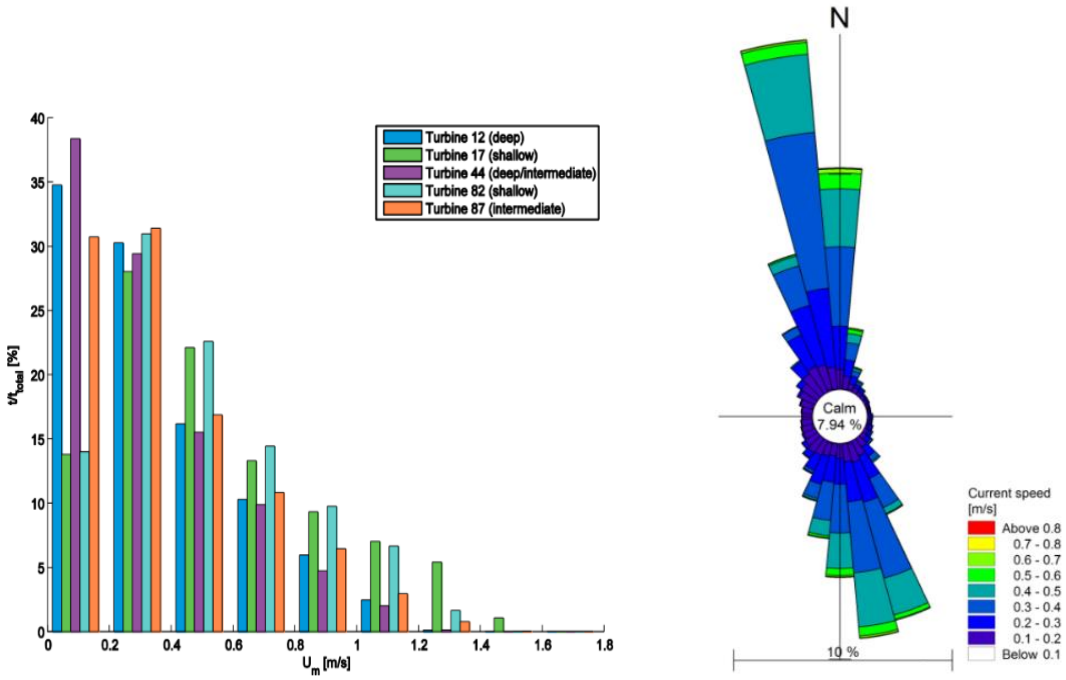

Fig. 5.3 – Distribution of maximum orbital velocities (left) and current speed at turbine 44 (right)

(taken from Nielsen *et al.*, 2014)

5.2 PROBABILISTIC DENSITY FUNCTIONS (PDF´S) – BASIC RANDOM VARIABLES

Defining every single variable and associate them with a probabilistic density function that describe its variation – mean, standard deviation and other parameters – is an extremely hard quest.

The availability of such data to characterize a variable is poor, when compared to what is needed to make statistical conclusions and approaches for rigorous studies. Such information is expensive and not always available.

With this, a problem in this thesis appeared. Statistical data for Horns Rev I is limited. Deep observations and measures are needed for a long range of time and that data was not obviously obtained.

Some papers describe some probability density functions but they are inconclusive because there is a difference in view of different authors.

In this thesis, the main objective in this sub-chapter is to define a probability density function for each variable that is desired for the limit state function – performance function. The variables were already described and its behaviour, fitted distribution and its explanation are made next to this text.

Table 5.3 – Pdf´s associated with variables

Variable	Probability Density Functions (Pdf´s)
Water Depth (m)	Normal
Wave Height (m)	Normal
Period (s)	Normal
D_{n50} (m)	Lognormal
Current Velocity ($m.s^{-1}$)	Normal

a) Water Depth

First, we have water depth. As said before, this parameter in Horn Rev I have a range between 6 and 13m. A study of the slope seabed is needed to apply and find a distribution to fit.

No scientific articles or studies were founded about this subject. Through this, assuming a linear sloping, the mean could be 9.5 m with a standard deviation of 3.5 m to full fill the range. A normal distribution is used for only having two parameters that are the easiest to access with a short list of data.

These values will be used in generation of other values knowing that a certain amount of uncertainty but future works could back fill this miss. The equation to define in algorithm is 5.1

$$d = normal\ (\ 9.5\ ;\ 3.5\ ) \tag{5.1}$$

b) Wave Height and Period

Wave height is an important variable in terms of scour protections designed (Nielsen *et al.*,2014*)*.

It is also important to refer that wave height is limited by water depth. Breaking wave criteria is one of the limitations, which means that for a confident extent of water depth, there are no breaking waves – one of the principle mechanisms of failure in scour protections.

Finding a probability density function to correct, use and predict wave heights is a complex study. Beside this, other problem appears in this section, period.

Period is related with wave height. From this point, it can be understandable that a correlation between them exists and it is important. This relation is different because it is not a direct relation.

To have such relation, observations of wave height and periods from meteorological or other institutes. For the propose of this thesis, Horns Rev I data was required, but there was no data given. With this obstacle, distributions can be not the most adequate for the careless of data.

On the other hand, information about Leixões harbour was provided by Instituto Hidrográfico Português.

LEIXOES - GLOBAL(1996-2011)

Hm0/Tp	3-5	5-7	7-9	9-11	11-13	13-15	15-17	17-19	19-21	%
0 - 1	0.4	0.6	3.1	5.3	2.4	0.5	0.1			12.4
1 - 2	0.6	3	6.5	17.4	13.3	3.2	0.9	0.2		45.2
2 - 3		0.6	2.2	5.7	11.1	4.9	1	0.1		25.7
3 - 4			0.3	1.2	3.9	3.8	1.3	0.1		10.6
4 - 5				0.3	0.9	1.6	1.1	0.1		4
> 5					0.3	0.6	1	0.3		2.2
%	1	4.2	12.1	30.1	31.8	14.6	5.5	0.7		100

Fig. 5.4 – Leixões Harbour – Significant Wave Height Vs Peak Period

LEIXOES - GLOBAL(1996-2011)

Hm0/T02	3-5	5-7	7-9	9-11	11-13	13-15	15-17	17-19	19-21	%
0 - 1	4.6	6.7	1							12.4
1 - 2	8.8	24.2	10.3	1.7						45.2
2 - 3	0.4	11.9	10	3.1	0.3					25.7
3 - 4		2	5.6	2.5	0.4					10.6
4 - 5		0.1	2.3	1.3	0.3					4
> 5			0.6	1.2	0.3					2.2
%	13.8	45	29.8	9.9	1.4	0.1				100

Fig. 5.5 – Leixões Harbour – Significant Wave Height Vs Mean Period

This two figures represent the typical data that is required to formulate a joint distribution function.

Visualizing and measuring is the work needed to perform such data but its importance is very high due to many studies and conclusion that can be made with this information.

Predictions for wave height are always being made and it is logical that from a certain amount of time, everything has an order and a distribution. Analysing such data can help to predict some phenomena that can occur.

About the function itself, it has two inputs correlated – the significant wave height and the period (peak and mean) – and an output which is the probability of a combination of both to occur.

The point of using this joint probabilistic function is that each variable can be analysed alone (i.e. we can know what is the probability of occurrence a wave with a significant height value between 1 and 2 m) and together (as said before with two inputs).

The data presented contains five years of measurements but for a deeper statistical analysis, a matrix with each value of wave (1.1, 1.2, …) and period with more precision is expected. Information presented only uses intervals which doesn't let we know correct value but despite this, it is good to have such information and it is known that if Leixões harbour was the case of study, all information it would be presented.

Analysing now figure 5.4, it can be observed that 45.2 % of waves are in the interval 1-2 m and that 61.8 % of wave periods range between 7 and 11m. This last one is important to compare with figure 5.5. At this last, the period is the mean period which of course is less than peak period.

A 3D model can be designed with the information in Matlab for the generation and extrapolation of new values.

Other important information is the relationship between wave height, significant wave height and design wave height (average of the 10 % highest waves).

In this thesis, for the probability density function, the variable considered was the design wave height and its relation to significant wave height states for Rayleigh distribution where design wave height is 1.27 times significant wave height.

Using this we are always overrating waves and of course for safety reason when choosing design stones. This relation is referred in subchapter 5.2.

For Horns Rev I case of study, no such data was received and it is difficult to relate the two variables. For this reason, the two variables were not considered correlated due to the limited information. Therefore, a normal distribution was chosen for both variables.

$$H_{1/10} = normal\ (\ 4.45\ ;\ 1.5) \tag{5.2}$$

$$T = normal\ (\ 9.4\ ;\ 3) \tag{5.3}$$

c) Sediment Graduation – Nominal Diameter

For the interpretation of this variable and its behaviour, Johnsons (1992) is an indispensable reference to review.

Johnson (1992) assumes the log-normal distribution for the sediment graduation and tested his hypothesis in laboratory. He used a correction factor to fit data, using calibrated data.

This thesis uses the same distribution for sediment graduation and due to gravel range – 0.35 to 0.55m – a value of 0.45 was chosen for the mean and 0.1 for the standard deviation.

To complete and to do a correct analysis, a full report from a company who provides stones is required. The sediments need to be characterized with a sieve and a grading curve can be created. This procedure is always used in construction works and in a scour protection it reveals a huge importance.

Scour protections need a wide grading otherwise there is more probability of failure. With a wide grading, smaller stones find a better shelter thanks to the larger stones (De Vos, 2011). Scour protection gets more full filled and it is more stable.

With a grade curve, a distribution function can be achieved representing the probabilities related to size of stones.

This work analyses needs to be done in a deeper study if this thesis analysis is used for any calculations or future works.

$$D_{n50} = lognormal\ (0.45\ ;0.1\ ) \tag{5.4}$$

d) Current Velocities

Finding a probability density function that evaluates the distribution of velocities in any sea or ocean is a search that involves lots of resources.

There are many studies and scientific papers that appraises and use various and different probabilistic density functions such as Gaussian (normal), Weibull and exponential but none of these studies refer the North Sea. Due to this a comparation between different probability density function is made and one is choose to apply in the Matlab code presented in this work.

Through this, he Normal distribution function is referred in Gille & Smith (1999). They used altimetry data from the Topex/Poseidon satellite to obtain ocean surface velocity which leaded them to use a normal distribution and to conclude that for simple statistical model, this pdf can be used. This is only useful when data velocities are not in a large range to count and correct the lateral flow inhomogeneity's. (Swenson and Niiler,1996). At Gille & Smith (1999), the data collected refer to the Atlantic Ocean and is used in this thesis to make an association with North Sea by analysing many forms of pdf´s and comparing them.

On the other side of the world, in Pacific Ocean several studies were made to analyse and fit a pdf to current velocities. The reference to this work is from Chu (2008). Using data from six different stations from Tropical Atmosphere Ocean project, his studies conclude data satisfies the two parameter Weibull distributions for the upper tropical Pacific.

About the exponential distribution, her use dues only to the shape of velocity forces field. It has a behaviour likely any exponential function.

The conclusions that can be drawn for this three different points of view is each that case depends on some variables, which are different from case to case. Comparing the Atlantic Ocean with Pacific it is an unrealistic situation because they are two different situations, since currents and waves are very different.

A detailed study for the North Sea in this thesis requires a data collection, analysis and post forward conclusions. Only with such instruments, a probability density function can be fitted to the data and be sure that is the right to use. Using statistical programs such as SPSS or others is interesting to make it easier to scrutinize all parameters from all pdf´s that needs to be analysed. Some probabilistic tests also need to be done.

There was no other choice to make other than assuming a distribution to current velocity. The choice was normal distribution because it is more comparable to the North Sea or to the Atlantic Ocean (despite their differences) than with Pacific (its temperature assumes an important role and a joint probability function may be needed). The values used for current velocity were 1.50 $m.s^{-1}$ for the mean and 0.5 for standard deviation

$$U \quad c = normal\ (1.5\ ;\ 0.5\ ) \tag{5.5}$$

5.3 PRELIMINARY ASSESSMENT OF THE RELIABILITY ALGORITHM

In order to understand if the reliability algorithm is correctly modelling the scour phenomena and the failure mode of the scour protection, it is important to assess the behaviour of the probability of failure according to each basic random variable. Therefore, the following analysis was performed to evaluate if the Matlab code is able to provide the expected tendency of the scour severity. The first basic variable that must be studied is the D_{n50} due to its importance in terms of the protection's resistance. The failure mode analysed in the present thesis corresponds to the erosion of the top layer, as defined in figure 5.6:

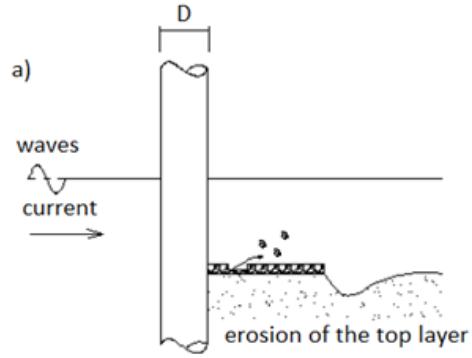

Fig. 5.6 – Mechanism of failure (De Vos, 2011)

This failure mode excludes the ones due to edge scour, loss of bed material through the top layer and flow slide occurrence. The present analysis uses the design example presented in De Vos (2011) as a reference situation, so that a design comparison can be made. This example is summarized in the following table 5.4:

Table 5.4 – De Vos design example

Data	Distribution	Mean	Standard Deviation
d	Normal	20	3
H_s	Normal	8.3	2
σ_D	-	2.5	-
T_p	Normal	11.2	3
U_c	Normal	1.5	0.5
D_{n50}	Lognormal	0.496	0.1

Regarding the erosion of the top layer, for higher dimensions of the protection blocks the resistance increases, since larger stones are difficult to be dragged. Hence if larger stones are used, it is expected that the protection is less likely to fail for the same hydrodynamic conditions, both for currents and waves. In the Shields' equation the basic random variable acts as a stabilizer of the protection since larger blocks present higher critical shear stress values. As it can be perceived from figure 5.7 the failure probability is decreasing with an increasing mean dimension of the protection units:

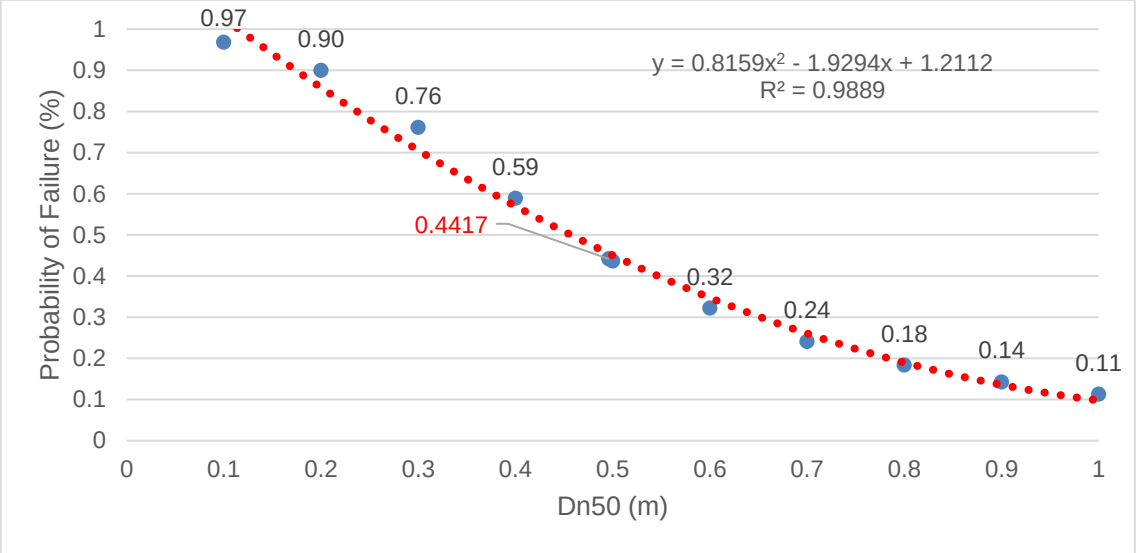

Fig. 5.7 – D_{n50} vs probability of failure

Such behaviour is expected and reasonably described by the empiric knowledge of the resistance increase provided by larger stones. An important aspect of the relationship found is the considerable difference between the probabilities of failure for this range of D_{n50} values. For the stones with 0.1 m of mean diameter the probability of failure is very high which is clearly expected, because the chosen diameter isn't enough for a statically stable protection, as it is shown in figure 5.8:

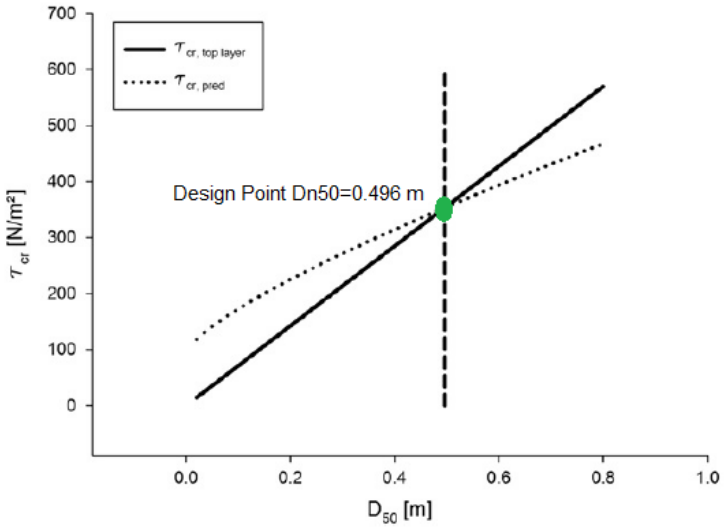

Example: $d = 20$ m, $U_c = 1.5$ m/s, $D_{85}/D_{15} = 2.5$, $H_s = 6.5$ m and $T_p = 11.2$ s. Comparison of $\tau_{cr,top\ layer}$ and $\tau_{cr,pred}$ as a function of D_{50}. $D_{50,stable} = 0.496$ m.

Fig. 5.8 – D_{50} vs τ_{cr} (De Vos, 2011)

On the other hand, stones with very large diameter are statically stable and the probability of failure is lower. In terms of design, it is important to note that besides the criterion of the threshold of motion, the installation and construction requirements of the protection must be respected. Therefore, although a D_{n50} equal to 1 m provides a much lower probability of failure (P_f=11.27%) it is not feasible in terms of pipe vessels installation. Usually pipe vessels deal with blocks that should not be larger than 0.85 m. This leads to the conclusion that, for design purposes, a balance should be achieved between a reasonable dimension and a feasible installation. As an approximation a parabolic curve was fitted with an R^2 of 0.9904, which can be used to compute P_f according to a specific D_{n50} for the hydrodynamic conditions used this example. This procedure could be used in other examples to develop new curves for a quick pre-assessment of the failure probabilities. For the suggested fit, it is possible to graphically confirm that the better fitting is achieved for D_{n50} higher than the design point proposed by De Vos (2011).

The standard deviation used in this simulation was 0.1 m which also contributes for very high failure rates in simulation with D_{n50} ranging from 0.1 m to 0.4 m. Naturally this values must be analysed as an indication, due to the very simplistic model assumed and the uncertainty of the parameters and distributions. Also the absence of correlation analysis

The design value proposed for a statically stable diameter was D_{n50} of 0.496 m, the associated probability of failure was 44.17% which might be considerably high for the investment made into installing and maintaining the scour protection. Such value is overestimated since the assumption of normal distributions and independent of basic variables tends to lead to overrate P_f (Chang, 1994).

In a similar way for the rest of the variables analysed in this chapter, it would be important to either perform a considerably large set of scour tests, by means of physical modelling work, in order to confirm the magnitude of the probabilities obtained. One of the major problems when conducting reliability based studies, related to scour protections, is the absence of field data or major laboratory research available to confirm *Pf*. The lack of information is added to other problems as the scaling issues, the probabilistic distributions and other uncertainties.

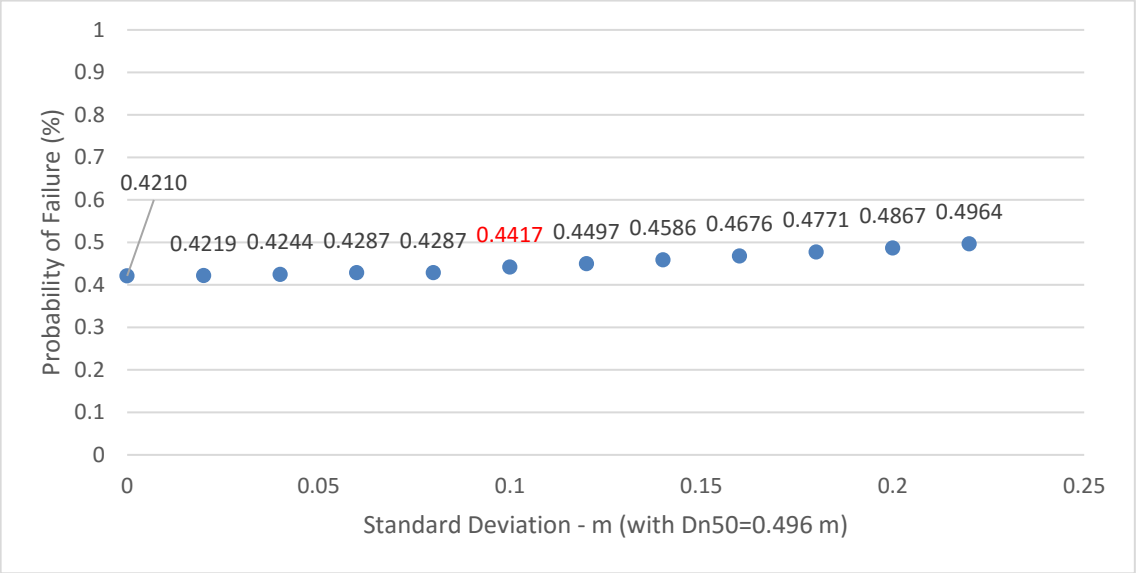

Fig. 5.9 – Standard deviation (with Dn50=0.496 m) vs probability of failure

As showed in figure 5.9 when simulating the scour protection's behaviour for Dn50 equal to 0.496, the influence of the standard deviation is also noticeable. A variation between 1 cm and 22 cm leads to differences of approximately 8% in the failure probabilities. When the standard deviation matches 0.1 m, the P_f value is equal to the one presented before (44.17%). Since this simulation corresponds to the reference situation used in De Vos (2011) the results should be consistent between the previous figures, which they are. Despite the simplifications made in the model the previous analysis shows that the MATLAB algorithm is giving a consistent relation between P_f and D_{n50}. If the protection blocks increase, the resistance increases and the failures probabilities are reduced.

The following basic variable that should be analysed is the current's average velocity. The current velocity has a strong impact in this failure mode. Note that the currents induced shear stress depends on the square velocity value (U_c^2). Therefore, increasing the currents loads means that the acting shear stress on the top layer will experience a considerable increase. On the other hand, the resistance shear stress computed with Shields' formula does not increase in the same proportion. Although the Reynolds number depends on the velocity and the type of flow, the present algorithm is assuming a fixed value of 0.035 for θ_{cr}, based on the methodology adopted. Hence the resistance shear stress does not compensate for the increased values of the acting currents, this leads to a higher probability for the stones to be dragged downstream. As it can be seen, the influence of this variable is also correctly described by the model.

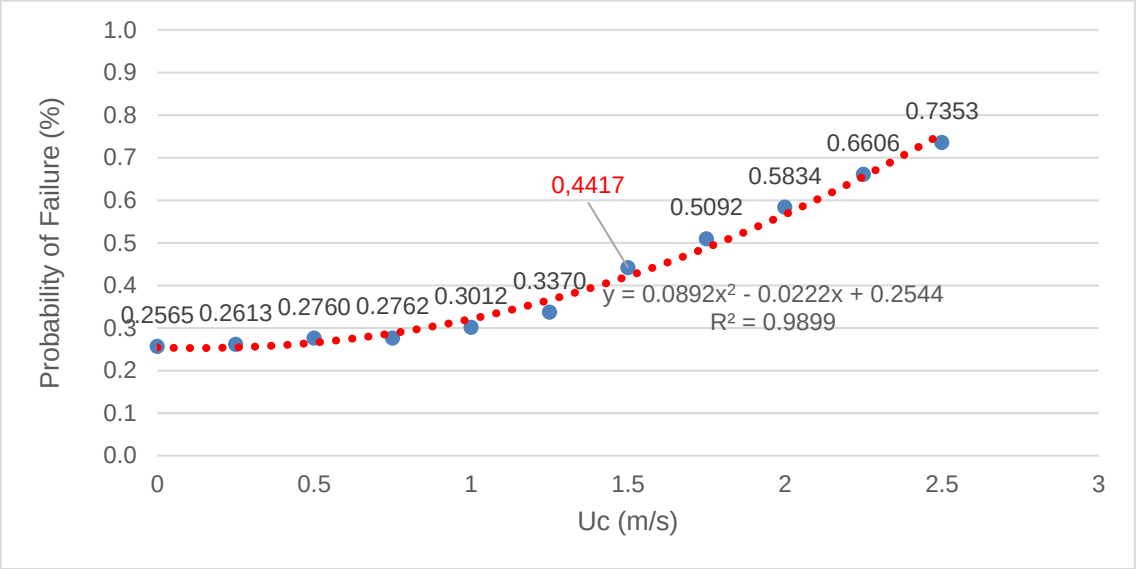

Fig. 5.10 – Current velocity vs probability of failure

In a similar way for the D_{n50} and the other variables studied, a fitting equation was applied leading to a quadratic law with a R^2 of 0.9899. This equation poses itself as an indicative fitting line between U_c and P_f. Nevertheless, the relation between D_{n50} and the probability of failure is more important, since the dimension of the stones is the actual design variable used for this failure mode.

Due to the nature of oceans currents, it would also be important in future works to use other statistical distributions, as the ones suggested by several authors, e.g. Gille & Smith (1999), Chu (2008) and Swenson & Niiler (1996) which indicate that U_c can also be modelled by means of Weibull or Exponential laws. However, due to the lack of information and since no specific analysis was made in terms of historical records available, the normal distribution was assumed as suggested in Gille & Smith (1999). The use of the normal distribution also helped to simplify the algorithm, since the present thesis concerned to the first stage of the code's implementation. A typical approach would imply the analysis of historical records coupled with confidence intervals and hypothesis analysis to determine a suitable distribution, that could be used later on in Monte-Carlo simulations.

These simulations provided the failure probabilities for the design point (D_{n50}=0.496 m) considering a velocity range of 0 to 2.5 m/s. In the North Sea, the velocities tend to be smaller than 2.5 m/s, as seen before. This implies that the stated probabilities above 1.5 m/s should not be considered typically expected values. Nevertheless, they allow us to understand that the algorithm is reasonably expressing the Pf's tendency in respect to velocity. If the velocity increases the protection is more likely to fail by top layer erosion.

Concerning the influence of the standard deviation, it can be seen in figure 5.11 that the changes in the velocity deviation have a similar influence in the probabilities magnitude, as the ones shown in the deviation of the stones nominal mean diameter (D_{n50}). In this sense it can be perceived that simulations performed with different standard deviations of U_c may produce results, which can vary around 10%, i.e. roughly between 42% and 53%, for D_{n50}=0.496 m.

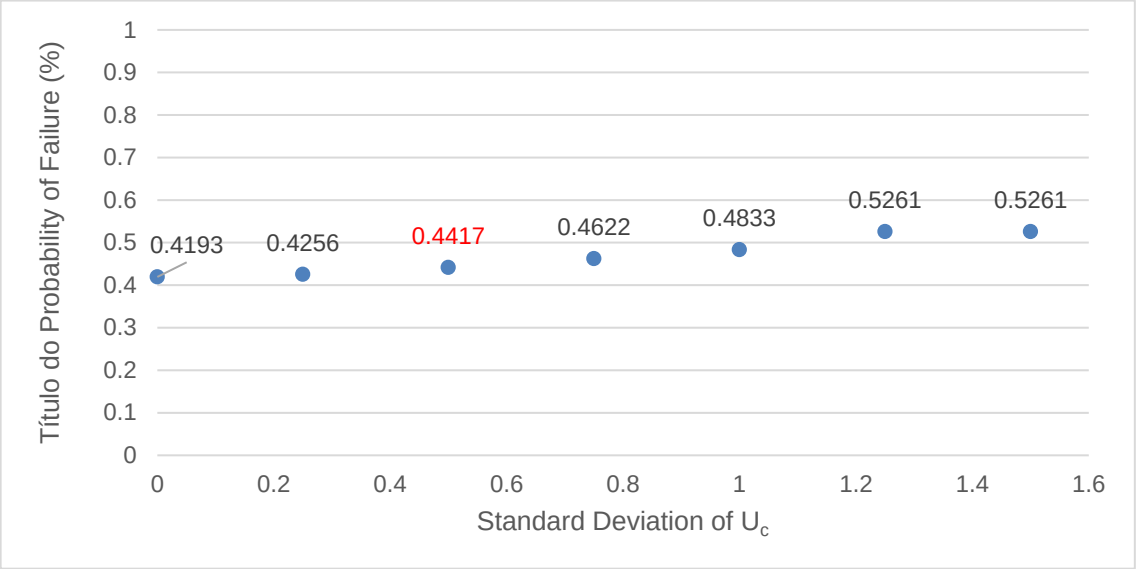

Fig. 5.11 – Standard Deviation (U_c) vs Pf

Another important aspect to be analysed is the influence of water depth. Typically, the scour phenomena in offshore environment tends to be less influenced by the water depth, since for the majority of the monopiles the water depth largely overcomes the pile dimeter (i.e. d>> D_p) (May & Willoughby, 1990 and Whitehouse, 1998).

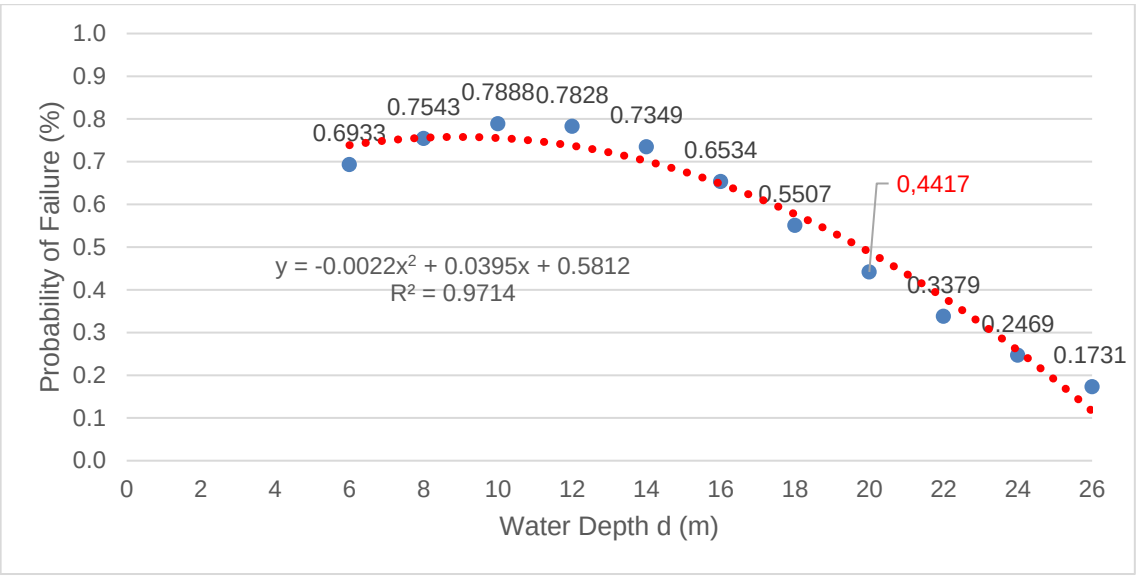

Fig. 5.12 – Water depth vs probability of failure

When designing a monopile for an offshore wind turbine, the effect of the water depth is negligible for d/D > 3 (Whitehouse, 1998). The same author also states that in deep waters this effect gets even more dissipated. Based on the amplification factor, Whitehouse recommends that when d/ $D_p \geq 5$ the monopile

is considered to be in deep waters. For shallow waters, the turbulence of the bed boundary layer is higher and the amplification of the shear stress increases, generating higher dragging forces. In shallow waters, also due to the possible existence of breaking waves, the scour phenomena on the top layer is more influenced by *d*. In the present example, according to De Vos (2008; 2011), *d* corresponds to 20 m and D_p is 5 m. This leads to d/ D_p equal to 5 which is already in deep water zone.

In these simulations, the water depth did not present a similar effect on the probability of failure as the D_{n50} and U_c. In a first part of the curve (figure 5.12) there is an approximate increase of 10% (Pf= [69.3%;78.8%]) in the failure probability for water depths ranging from 6 to 10 m. In this case the ratio d/ D_p varies between 1.2 to 2. These limits are clearly bellow 3, hence the water depth has a considerable influence in the phenomena. Besides that, these values present a wave modelling problem, because $H_{1/10}$ was equal to 8.3 m ($H_{1/10}$=1.27H_s). For *d*=10 m the wave breaks. The present algorithm was designed to compensate for such fact, by substituting these cases for a new wave height equal to 78% of the water depth (according to wave breaking criteria – linear theory).

A possible way to avoid this problem would be either to compute the specific shear stress for the breaking wave event or to incorporate the field data for the wind turbine location, in the Matlab code. In the present case, since this simplification was made, the results must be carefully interpreted. It is suggested that the present algorithm is used for deep water limits, where the generated wave is less likely to break.

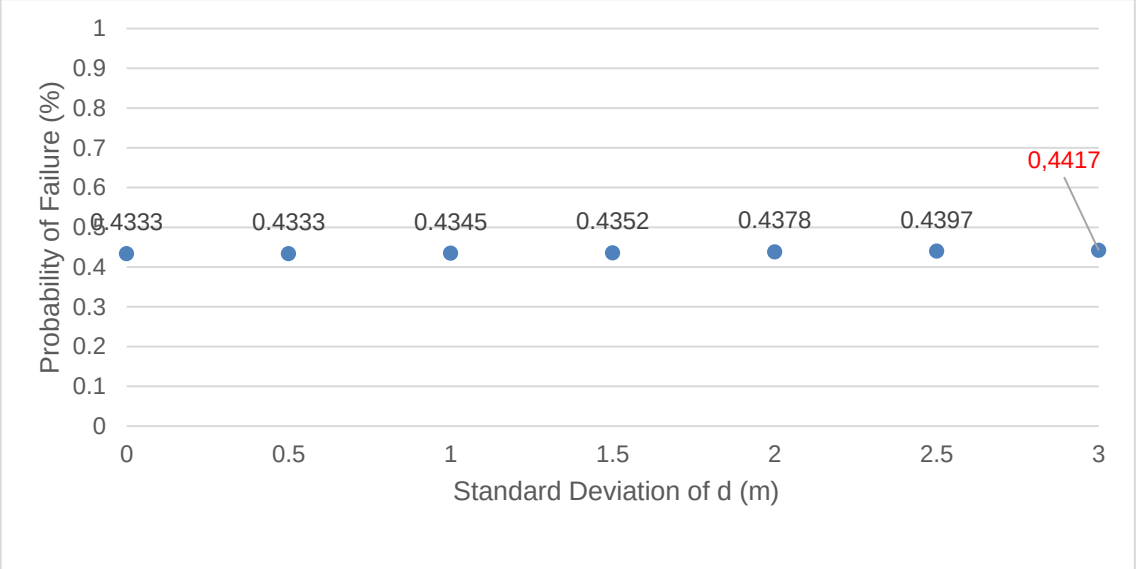

Fig. 5.13 – Standard deviation (d) vs Pf

In order to correctly model the water depth, future versions of the present algorithm should also include proper data regarding the variation of the water surface (η) and the tidal influence in the offshore wind farm. At this stage of the research it wasn't possible to acquire the desired information and the water depth was assumed as d=20 m with the standard deviation of 3 m.

The variation of the probability of failure with respect to the standard deviation of the water depth was also analysed. As it can be perceived by figure 5.13, there is not a considerable impact in the probabilities. With a standard deviation varying from 0 (deterministic situation) to 3, P_f ranges from

43.33% to 44.17%, which corresponds to a difference of less than 0.2%. This difference is comparatively lower than the ones presented for D_{n50} and U_c. Such small variations were expected since the simulations included the deep zone case with h=20 m and σ_h=3 m, indicating that the water depth did not have a strong effect on the scour phenomena. In the Gaussian curve applied to the water depth, according to confidence intervals' theory, 95.44% of the cases are included within the range of $d=[\mu \pm 2\sigma] = [14;26]$.

Therefore, if this algorithm is applied to deep water zones $d/ D_p \geq 5$ ($h \geq 20$ m), no major problems should be expected in terms of the influence of the generation, particularly if it is considered the fact that for $d/ D_p > 3$ (d=15 m) the water depth already has a negligible influence in the scour of the top layer (Whitehouse, 1998).

In summary, the water depth generation is based on simplified assumptions, meaning that the present algorithm should be applied for deep water cases and future research should also be focused on improving the water depth modelling both considering the tidal effects, the free surface and the wave breaking criteria.

Finally, concerning the acting shear stress, there is also a dependency on the waves induced stress. It is important to take into account the behaviour of the waves characteristics. Therefore, the behaviour of the probability of failure according to the waves' peak period and the design wave height ($H_{1/10}$) was studied as follows.

The relationship between the peak wave period and the design wave height is not linear, in fact, a perfect algorithm should be able to compute the specific wave length for a certain wave height and the associated period. On top of that, it is important to note that each wave height should be associated to the expected return period. In this case, this does not happen, since both basic variables are being generated according to separated normal distributions. The most suitable way to develop the wave induced shear stress, should be to account for the joint probability function (H; T), based on field data collected from the location site of the wind turbine.

During this research, and as stated before, there was no possibility to have access to such information. However, this analysis helped us to gain an idea on how the algorithm reacts to univariate changes in the wave height and period. While interpreting the results, it is crucial to take into consideration the effect of this changes in the wave length, which was computed by the commonly used dispersion relationships, which can be consulted in Wiegel (1964).

The following figure provides the effect of the wave height in the probability of failure, when maintaining the other basic variables with the original parameters assumed in De Vos (2011).

A range of $H_{1/10}$ from 6 to 11m was tested, representing extreme shear stresses applied to the top layer, with a standard deviation of 3 m. Although Normal distribution was applied, in future work the wave heights should be tested with other statistical laws, such as the Rayleigh Distribution.

The influence of the wave height is considerable, with the probabilities of failure roughly varying between 16 to 77%. For $H_{1/10}$ equal to 8.3 m, the probability of failure of 44.17% is consistent with the previous simulations.

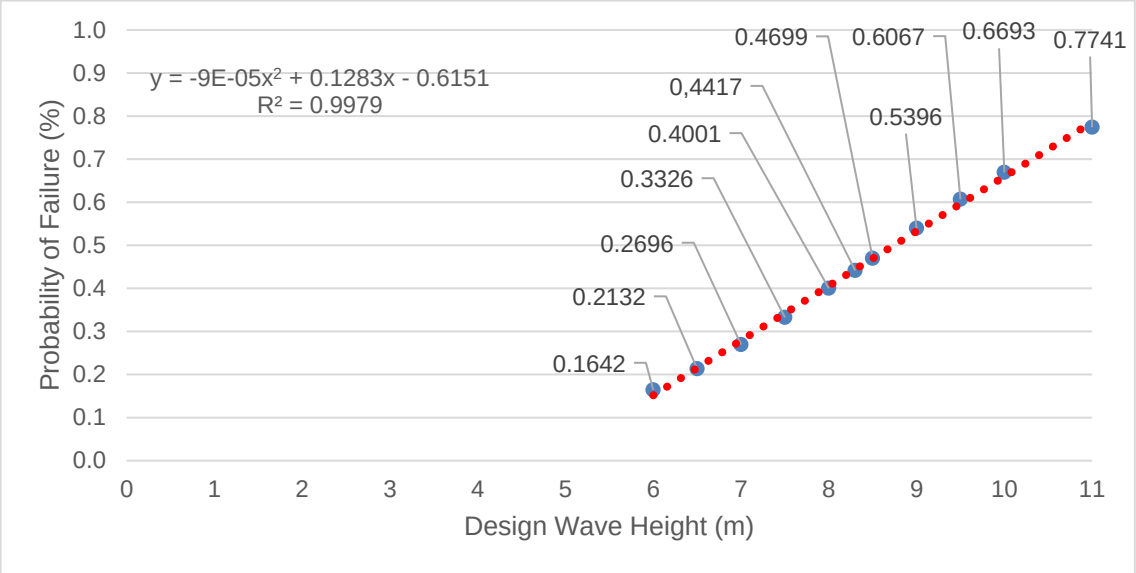

Fig. 5.14 – $H_{1/10}$ vs probability of failure

In a similar way to the water depth it was possible to confirm that the standard deviation did not present a very high influence on the failure probabilities.

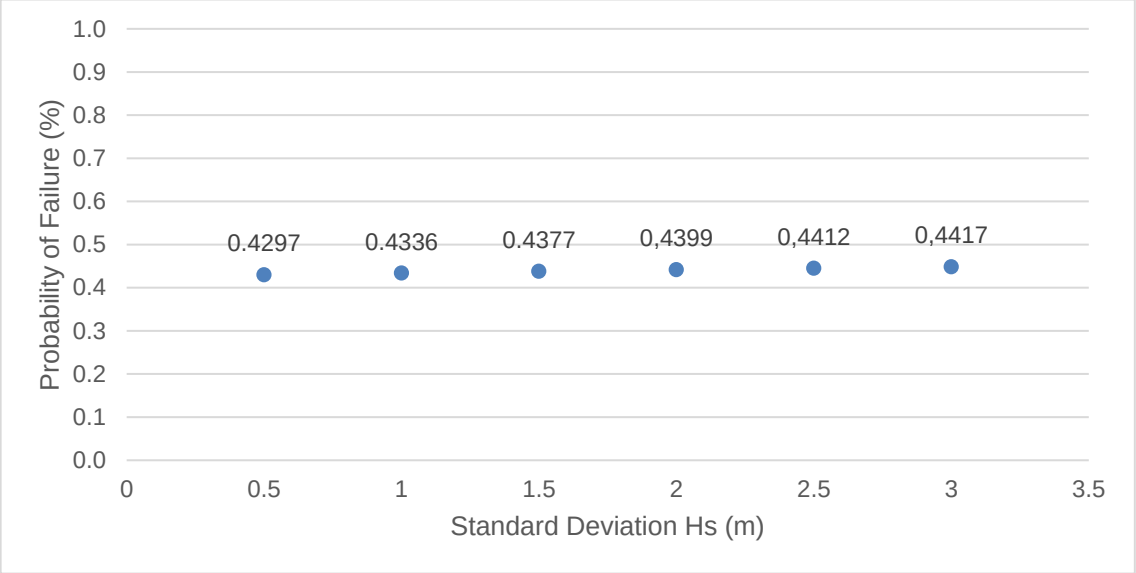

Fig. 5.15 – Standard Deviation ($H_{1/10}$) vs probability of failure

The wave induced shear stress is proportional to the square orbital velocity (U_m), which is proportional to the design wave height. Therefore, it is expected that if the wave height increases the probability of failure also tends to increase. The resistant shear stress obtained from the Shields parameter is not compensating for the increasing acting stress, hence the scour protection is more likely to fail through the top layer erosion mechanism.

Although in figure 5.14 the relationship between P_f and $H_{1/10}$ seems to be linear, for the tested range, the best approximation was achieved for a quadratic equation, with an R^2 equal to 0.9979. A better perception of this could be given if lower values of $H_{1/10}$ were tested. However, for such values the wave induced shear stress is significantly reduced and the probabilities of failure are lower. For example, simulating for $H_{1/10}$ equal to 2 m and 4 m, *Pf* is respectively equal to 3.09% and 9.29%. The algorithm was able to represent the increasing severity of the scour phenomena according to the increasing acting/design wave height.

The analysis of the wave period is a complex one, not only for its relation with the wave heights but also due to its influence in the wave length calculation which is used to obtain the orbital velocity values. For fixed parameters of the remaining basic variables, it is possible to conclude that the combined effect of the period on the orbital velocity and the wave length, for positive values, tends to infinite although at a very slow rate.

Within this mathematical perception it seems reasonable to indicate there is an increasing tendency for the probability of failure with the increasing wave period, as show in figure 5.16. A more detailed analysis on such variation should be performed in future research. Regarding the standard deviation, it is possible to see that a variation in the wave period generates a considerable fluctuation in the probabilities of failure. Nevertheless, for the present range of tested values the relation is clear, if T increases *Pf* also does.

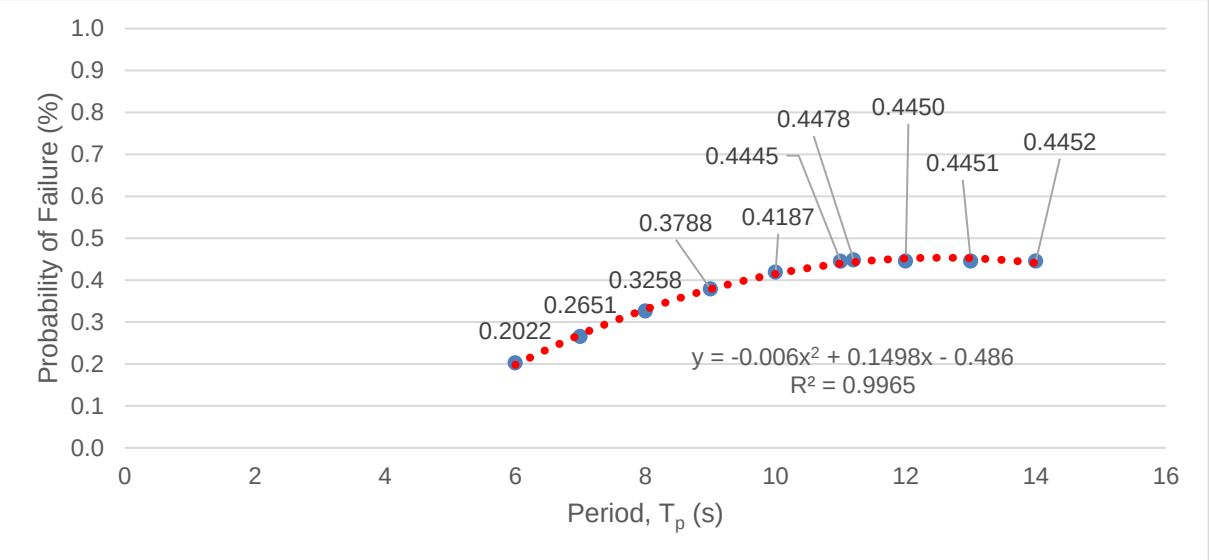

Fig. 5.16 – Period (T_p) vs P_f

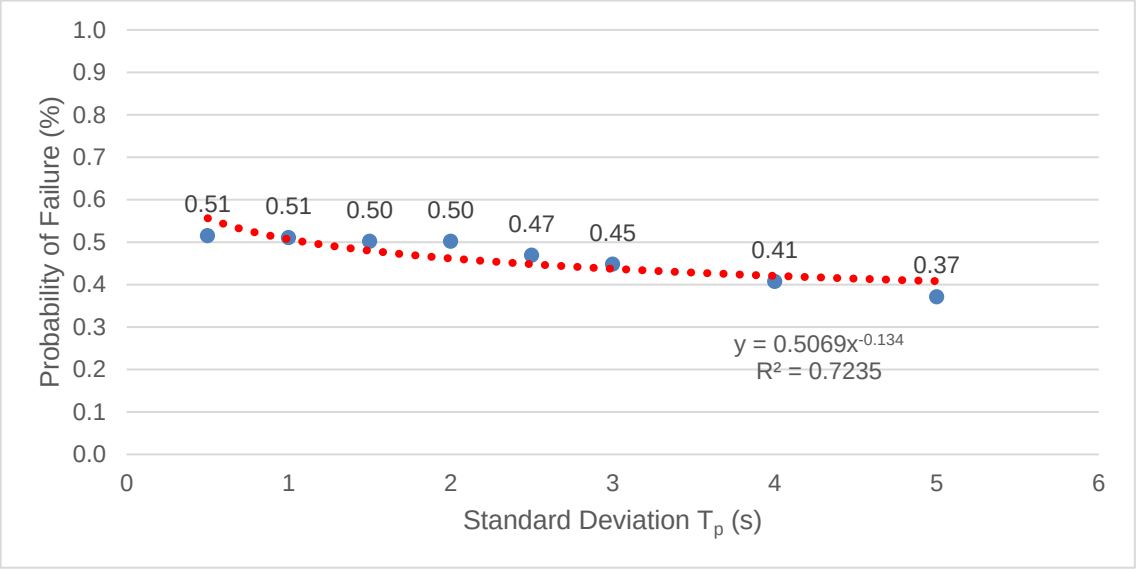

Fig. 5.17 – Standard Deviation (T_p) vs P_f

The analysis of the basic variables influence should be carefully interpreted due to the simplifications made and the uncertainty of the parameters, as explained before. However, a rough estimate of their influence, in the probabilities behaviour, is crucial to ensure that the algorithm is correctly translating the phenomena for the small range of values tested in the example.

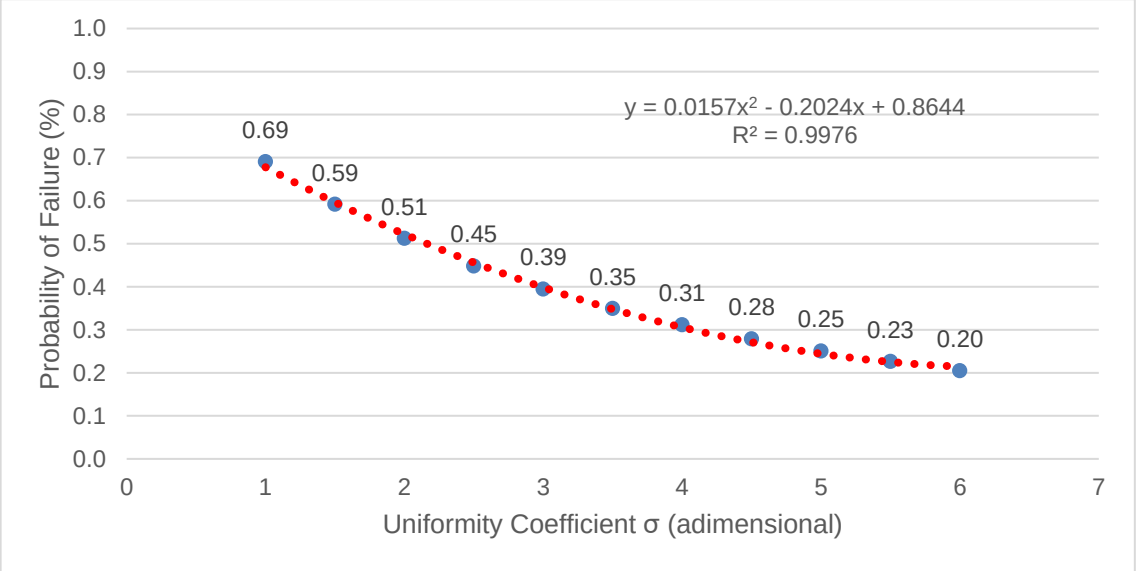

Fig. 5.18 – Uniformity Coefficient vs probability of failure

The uniformity coefficient is of greater importance when trying to analyse the resistant shear stress of the protection. Several authors, e.g. Soulsby (1997), De Boon (2004) and Fazeres-Ferradosa (2016), state that scour protections with a wider grading appear to be more stable, than the ones with a very

narrow grading curve. Higher values of σ correspond to a wider range of stones existing between the D_{85} and the D_{15}.

A possible reason for the increasing stability with higher values of the uniformity parameter is the fact, that smaller stones are able to find shelter between the larger ones. Hence being less exposed to drag forces. Although the design parameter θ (Shields factor) is usually defined for the scour protection as a whole, smaller stones tend to be dragged first. In fact, the θ_{cr} is based on the D_{n50} value but it does not describe the behaviour of all the protection units.

This is also a justification why typically designed scour protections fail although they have been placed to resist to the threshold of motion criterion. If smaller stones are dragged the protection can fail by loss of filter material or sinking effect. More recently some studies have been conducted in order to analyse new configurations for the scour protection, where the filter layer is not placed and the protection is made only with a very widely graded material, e.g. Schendel *et al.* (2015).

In the present case, as shown in figure 5.18 the probability of failure is decreasing with the increasing uniformity coefficient, which is in agreement with the previous observations.

As an overall idea, it is possible to conclude that the present algorithm is providing interesting and reasonable matches between the basic random variables and the erosion of the top layer. Several simplifications and assumptions were made and the reliability algorithm presents a considerable improvement margin, as it will be discussed further on. Another important aspect to be further developed is the choice of the probability density functions and the parameters estimation, which can be enriched by data gathering concerning the present design variables. Nevertheless, the code implemented allows the selection of new probabilistic laws and other parameters, which enables the application of the reliability based assessment for other scour protections.

5.4 Algorithmic Optimisations – Latin Hypercube Sampling Method and Minimum Number of Simulations

The Latin Hypercube Sampling Method is an algorithm typically used in order to reduce the number of Monte-Carlo Simulations required for a stabilised probability of failure.

In proper conditions, this algorithm may allow an optimisation that reduces 10 times the amount of simulations needed to obtain a realistic value of P_f. In the present case, this algorithm was applied through an optimisation tool of the MATLAB code. During its application it was concluded that further improvement was required, as it will be explained further on.

Although all the variables were considered statistically independent, the physical coherence of the phenomena must be respected, to ensure that the obtained probabilities are in the expected order of magnitude. In the present case, and as discussed before, the wave heights and the wave periods depend on each other. The correct way to generate (H; T) pairs is according to the joint probability function, which wasn't available for the present study. Nevertheless, once the pairs are generated it is important to keep them paired to avoid a misrepresentation of the physical characteristics of the sea wave generation. Although the joint probability function was not used, this code took into account the need to maintain the originally produced (H; T) pairs. Such detail enables an accurate incorporation of the joint probability density function in future works, if field data is available.

Another important variable that will require a deeper analysis when using the Latin Hypercube algorithm is the water depth, due to its importance for the wave breaking phenomena. However, if field data is

available, the generation of tri-dimensional pairs (H; T; d) will be able to include reasonably associated values, since the parameters and probabilistic functions are based on real data. Of course, if field data indicates that the waves are breaking at the wind turbine location, the shear stresses should take this fact into consideration, and other changes might be required to the present code. Nevertheless, if the offshore wind turbine is located in deep water zones, this is expected to be correctly functioning. Note that according to DNV-OS-C201 (DNV, 2015) monopiles are used up to 30 m, which for a monopile diameter of 6 m already respects the minimum ratio d/ $D_p \geq 5$. At the present, XL monopiles can be installed in water depths up to 45 m (Navigant Consultant Inc., 2014).

Due to the previously stated, the hypercube sampling method was applied to basic random variables concerning to water depth (d), current average velocity (U_c) and the average nominal diameter of the blocks (D_{n50}). It was not applied to the wave heights and periods, in order not to rearrange these pairs.

The following figure provides a sample of simulations where the hypercube algorithm was applied (blue lines) and not applied (red lines). No major differences were noted in terms of the probabilities stabilisation, which leads one to wonder why the Latin Hypercube has not significantly contributed to a quicker stabilisation of the probability of failure.

Several hypotheses can be pointed as possible reasons for this to occur. Firstly, it is important to understand the minimum required number of simulations (N) to reach a reasonable estimate of the failure probability. There are different criteria that can be used to assess this (DNV, 1992; Das & Zhang; 2003).

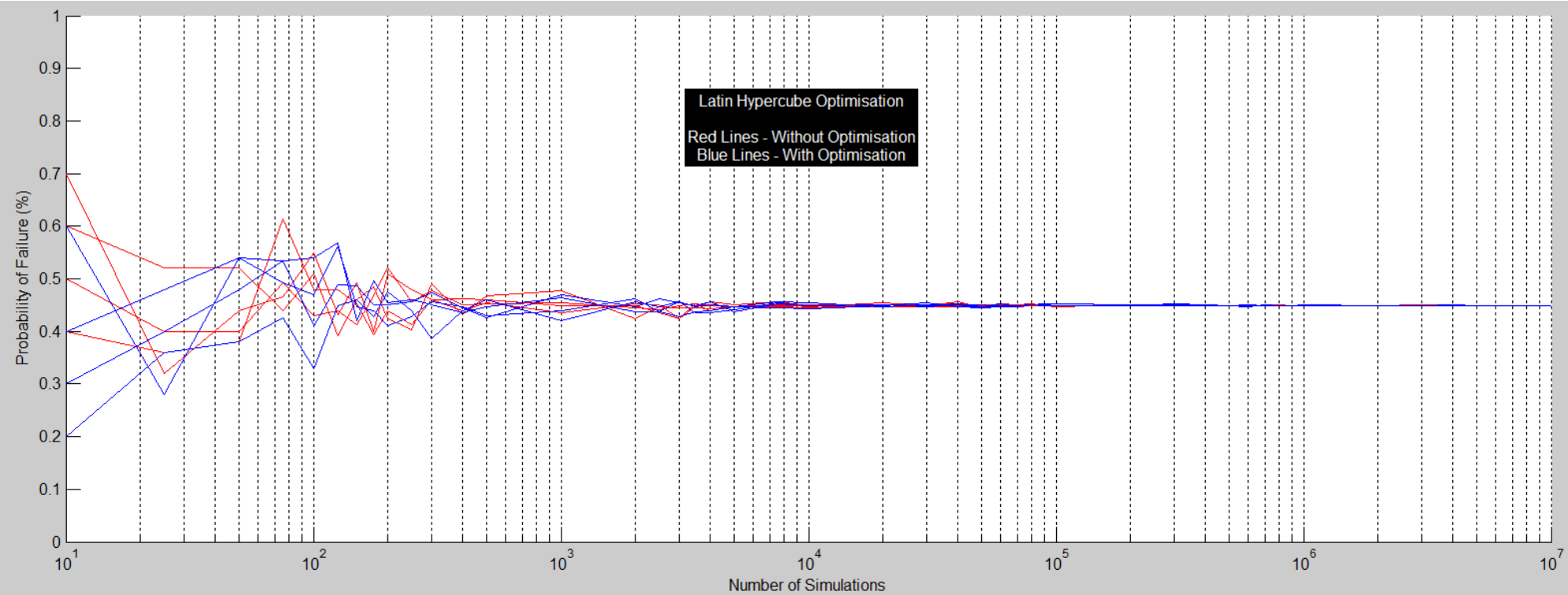

Fig. 5.19 – Number of simulations vs Pf - Algorithmic Optimisation

A first idea of the number of simulations needed for a certain desired confidence level and probability of failure can be given as $N>-ln(1-C)/P_f$ according to Broding (1964). Another possibility often consists in analysing the behaviour of the probability of failure with the increasing number of simulations.

Johnson (1992) studied the probability of failure in scour at bridge piers, coupling Monte Carlo method with variance reduction techniques (antithetic variates and conditional expectation). In this research the stabilization of *Pf* was reached after N=4000 cycles for a pier depth equal to 0.8 and 1.4 times the scour depth. If the probability of failure is plotted *versus* the number of simulations another possible criterion for N is the correspondent value associated to the limit of *Pf* when $N \to \infty$.

Fazeres-Ferradosa (2016) states that variance tends to diminish with the increasing number of simulations (samples). Nevertheless, it is important to note that the rate of convergence and its stability can depend, to some extent, on the quality of the random number generator used. Therefore, in some unfavourable circumstances, it is possible to obtain an apparent convergence, which is not real. Some engineering practices present their own criteria, e.g. DNV (1992) suggests that simulations based on Monte Carlo method should be carried with $N_{minimum}=100/Pf$ while other methods must be carried for an estimate of *Pf* with a coefficient of variation lower than 10%.

For the parameters defined in the De Vos example (2011), for a design wave height of 8.3 m, the obtained probabilities were close to 44%. Broding's formula (1964) would imply that N>4600 simulations, for a confidence level of 99% and a P_f of 0.1% while DNV (1992) would require 10000 simulations for the same P_f equal to 0.1%.

In this dissertation, a maximum of 10 000 000 simulations was applied, which is clearly above the necessary limit for such high values of P_1, as the 44% obtained in the example studied before. For such high values of probabilities, it is expected that the Latin hypercube algorithm does not add any considerable optimization. This type of algorithms is typically applied for large data bases, and engineering problems, were P_f is legally restricted to very low values, as it occurs for example in structural design problems limited by Eurocodes or similar norms. Therefore, the added value generated by this optimization is not quite clear in this case.

Another important aspect, already mentioned, is the fact that the pair (H; T) was excluded of the Latin hypercube sub-algorithm. Therefore, only three variables (d; D_{n50}; U_c) were rearranged in order to optimize the probabilities' convergence, besides that the standard deviation of the water depth presented a very low influence on the probability of failure, which may also contribute for a smaller difference in this stabilization.

As an overall view of the Latin Hypercube algorithm, it can be stated that further research is needed. Nevertheless, the non-significant gains in terms of the stabilization might be due to:

1- The high values of P_f associated to the chosen example;
2- The low amount of basic random variables included in the rearrangements.

However, it was important to program this and incorporate it the computational code, so that it can be used in further research, namely, when design the scour protection for very low values of the failure probability. Besides that, if the possibility of using field data appears in the future, this will be enable a more evident optimization, since the code is already developed to include such information in the hypercube combinations. The fact that the final results tended to provide the same values for P_f, both using and not using the optimization, shows that the rearrangements made to the tri-dimensional (d; D_{n50}; U_c) pairs did not affect the final outcomes.

5.5 IMPROVEMENTS NEEDED FOR THE ALGORITHM

In the previous sections of the present chapter, it was possible to assess the applicability of the reliability algorithm developed in order to compute the probability of failure of a riprap scour protection. Based on the assessment made, it is crucial for the results interpretation and future developments to understand the "flaws" of the system and to present possibilities for further improvement.

The first major improvement that should be considered is the deep study and detailed statistical modelling of the basic random variables. Although this fact does not actually concern to the algorithm itself, it has a very important impact on the final outcome of this approach, because the random variables generation depends on the correct modelling of their statistical properties. Therefore, it would be important to accurately assess which probabilities density functions should be used and properly estimate their population's parameters. There is a clear lack of freely available metaoceanic data to be used for purposes of design of offshore wind foundations. This occurs mainly due to confidential policies between the companies in the energy market, as seen before.

Important field data should also be acquired concerning scour depths, erosion and deposition on the top layer of the installed protections. This would enable a particularly detailed scour monitoring that could be used in order to calibrate this algorithm and the random number generator.

Still concerning data acquisition, the physical modelling of the scour phenomena is a major contribution for a more reasonable statistical modelling of the variables. Nevertheless, since the majority of scour tests, performed at experimental facilities, are quite expensive the data availability is low, particularly when considering the sampling sizes needed for proper modelling. Added to this, the scale effects concerning this experiments tend to propagate errors to the probabilities obtained.

Concerning the basic random variables, table 5.5 briefly presents some notes on future aspects that can be considered when improving the present algorithm:

Table 5.5 – Basic Random Variables – Modelling problems and future improvements

Basic random variables	Modelling problems	Future improvements
$H_{1/10}$ and T_p	No joint probability was applied; Other distributions could be used for comparison, as Rayleigh or Weibull. Time series – no time series dependency was used.	Test other distributions and gather field data to build the empiric joint probability. Use time series dependent Monte-Carlo simulations, in order to ensure that the generated waves are time dependent, which represents the real life situation in a more realistic way.
D_{n50}	No major problems were experienced and the logarithmic distribution seemed a reasonable approach.	Hypothesis tests should be performed in the future to exactly quantify the properness of the distribution.
U_c	Other distributions could have been used, namely the Weibull distribution.	Field data must be acquired for future calibration.

d	Although some norms, as DNV, ROM or BSI recommend that the water surface (η) should be modelled by a Gaussian distribution and the tidal levels should be modelled on historical records, it was not possible to do it within the timetable available.	Take into consideration the need to separate d into its components: bathymetry, water free surface and tidal variations.

The present methodology was mainly based on the Monte-Carlo simulations. However, it would be very interesting to analyse and compare the results with other methodologies, including for example, the First and Second Order Reliability Methods, which are easier to apply since they work in the normalised space. This would help to analyse if the Monte-Carlo results are similarly achieved with simplified models, which enable quicker simulations. This algorithm could also be updated for even more complex statistical approaches, such as the surface response method coupled with sensitivity analysis.

Still concerning the Monte-Carlo Method, the dependency between variables should be a major concern for future developments of the code. Mathematically speaking, programming such relations is not difficult, being just a matter of re-writing the algorithm to consider the correlation matrix of basic variables.

However, it becomes a difficult task when trying to define the specific matrix to be used, i.e. to assess the real correlations between the basic random variables. Such task must, once again, rely on proper field information to quantify the correlation coefficients applicable to each variable. Besides that, a multivariate analysis should be considered in order to fully account for cross effects on the scour protection's resistance and loads.

The way that resistances and loads interact is very important, not only in terms of the basic variables, but also regarding the failure mode considered, i.e. the performance/limit state function g(x) and the failure criterion applied. Therefore, the research of other criteria and other limit state functions should also be analysed. The present algorithm could be further improved if it is programmed to compute the probability of failure according to other functions. New ones could be considered based on similar variables, namely, taking into consideration the following quantities:

- Dimensionless grain size D* or the Critical grain size D_{cr};
- Critical Velocity (U_c) or the Bottom friction velocity (u*);
- Amplification factor α;
- Stability Parameter ($Stab=\theta_{max}/\theta_{cr}$);
- Dimensional Damage Number S_{3D};
- Others.

In terms of the limit state function applied in this research, some aspects can be mentioned, which might be related to the way P_f is obtained. For example, the equation used in this work, does not directly depend on the pile diameter (D_p).

As it empirically known, the scour process depends on the flow-structure interaction, which is the same as saying that the dimension of the monopile will affect the downward flow responsible for the horseshoe vortex and lee-wake ones. Therefore, the pile diameter seems a major variable which affects the scour severity. This leads to the reasonable conclusion that D_p should be considered in G(x) formulation.

Including this variable into G(x) enables to consider the flow-structure interaction, which was not directly accounted for, because the limit state function was designed based on shear stresses only. Besides that, the function applied, which combines De Vos (2011) predictions with the Shields criterion, does not consider the fact that different zones of the top layer tend to fail more often than others. In 2013, during the MARINET proposal 61 project (MARINET, 2013), scour tests were performed at 1:50 scale, for a monopile subjected to waves and currents combined and it was concluded that the top protection is more likely to fail immediately downstream and at the upstream edge of the monopile (Fazeres-Ferradosa, 2016), as shown in figure 5.20. In the overall tests performed with 5000 waves in each experiment, more than 55% of the failures occurred in blue areas (sectors).

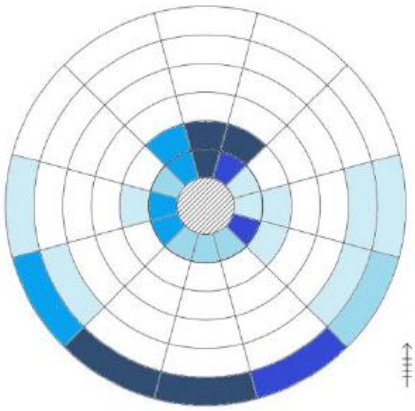

Fig. 5.20 – Matrix of scour failures for Marinet proposal 61, edge failures and in the nearest ring of the pile (MARINET, 2013)

Those tests confirmed that the scour protection failure depends on the specific distributions of the shear stresses, which means that the amplification factor, that describes the stress around the monopile, plays a major role in the top layer failure.

Thus it is possible to state that scour depends on the spatial distribution of the shear stresses and the pile diameter. Therefore, other limit state functions should be developed to take this factors into consideration, among others.

Although the present section of this work could be further presented in the future work considerations, it was important to include it in this stage of the discussion. Mainly because the algorithm limitations affect the way the results should be interpreted. A careful analysis to the limitations hereby presented, enables to outline the future priorities for code development.

Nevertheless, this algorithm provides the basis for a reliability-based assessment of scour protections in offshore foundations. Hence providing interesting possibilities for a reliability design methodology of the protection, in terms of their blocks' dimensions. The new methodology also enables the association between the protection's design and a measure of reliability, which can be intuitively interpreted not only as a measure the system's safety but also on the uncertainty surrounding the problem.

5.6 RELIABILITY BASED ASSESSMENT OF THE CASE STUDY´S SCOUR PROTECTION

The present section will be devoted to the analysis of the failure probabilities, of the scour protections installed at the Horns Rev 1 offshore wind farm.

Regarding the design values to be considered, different information and sometimes not so consistent can be found, e.g., Nielsen *et al*. (2014), Hansen *et al.* (2007) and Orlando (2015). In order to analyse the protection reliability, a situation close to the limit state (B) and another one, described as the typical values for this case study (A), were considered as in the following table 5.6.

Table 5.6 – Situation A and B – Defining values for variables

Situation Description	**d (m)**	**Hs (m)**	**$H_{design}=H_{1/10}$ (m)**	**T_p (s)**	**U_c (m/s)**	**D_{50} (m)**	**D_{n50} (m)**
Situation A – as in Nielsen *et al.* (2014)	9.5	3.5	4.45	9.4	0.4	0.45	0.38
Situation B – as in Whitehouse *et al.* (2011)	13.5	4.43	5.63	12	0.8-1.2	-*	-
	σ_d (m)	**-**	**$\sigma_{H1/10}$ (m)**	**σ_{Tp} (m)**	**σ_{Uc} (m/s)**	**σ_{Dn50}** (m)**	**-**
According to data base information of: LORC and 4COffshore (LORC, 2016; 4COffshore, 2016)	3.5	-	1.5	3	1	0.1	-

* as in Nielsen *et al.* (2014);
** Standard deviation of D_{n50} do not confuse with the uniformity parameter $\sigma=D_{85}/D_{15}$
*** Although the standard deviation of U_c overcomes the mean was only modelled with values always equal or higher than 0. The simulations were performed considering the following pairs $(\mu_{Uc}; \sigma_{Uc}) = (0.8;1)$ and $(\mu_{Uc}; \sigma_{Uc}) = (1.2;1)$

Situation A

If the previously defined parameters are provided as inputs to the reliability algorithm, it is possible to compute the probabilities of failure associated to the general design of the scour protections applied in Horns Rev 1.

Several cycles of Monte-Carlo simulations were applied, following the same procedure as the one used in the example provided in section 5.3. It was concluded that the rounded up mean probability of failure, stabilised for 45.9%.

Taking into consideration the general example analysed before (based on De Vos, 2011 - P_f =44.17%) it can be seen that the values are similar, although the load parameters are quite smaller than the ones tested before. For example, $H_{1/10}$ equal to 4.45 m and U_c equal to 0.5 m/s used for Horns Rev 1 respectively compare with 8.3 m and 1.5 m/s used in section 5.3. This leads to a reasonable question which is: "if the load parameters are less severe in Horns Rev 1 analysis, why does the P_f remain so similar?" Despite the differences in the loads' parameters, it is important to note that the scour protection

applied in the present wind farm has much lower resistance, since D_{n50} is equal to 0.38 m instead of the 0.496 m provided in the other example.

Due to this fact both probability of failures is similar (O (0.4) – order of magnitude – 40%) because the lower values for the loads are now compared with smaller resistances. The figure 5.21 provides a series of tests performed with the algorithm, in order to confirm the probability stabilisation and its order of magnitude.

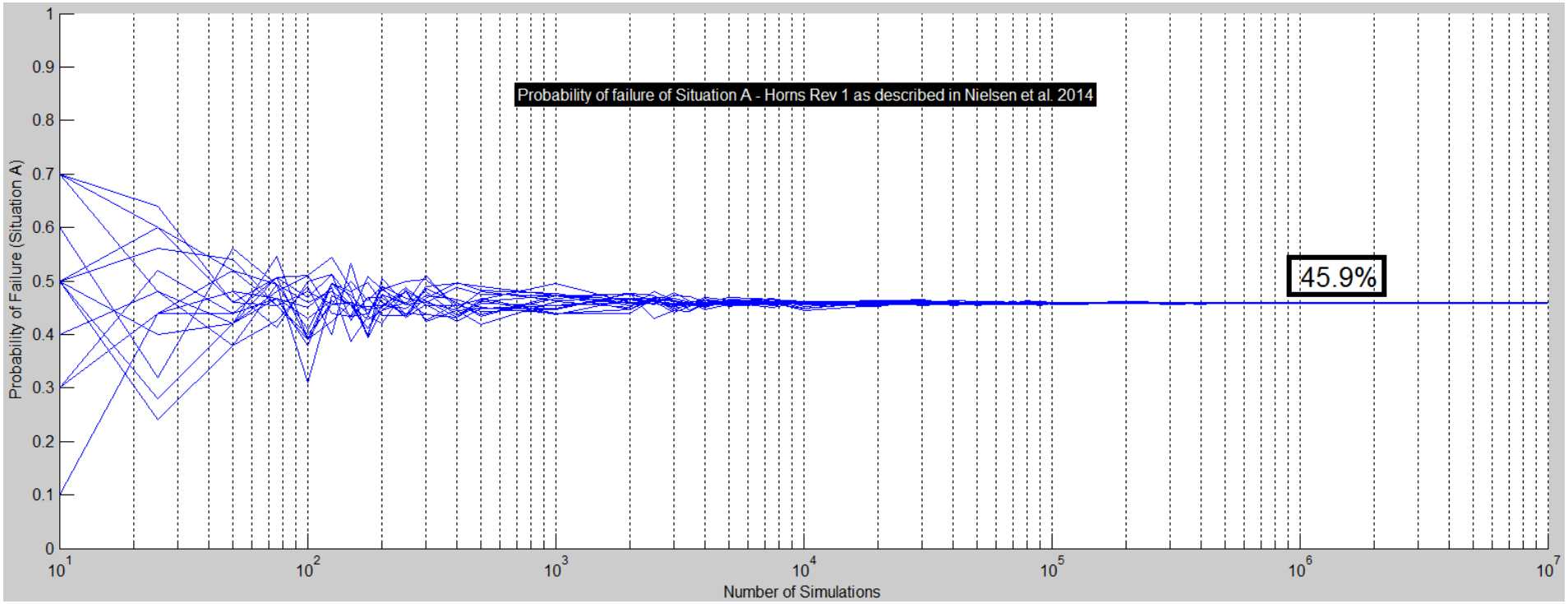

Fig. 5.21 – Number of simulations vs probability of failure - Situation A

When compared to other realities of civil engineering it is possible to confirm that the present probabilities of failure might be considered quite high. In structural problems it is normal to deal with 1x10-4 to 1x10.-6. Thus one may think that the magnitudes hereby presented are very high. Regarding this matter, it should be noted that the uncertainty surrounding the scour phenomena is much larger than in typical structural problems, where for example the concrete resistance to tension and compression is studied, certified and ultimately provided by the manufacturer. In fact, Negro *et al.* (2014) conducted a major study concerning the uncertainties in the design of support structures and foundations for offshore wind turbines, stating that scour phenomena and the empiric nature of the protection design are both major sources of uncertainty in the design of these structures. This leads to the conclusion that such order of magnitude in the probability of failure may not be as unexpected as it may seem.

On the other hand, besides the uncertainty in the phenomena and the protection, other uncertainties can be attributed to the installation and construction methods. According to Nielsen & Sumer (2015) rock/ stone dumping is one of the methods widely used for scour protection, in which a stone cover is installed around the pile (with or without a filter layer between the seabed and the stone layer), extending over an area of three to four times the pile diameter. The stone dumping often originates misplaced stones in the armour layer of the protection, which will contribute for the upper mentioned high failure rates.

A survey reported in Whitehouse *et al.* (2011) from 2002 to 2005 showed that a lowering of the surface, both within and around the scour protection occurred, which backs up the failure occurrence in this offshore windfarm. Furthermore, Nielsen *et al.* (2014) also developed an extensive research concerning the sinking failure of the monitored protections, concluding that several of them actually failed. Whitehouse *et al.* (2011) also reported a lowering of 1.5 m in the protection's sectors adjacent to the monopile. Besides the use of a thicker filter layer, the same author states that the top layer of the armour should be included as part of a maintenance programme, which corroborates the possibility that the top layer failure, analysed in this dissertation, might have contributed for the sinking of the protection.

According to the existing field surveys, other offshore wind farms such as Arklow Bank, Scorby Sands, Egmond Zee present even more severe failures in terms of scour protections, e.g. in March 2004 Scorby Sands Wind Farm presented a 5 m average scour, compared to 2.6 and 3.2 in July of 2004 and November 2006 respectively. Due to the lack of time and information constraints it was not possible to confirm if these wind farms present higher values of P_f matching with encountered severest scour. Nevertheless, not only this could be used to analyse the values of the probabilities as it could be further incorporated to the algorithm's calibration.

Based on the literature and the analysis previously made, the obtained probability of failure for situation A (45.9%) seems to be a reasonable value. Particularly if taken into account the fact that this offshore wind farm already has suffered from top layer refills, meaning that actual failures have occurred.

Table 5.7 – Situation A description

d (m)	**Hs (m)**	**$H_{design}=H_{1/10}$ (m)**	**T_p (s)**	**Uc (m/s)**	**D_{50} (m)**	**D_{n50} (m)**
9.5	3.5	4.45	9.4	0.4	0.45	0.38
σ_d (m)	**σ_{Hs} (m)**	**$\sigma_{H1/10}$ (m)**	**σ_{Tp} (m)**	**σ_{Uc} (m/s)**	**σ_{Dn50} (m)**	**-**
3.5	-	1.5	3	1	0.1	-
***Pf* (situation A)**				**45.9%**		

Situation B

In order to analyse the situation B, the same procedure was applied. In this case the loads are expected to provide additional solicitations to the protection. Higher values were considered in terms of the water depth and the wave height, a slightly increased current velocity was also applied.

As it was seen before, the changes on the probability of failure will mainly depend on the combined effects of each variable. For example, increasing design wave height and current average velocity tend to increase the failure probability. However, this effect may be diminished by the increasing water depth considered.

Taking into consideration the reference situation, described in table 5.8 with a lower limit of U_c=0.8 m/s the probability of failure obtained was 46.2%, while the limit of U_c=1.2 m/s corresponded to 52.9%.

Table 5.8 – Situation B description

d (m)	**Hs (m)**	**$H_{design}=H_{1/10}$ (m)**	**T_p (s)**	**U_c (m/s)**	**D_{50} (m)**	**D_{n50} (m)**
13.5	4.43	5.63	12	0.8-1.2	0.45	0.38
σ_d (m)	**-**	**$\sigma_{H1/10}$ (m)**	**σ_{Tp} (m)**	**σ_{Uc} (m/s)**	**σ_{Dn50} (m)**	**-**
3.5	-	1.5	3	1	0.1	-
***Pf* (situation B – U_c=0.8 m/s)**				**46.2%**		
***Pf* (situation B – U_c=1.2 m/s)**				**52.9%**		

Although the probability increases due to the higher values of the velocity, both between situation A and the cases considered in situation B, as showed in table 5.8, this increase is quite small. The probabilities of failure roughly changed 0.3% from situation A to B with U_c of 0.8 m/s and about 7% from situation A to B with U_c equal to 1.2 m/s

A possible reason for the small increase in P_f could be the fact that the water depth also increased from 9.5 m to 13.5 m, contributing to diminish the negative effect of the new velocities considered.

When De Vos (2011) example was analysed, in section 5.3, it was concluded that the water depth did not provide a linear and monotonic proportional effect on the probability of failure. A peak zone was identified for depths ranging from 8 s to 14 s, which also includes the periods tested in Horns Rev 1. A multivariate and deeper analysis should be performed in order to exactly assess if there is a positive influence of the water depth, that reduces the increasing probability of failure generated by a higher current speed velocity. Added to this uncertainty, the increased period from 9.4 s to 12 s also played a role in the probability effect, that might be hard to quantify as seen in section 5.3. Future research should consider the importance of clarifying these effects. As it can be seen in figure 5.22, there is a decreasing failure probability with the increasing water depth for this situation B. This might have played a major role in the small overall increasing P_f from situation A to situation B.

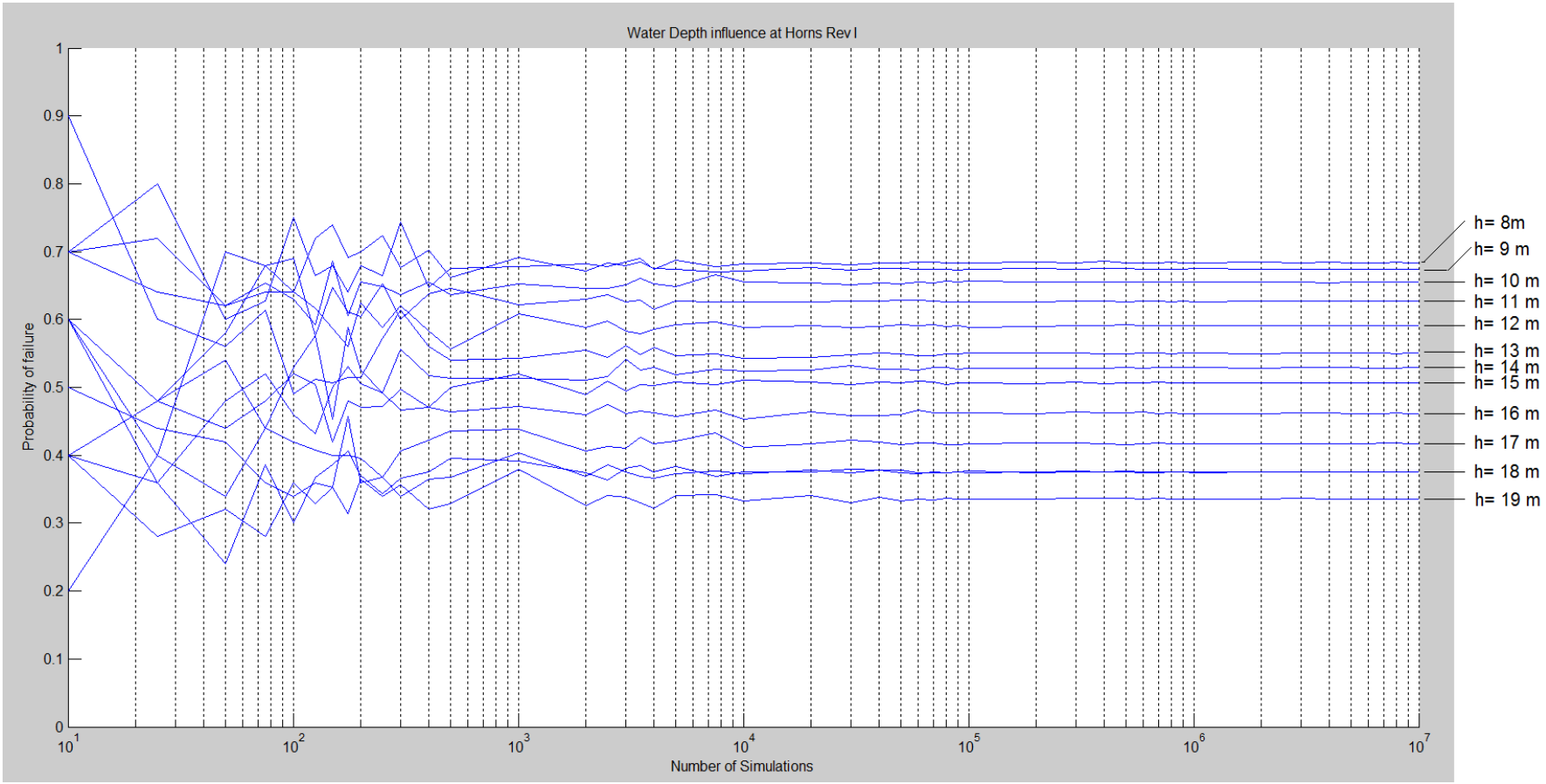

Fig. 5.22 - Probability of failure *vs*. water depth (h=d), for situation B

Another interesting aspect is that Whitehouse *et al.* (2011) states that Horns Rev 1 is a location with particularly adverse hydrodynamic conditions, both in terms of the waves and in terms of the current speeds, in the surveys conducted during the monitoring season, a maximum wave height of 8 m was registered. When the new water depth goes from 9.5 m to 13.5, this maximum wave height becomes possible, since the algorithm does not require a wave height replacement due to the breaking wave criterion explained in section 5.3.

Despite the hidden effects between the basic random variables and the need for further research aiming at these results confirmation, the present algorithm enabled a first measure of reliability, in each case studied. Such measure becomes very important in order to mitigate future risks of failure for scour protections already placed in specific sites and to be used in future projects that are still being designed.

6
CONCLUSIONS AND FUTURE WORKS

The present work aimed at the development of structured algorithm to assess the reliability of scour protections by means of the probability of failure concept. A laboratorial work regarding scour tests with movable sands was also performed, in order to contribute for future scour research to be performed in the Hydraulics Laboratory of the Hydraulic, Water Resources and Environmental Division, of the Civil Engineering Department at FEUP.

The research successfully provided a reliability measure for the specific location of Horns Rev 1 Offshore Wind Farm, based on the previously validated model based on De Vos (2011) experiments. In addition, some conclusions were obtained with the experimental work performed, and several improvements needed to be made were identified.

In addition to the conclusions and the discussions previously made, the following points summarize major outcomes and aims to provide a possible research course for future work, taking into consideration the problems and proposed solutions in chapters 4 and 5.

Concerning the experimental work:

- A first approach to the wave tank adaptation in order to simulate currents was made;
- It was not possible to ensure a symmetric and reproducible flow pattern. Improvements must be made, including the use of more than one pump to ensure higher friction velocities and higher current stresses;
- The first trial registered minimum scour with 2 failure occurrences at 6.5 and 10.5 cm away from the pile;
- The second trial did not register any significant scour, without the protection installed. This could have been due to the devices used for measuring the scour depths, at the face of the pile, or because the maximum depth tends to move to a 30^{o} degree line instead of remaining in the centre profile;
- Data acquisition problems in the wave probes led to the impossibility of using 4 other tests in this thesis;
- These waves' probes must be re-checked before considering future studies;

- The 2Bed Profiler must be fixed and its software updated. Malfunctioning was detected during data acquisition. Profiler tended to stop at the middle of the measuring process.
- This profiler was later on substituted by an ADV Vectrino plus device, adapted for depths measuring, this change led to the conclusion that ADV can be faced as a good alternative to HR Wallingford's 2D Bed Profiler.
- The sediments and its´s own characteristics must be studied in more detail, for a better representation of specific site's characteristics, once again field data is essential in this matter;
- The use of a larger scale in model should present more benefits and more accurate results;
- It was concluded in during this work that a scale of 1:100 might be unsuitable for proper comparison with other studies that have used 1:50 scales. The scale effects on the results presented in chapter 4 were not quantified;
- It was also concluded that the ADV device measurements within the wave tank had suffered from reflection problems in the acoustic signal. Hence providing noisy results that should be further checked.

In respect to the algorithm application, in chapter 5, the following conclusions might be drawn:

- A first base for reliability assessment was successfully developed, by means of a bed shear stress limit state function, for the top layer failure mode, which is one of the major mechanisms in scour protections failure;
- This algorithm still presents some sources of inaccuracy, namely, in the simplifications made concerning the variables independency and their probabilistic distributions;
- The example from De Vos (2011) was used to validate the model tendencies, providing interesting and promising results, with reasonable relations when compared with the existing knowledge concerning scour phenomena;
- Horns Rev I was used as a case study, and it was possible to compute the probabilities of failure in a reasonable way;
- The validation and case studies results showed similar magnitudes, e.g. O (40%)
- The following relations were obtained between the probabilities of failure and the structural and environmental parameters according to the chosen limit state function:
    - If the wave height increases the sour increases;
    - Wave heights and periods do not have direct and monotonic proportion with the scour depths;
    - Wave heights and periods have an effect on P_f is also dependent on the wave length;
    - Increasing water depths led to less scour failures of the top layer;
    - Increasing the mean blocks diameter leads to more stable protections;
    - The uniformity parameter also affects the resistance component of the limit function;
    - The current velocity plays a major role in failure situations, because it tends to increase significantly the probabilities behaviour.
    - In this matter situation B with Uc =0.8 and 1.2 gave consistent results with situation A, although more severe due to the increased velocities.

- Further developments of the code are needed in order to revert the process and go from the reliability assessment to a final methodology of reliability based design.

For the future works, the following main research topics should be considered in order to achieve more realistic results and a more precise assessment of the protection's reliability:

- Field data gathering for purposes of obtaining an accurate statistical model of each basic random variable;
- Perform tests with higher scales to analyse scale effects;
- Analyse and study the probability density functions and adjust them to some variables to better define them;
- Improving the setup conditions for a proper combination of waves and currents environment;
- Develop the algorithm's precision according to the previous point, incorporating the field data analysis and eventually optimising the Monte-Carlo simulations, by using time-series ad accounting for variables correlation.

REFERENCES

4C Offshore (2016, June 15). 4COffshore. Retrieved from 4C Offshore – Offshore Wind Farms Database: http://www.4coffshore.com/windfarms/xiangshui-intertidal-pilot-project---goldwind---gw-100-2500-china-cn48.html.

Athanasia, A., Anne-Bénédicte, G., Jacopo, M., (2012). *The offshore wind market deployment: forecasts for 2020, 2030 and impacts on the European supply chain development. Energy Procedia*, Vol 24, pp.2-10, DOI: 10.1016/j.egypro.2012.06.080.

Breusers, H.N.C. (1971), *Local scour near offshore structures*, Symposium on offshore hydrodynamics, Wageningen, Netherlands.

Breusers, H.N.C, g Nicolet G., Shen H.W., (1977). *Local scour around cylindrical piers*, Journal of Hydraulic Research, IAHR, 15(3): 211-252.

Breusers H. & Raudkivi A. (1991). *Scouring-hydraulic Structures Design Manual*, International Association for Hydro-Environment Engineering and Research.

British Broadcast Corporation (2016, June 1) http://www.bbc.com. Retrieved from BBC news website: http://www.bbc.com/news/world-europe-13592208.

Broding W., Diedderich F., Parke P. (1964). *Structural optimization and design based on a reliability design criterion*. Journal of Spacecraft, Vol. 1, No. 1.

Carstens MR (1996). *Similarity laws for localized scour. Journal of the Hydraulics Division*, ASCE. 92(3), 13-16.

CEM (2008). *Coastal Engineering Manual*. EM 1110-2-1100.

Chang C. & Tung Y (1994). *Discussion of "Reliability-Based Pier Scour Engineering" by Peggy A. Johnson*. Journal of Hydraulic Engineering. Vol. 118, No.10.

Chee RKW (1982). *Live-bed scour at bridge piers*. Report No. 290. School of Engineering, The University of Auckland, 79.

Chiew YM (1995). *Mechanics of riprap failure at bridge piers*. Journal of Hydraulic Engineering, ASCE. Vol. 121, No9, 635-643.

Chu PC (2008). *Probability distribution function of the upper equatorial Pacific current speeds*. Geophysical Research Letters, American Geophysical Union, 35.

Colebrook CF & White CM (1937). *Experiments with fluid friction in roughened pipes*. Proceedings of the Royal Society of London. Series A, Mathematical and Physical Sciences, 161(906): 37-381.

Das, P., Zhang, W., (2003). *Theoretical methods of structural reliability. In: Guidance on structural reliability analysis of marine structures*, pp.22-51. Department of Naval Architecture and Marine Engineering, University of Glasgow, University of Strathclyde, United Kingdom.

De Vos L., Rouck J., Troch P., Frigaard P. (2011). *Empirical design of scour protections around monopile foundations*. Part 1: Static approach, Coastal Engineering, Vol. 58, 540-553.

De Vos L., Rouck J., Troch P., Frigaard P. (2012). *Empirical design of scour protections around monopile foundations*. Part 2: Dynamic approach, Coastal Engineering, Vol. 60, 286-298.

De Vos, L., (2008). *Optimisation of scour protection design for monopiles and quantification of wave run-up – Engineering the influence of an offshore wind turbine on local flow conditions*. Ph.D. thesis, Faculteit Ingenieurswetenschappen, Universiteit Gent, Belgium.

Den Boon H., Hessels J., van Rooij J. (2003). *Cost reduction of offshore wind parks by low cost load monitoring of pile foundations*. Offshore wind energy in Mediterranean and other European Seas (OWEMES), Napels, Italy.

Den Boon H., Sutherland J., Whitehouse R., Soulsby R., Stam C., Verhoeven K., Høgedal M., Hald T. (2004). *Scour behaviour and scour protection for monopile foundations of offshore wind turbines*. European Wind Energy Conference & exhibition (EWEC), London, UK.

Den Boon JH, Sutherland J, Whitehouse R, Soulsby R, Stam CJM, Verhoven K, Hogedal M, Hald T (2005). *Scour Behaviour and Scour Protection for Monopile Foundations of Offshore Windfarms*. Proceedings of the European Wind Energy Conference, 2004, London. UK, UWEA, 14.

Dixen M, Hatipoglu F, Sumer BM, Fredsϕe J (2008). *Wave boundary layer over a stone-covered bed*. Coastal Engineering. Vol 55(1): 1-20.

DNV – DET NORSKE VERITAS (1992). *Structural reliability analysis of marine structures*, classification notes. Number 30.6. Norway.

E-Connection, (2002-2004). Vestas Wind Systems, D.K., Lloyd Germanischer, D. Windenergie, OPTIPILE, Fifth Research and Technological Development Framework Programme.

EWEA – European Wind Energy Association (2016). The European offshore wind industry – key trends and statistics 2015. Available at: www.ewea.org

Faber M. (2009). Risk and Safety in Engineering, Swiss Federal Institute of Technology Zurich, 5.1-5.14.

Fazeres-Ferradosa (2012). *Scour around marine foundations in mixed and layered sediments*. Master thesis in Civil Engineering. College London and University of Porto, Civil Engineer Department.

Fazeres-Ferradosa T & Taveira-Pinto F (2015). *A start for risk analysis application to scour dynamical protection systems for offshore foundations optimization*. 1st Doctoral Congress in Engineering. Portugal.

Fazeres-Ferradosa T & Taveira-Pinto F (2016). *Probability of failure of monopile foundations based on laboratory measures*. CoastLab16 – 6th International Conference on the Application of Physical Modelling in Coastal and Port Engineering and Science. Canada.

Fazeres-Ferradosa T, Taveira-Pinto F, Oliveira B, Simons R (2014). *ECHO-sounder profiles 2D analysis on scour around marine foundations in mixed and layered sediments*. 5th Conference on the Application of Physical Modelling to Port and Coastal Protection. CoastLab 2014. Bulgaria.

Franzetti, S., Larcan, E. and Mignosa, P. 1982. *Influence of tests duration on the evaluation of ultimate scour around circular piers. International Conference on the Hydraulic Modeling of Civil Engineering Structures*. Organised and Sponsored by BHRA Fluid Engineering, University of Warwick, Coventry, England, 16.

Garde (1970). *Initiation of motion on hydrodynamically rough surface – Critical velocity approach*. J. Irrig Power 27(3): 271-282

Gille & Smith (1999). *Velocity Probability Density Functions from Altimetry*. American Meteorological Society.

Goncharov (1964). *Dynamics of channel flow. Israel Programme for Scientific Translation*. Moscow, Russia

Grune, J., Sparboom, U., Schmidt-Koppenhagen, R., Oumeraci, H., Mitzlaff, A., Uecker, J. and Peters, K. (2006). *Innovative scour protection with geotextile sand containers for offshore monopile foundations of wind energy turbines*. Proceedings Third International Conference on Scour and Erosion, November 1-3, 2006 (CD-ROM). © CURNET, Gouda, The Netherlands, 2006.

GWEC – Global Wind Energy Council (2014). Global Wind Report – Annual market update 2013.

GWEC – Global Wind Energy Council (2016). Global Wind Report – Annual market update 2015.

HTB Electrical (2016, 15 June). Retrieved from HTB Electrical – Case studies http://htbelectrical.co.uk/case-studies.html

Hansen NEO and Gislason K (2005). *Movable scour protection on highly erodible sea bottom*. International Coastal Symposium.

Hansen, J., 2007: Climate catastrophe. *New Scientist*, Vol. 195, No. 2614), 30-34.

Henriques, A., (1998). *Aplicação de novos conceitos de segurança no dimensionamento do betão estrutural*. Ph.D. thesis, Faculdade de Engenharia, Universidade do Porto, Portugal

Henriques, A., (2015). *First order second-moment propagation of uncertainty*. Lecture notes on Uncertainty Modelling and Risk Analysis, Infrarisk Ph.D. program, Faculdade de Engenharia, Universidade do Porto, Portugal.

Hjorth P (1975). *Studies on the nature of local scour*. Institute of Technology, Dept. of Water Resources Engineering.

Hoffmans G. (2008). *Closure problem in jet scour*. Ministry of Transport, Public Works and Water Management, Road and Hydraulic Engineering Institute, Delft

Hoffmans G. & Verheij H. (1997). *Scour manual*, Balkema, Netherlands (1997), pp. 224.

HTB Eletrical. (2016). Case Studies. Retrieved 6

Hughes S (2003) *Review of The Mechanics of Scour in the Marine Environment* by Mutlu Sumer and Jφrgen Fredsφe. Journal of Waterway, Port, Coastal, and Ocean Engineering. Vol 129. Issue 6.

Hughes, S. (1993). *Physical models and laboratory techniques in coastal engineering*. Singapore: World Scientific Publishing Co. Pte. Ltd.

IEA – International Energy Agency (2015). Key world energy statistics

Johnson, P., (1992). *Reliability-based pier scour engineering*. Journal of Hydraulic Engineering, Vol. 118 (10), pp-1344-1358, ISSN: 0733-9429/92/0010

Kirkegaard L., Hebsgaard M., Jensen O. (1998). *Design of scour protection for the bridge piers of the Øresund link*. International Conference on Coastal Engineering, Copenhagen, Denmark, pp. 3634–3642

Kobayashi, T. & Oda, K. (1994). *Experimental study on developing process on the local scour around a vertical cylinder*. International Conference on Scour and Erosion.

Kortenhaus, A., Van Der Meer, J. W., Buurcharth, H. F., Geeraerts, J., Pullen, T., Ingrand, D.,Troch, P. (2005) – D40 report on conclusions of scale effects. CLASH WP7- Report.

Kothyari, U. C., Garde, R. J., Ranga Raju, K. G. (1992). *Temporal variation of scour around circular bridge piers*. J. Hydrol. Eng. ASCE 118 (8),1091-1106

LeBlanc C. (2004). *Design of offshore wind turbine support structures*, Ph. D. thesis, Technical University of Denmark, Copenhagen, Denmark.

Leite O. (2015) *Review of design procedures for monopile offshore wind structures*. Master thesis in Civil Engineering. Faculty of engineering of University of Porto, Civil Engineering Department.

Liu Z. (2001). *Sediment transport*, Aalborg.

LORC – Lindoe Offshore Renewables Center (2016) - www.lorc.dk

MARINET (2013). *Optimising the design of dynamic scour protection around offshore foundations*. Technical Report, Marinet Research Program, FEUP, HR Wallingford, IMDC, University of Gent & Aalborg, at Aalborg, Denmark.

Matutano, C., (2013). *Caracterización de los sistemas de protección basados en materials naturals destinados al control de la socavación en obras marítimas presents en instalaciones eólicas marinas*. Ph.D thesis, Departamento de Ordenación del Territorio, Urbanismo y Medio Ambiente, Universidad Politécnica de Madrid, Spain.

May & Willoughby (1990). *Local scour around large constructions*. Technical Report, Hydraulics Research Wallingford.

May RWP, Ackers JC, Kirby AM (2002). *Manual on Scour at Bridges and Other Hydraulic Structures*. CIRIA.

Miranda (2014). *Análise de fiabilidade de estruturas com funções de estado limite implícitas*, Master thesis in Civil Engineering. University of Lisbon, Civil Engineer Department.

Navigant Consulting Inc. (2014). *Offshore Wind Market and Economic Analysis*. Department of U.S. Department of Energy. Document Number DE-EE0005360.

Negro, V., López-Gutiérrez, J., Esteban, M., Matutano, C., (2014). *Uncertainties in the design of support structures and foundations for offshore wind turbines*. Renewable Energy, Vol. 63, 125-132, DOI:10.1016/j.renene.2013.08.041

Neil (1967). *Note on initial movement of coarse uniform bed-material*. Journal Hydraulic Research 6:173–176

Niedoroda, A.W. and Dalton, C. (1982). *A review of the fluid mechanics of ocean scour*. Ocean Engineering. 9(2):159-170.

Nielsen P (1992). *Coastal Bottom Boundary Layers and Sediment Transport*. Advanced Series on Ocean Engineering. Vol 4. World Scientific.

Nielsen AW, Sumer BM, Petersen TU (2014). *Sinking of scour protections at horns rev1 offshore wind farm*. Coastal Engineering Proceedings.

Pang A.L.J., Skote M., Lim S.Y., Gullman-Strand J., Morgan N., (2016). *A numerical approach for determining equilibrium scour depth around a mono-pile due to steady currents*. Applied Ocean Research, Vol.57, Pages 114-124

Porter K, Simons R, Harris J, Fazeres-Ferradosa T (2012). *Scour development in complex sediment beds*. Coastal Engineering Proceedings.

Prendergast L, Gavin K, Doherty P. (2015). *An investigation into the effect of scour on the natural frequency of an offshore wind turbine*. Ocean Engineering, Vol. 101., 1-11.

Prendergast L, Hester D, Gavin K, O'Sullivan J. (2013). *An investigation of the changes in natural frequency of a pile affected by scour*. Journal of Sound and Vibration, Vol. 332. 6685-6702.

Reeve D (2010). *Risk and Reliability: Coastal and Hydraulic Engineering*. Spoon Press.

Rodrigues S, Restrepo C, Kontos E, Teixeira Pinto R, Bauer P (2015). *Trends of offshore wind projects*. Renewable and Sustainable Energy Reviews, 49, 1114-1135.

Schendel, A., Goseberg, N., and Schlurmann, T. (2015*). Erosion Stability of Wide-Graded Quarry-Stone Material under Unidirectional Current.* Waterway, Port, Coastal, Ocean Eng., 10.1061/(ASCE)WW.1943-5460.0000321, 04015023.

Schürenkamp D., Bleck M., Oumeraci H. (2012). *Granular Filter Design for Scour Protection at Offshore Structures*. ICSE6 Paris - August 27-31, 2012, Technische Universität Braunschweig, Gemany.

Shields A (1936). *Anwendung der Aehnlichkeitsmechanik und der Turbulenzforschung auf die Geschiebebewegung*. Preussische Versuchsanstalt fur Wasserbau und Schiffbau.

Soulsby, R. (1997). *Dynamics of marine sands a manual for practical applications*. Thomas Telford Services Limited, London.

Sumer, B, Christiansen, N, & Fredsϕe, J. (1997). *The horseshoe vortex and vortex shedding around a vertical wall-mounted cylinder exposed to waves*. Journal of Fluid Mechanics, 332, 41-70.

Sumer, B. & Fredsøe J. (2002). *The mechanics of scour in marine environment*. World Scientific, Singapore.

Sumer, B. (2002). *Physical and mathematical modeling of scour*. 2nd International Conference on Scour and Erosion

Sumer, B., Christiansen, N., & Fredsϕe, J.(1992). *Scour Around Vertical Pile in Waves*. Journal of Waterway, Port, Coastal and Ocean Engineering, 118(1), 15.

Sumer, B., Hatipoglu, F., & Fredsϕe, J . (2007). *Wave Scour around a Pile in Sand, Medium Dense, and Dense Silt.* Journal of Waterway, Port, Coastal, and Ocean Engineering, 133(1), 14.

Sumer, M., & Fredsøe, J. (2003). *Review of The Mechanics of Scour in the Marine Environment*. Journal of Waterway Port Coastal and Ocean Engineering, Vol. 129 (6), 297

Swenson, M. S., and P. P. Niiler, (1996). *Statistical analysis of the surface circulation of the California Current*. J. Geophys. Res., 101, 22 631–22 645.

Teixeira, A.P., (2007). *Dimensionamento de Estruturas Navais Baseado no Risco e na Fiabilidade*. Tese de Doutoramento em Engenharia e Arquitectura Naval, Universidade Técnica de Lisboa, Instituto Superior Técnico, Lisboa, Portugal

van Rijn LC (1993). *Principles of Sediment Transport in Rivers*, Estuaries and Coastal Seas. Aqua Publications.

Whitehouse RJS, Sutherland J, O'Brien D (2006). *Seabed scour assessment for offshore windfarm*. International Conference on scour and erosion. Nanyand University. Singapore.

Whitehouse, R, Harris, J, &Sutherland, J. (2010). *Evaluating scour at marine gravity structures*. Report HRPP 442, HR Wallingford

Whitehouse, R. (1998). *Scour at marine structures*. Thomas Teldford Limited, London.

Whitehouse, R., Brown, A., Audenaert, S., Bolle, A., de Schoesitter, P., Haerens, P., Baelus, L., Troch, P., das Neves, L., Ferradosa, T., Pinto, F., (2014). *Optimising scour protection stability at offshore foundations*. In: 7th International Conference on Scour and Erosion, ICSE7, December 2nd – 4th, Perth, Western Australia.

Whitehouse, R., Harris, J., Sutherland, J., Rees, J., (2011). *The nature of scour development and scour protection at offshore windfarm foundations*. Marine Pollution Bulletin, Vol. 62, 73-88, DOI: 10.1016/j.marpolbul.2010.09.007

Wiegel R.L. (1964) *Linear Theory of Ocean Surface Waves*, Oceanographical Engineering, Englewood Cliffs, New Jersey

Zaaijer, M., van der Tempel, J., (2004). *Scour protection: a necessity or a waste of money?*. Proceedings of the 43rd IEA Topical Expert Meeting Stockholm, Sweden, 43-51.